



**Progress and prospective on high voltage and safety electrolytes in advanced lithium batteries: from liquid to solid**

Journal:	<i>Journal of Materials Chemistry A</i>
Manuscript ID	TA-REV-04-2018-003358.R1
Article Type:	Review Article
Date Submitted by the Author:	21-May-2018
Complete List of Authors:	Chen, Shimou; Institute of Process Engineering, Chinese Academy of Sciences, Wen, Kaihua; Institute of Process Engineering, Chinese Academy of Sciences, Fan, Juntian; Institute of Process Engineering, Chinese Academy of Sciences Beijing, CN 100190 Bando, Yoshio; National Inst for Materials Science, Advanced Materials Lab and Nanomat Lab Golberg, Dmitri; National Institute for Materials Science,



## REVIEW

## Progress and prospective on high voltage and safety electrolytes in advanced lithium batteries: from liquid to solid

Received 00th January 20xx,  
Accepted 00th January 20xx

DOI: 10.1039/x0xx00000x

www.rsc.org/

Shimou Chen, ‡\*<sup>a</sup> Kaihua Wen, ‡<sup>ab</sup> Juntian Fan, ‡<sup>ab</sup> Yoshio Bando,<sup>cd</sup> and Dmitri Golberg<sup>ce</sup>

(This paper is Dedicated to Prof. Yoshio Bando on the occasion of his 70th birthday)

Developing the next generation high energy density and safe batteries is of prime importance to meet the emerging challenges in electronics, automobile industries and various energy storage systems. High voltage lithium ion batteries (LIBs) and solid state batteries (SSBs) are two main directions gaining increasing interests in recent years, due to their visible applications in the near future. In both of the two kinds of batteries, the electrolytes play a pivotal role but also create several bottle-neck problems. In this review, recent progress in designing electrolytes for high voltage LIBs and SSBs is summarized. First, the solvents, additives, ionic liquids and super-concentrated salts strategy for constructing the high voltage liquid electrolytes are reviewed, and then the applications of inorganic solids, solid polymers, gel and ionic liquids in solid state electrolytes are presented. Finally, the general design rules of the electrolytes and their current limitations and future prospects are briefly discussed.

### 1. Introduction

Recently, growing demands for electronic devices, electric vehicles and mass energy storage systems have spurred the research on Li-

based batteries with high power/energy density and safety. Developing new materials and systems for the Li-based batteries play a key role for this challenge, because the present Li ion batteries (LIBs) cannot satisfy the increasing requirements of their applications, especially for the rapid developments of electric vehicles. It is widely recognized that the advanced LIBs should bring a combination of high-voltage cathodes, high capacity anodes and the corresponding high-voltage electrolytes.<sup>1-5</sup> However, conventional carbonate solvent-based electrolytes exhibit inferior anodic stability of lower than 4.3 V vs. Li/Li<sup>+</sup>, which makes them highly unstable against high-voltage cathodes. With the development and commercialization of high-voltage cathode materials, designing electrolytes at voltages greater than 4.3 V vs. Li/Li<sup>+</sup> and mitigating the undesirable oxidative decomposition of electrolytes have become the decisive factors to restrict electrode capacity of high-voltage LIBs. These issues have gained much

<sup>a</sup>Beijing Key Laboratory of Ionic Liquids Clean Process, CAS Key Laboratory of Green Process and Engineering, Institute of Process Engineering, Chinese Academy of Sciences, Beijing 100190, P. R. China. E-mail: chenshimou@ipe.ac.cn.

<sup>b</sup>University of Chinese Academy of Sciences, Beijing 100049, P. R. China.

<sup>c</sup>International Center for Materials Nanoarchitectonics (MANA), National Institute for Materials Science (NIMS), Namiki 1-1, Tsukuba, Ibaraki 305-0044, Japan.

<sup>d</sup>Australian Institute of Innovative Materials (AIIM), University of Wollongong (UOW), Squires Way, North Wollongong, NSW 2500, Australia.

<sup>e</sup>School of Physics, Chemistry and Mechanical Engineering, Science and Engineering Faculty, Queensland University of Technology (QUT), 2nd Georgest., Brisbane, QLD 4070, Australia.

‡These authors contributed equally to this work.



Shimou Chen received his B.S. degree from Zhengzhou University in 2002, and his PhD degree from Shanghai Institute of Applied Physics, Chinese Academy of Sciences in 2007. In Apr. 2008, he moved to Nagoya University as a JSPS postdoctoral fellow. From 2011 to 2012 he was a Research Associate at National Institute for Materials Science (NIMS), Japan. In April, 2012, he joined Institute of

Processing and Engineering as a professor funded by "Hundred Talent Project" of Chinese Academy of Sciences. His research interests include structure and properties, application of ionic liquid in lithium-ion battery, development of advanced energy storage systems, etc.



Kaihua Wen obtained his B.S. degree from the School of Chemical Engineering and Environment, Beijing Institute of Technology in 2015. He is currently pursuing his M.S. degree under the supervision of Professor Shimou Chen at Institute of Process Engineering, Chinese Academy of Sciences. His research interests mainly focus on the design, synthesis and applications of ionic liquids based novel solid electrolytes for lithium batteries.

## REVIEW

attention from both the academia and industry.<sup>6</sup>

On the other hand, as a key component in LIBs, the commonly used electrolytes are organic liquids, which are volatile and flammable. When the liquid electrolytes are replaced by inorganic solid, gel polymer or solid polymer electrolytes, the safety risks can significantly be lowered. Thus, developing solid state batteries is considered as the ultimate solution for the safety of Li-based batteries. Furthermore, because the solid electrolytes can suppress the lithium dendrite growth, lithium metal anodes can be adopted increasing the energy density of the battery remarkably. However, there are still many challenges for the solid state electrolytes, such as low ion conductivity, bad electrolyte/electrode interface, high cost, too sensitive, etc.<sup>7-13</sup> Therefore, how to design a suitable solid electrolyte is also the key issue to develop practical solid-state lithium based batteries.

Considering the advanced Li-based batteries and solid state batteries are the two kinds of batteries widely studied and used in the following years, they show the main-stream research direction for the near-future electric vehicles and energy storage systems (Fig. 1). The suitable electrolytes for the two systems create the bottleneck problems for real applications. In this review, we mainly focus on how to design the high voltage electrolytes and solid electrolytes for the advanced Li-based batteries and solid state batteries, respectively. We summarize the recent progress on how to design the functional solvent, additives, ionic liquids and lithium salts and for the high-voltage electrolytes. For the solid electrolytes, we consider three main categories: solid inorganic electrolytes, solid polymer electrolytes and gel polymer electrolytes. Then we discuss the state-of-the-art progress in ionic liquid-based electrolytes, exemplifying how ionic liquids can contribute to high voltage LIBs



*Juntian Fan is currently working as a graduate student (towards a Master's degree) at the Key Laboratory of Green Process and Engineering in the Institute of Process Engineering, Chinese Academy of Sciences. Her current research focuses on the high voltage electrolytes and their applications in the energy storage.*



*Prof. Yoshio Bando received his PhD degree from Osaka University in 1975 and joined the National Institute for Research in Inorganic Materials (at present NIMS) in the same year. From 1979 to 1981 he also worked as a visiting researcher at Arizona State University. Currently, he is a consulting researcher of the International Center for Materials Nanoarchitectonics (MANA) of NIMS. His research concentrates on the synthesis and properties of various inorganic nanostructures and their TEM characterizations.*

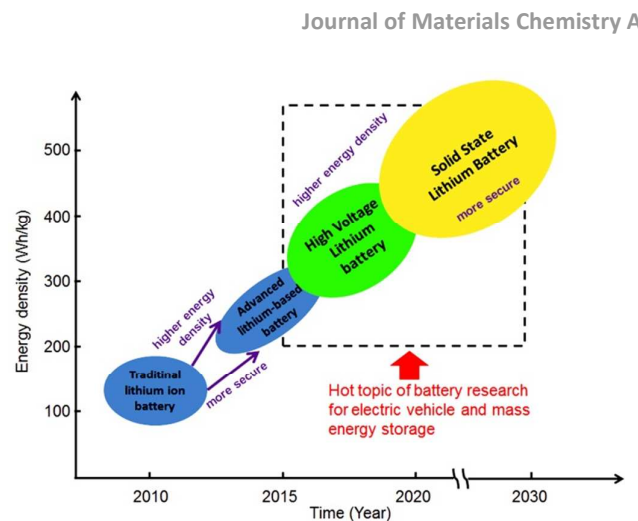


Fig. 1 The roadmap for the Li-based batteries development.

and SSBs systems. Finally, this review ends up with an outlook and proposed directions toward future safe and high performance electrolytes.

## 2. High voltage non-aqueous electrolytes

Lithium-based batteries have already been successfully commercialized in various flexible electronic devices due to their many outstanding properties, including no memory effect, long cycle life, high capacity and energy density.<sup>14-16</sup> To satisfy the increasing demands for the next generation electronic devices like electric vehicles, Lithium-based batteries with better safety, longer cycle life and higher energy densities are urgently required, and as a result they have been achieved intensive progress.<sup>17-24</sup> It is well known that the general method to improve the energy densities of the batteries is exploring the cathode materials having high working voltages or high specific capacities.<sup>25</sup> For example, novel high capacity cathode materials such as  $\text{Li}_2\text{FeSiO}_4$ , and high voltage cathode materials such as  $\text{LiNi}_{0.5}\text{Mn}_{1.5}\text{O}_4$  have been successfully tried.<sup>26</sup> However, the oxidative decomposition of traditional electrolyte has restricted their practical applications. Electrolyte is indispensable in all lithium-based batteries and its basic function is serving as a medium to transport  $\text{Li}^+$  between the cathode and anode, thus ensuring the effectiveness of inner



*Prof. Dmitri Golberg obtained his B.S., M.S. and PhD degrees in Moscow, Russia, and in 1995 joined the National Institute for Materials Science (NIMS), Tsukuba, Japan. From 2017 he became a Professor of the Queensland University of Technology (QUT), Australia. Dmitri's numerous awards include "Tsukuba Prize", "Thomson Reuters Research Front Award" and "Seto Award" from the Microscopy Society of Japan. Over the last consecutive years he was nominated as a Highly-Cited Researcher by "Thomson Reuters" being currently listed among top-200 most-cited world materials scientists on the Web of Science. His research is focused on inorganic nanotubes, nanowires and nanosheets and their in situ TEM studies.*

circuit.<sup>6, 27</sup> The volume between particles of cathode and anode should be filled with the electrolyte, so the electrolyte can set off chemical reaction on both of them. So, the interfaces between the electrolyte and the two electrodes become crucial for the cycling performance of an electrochemical device.<sup>4, 28</sup> To transport  $\text{Li}^+$  between cathode and anode (and being compatible with the electrodes), the electrolytes used nowadays are mainly composed of carbonate solvents, lithium salts and diversified additives. In the first generation of commercial LIBs, the superb physical properties of propylene carbonate (PC), such as low melting point ( $-49.2\text{ }^\circ\text{C}$ ), high boiling point ( $241.7\text{ }^\circ\text{C}$ ) and high flash point ( $132\text{ }^\circ\text{C}$ ), made it excellent low-temperature properties and safe solvent compatible with petroleum coke by "Sony Corporation". Following the energy revolution, the graphite anodes have achieved enormous success owing to their ability to intercalate/de-intercalate  $\text{Li}^+$  reversibly. Further investigations have indicated that ethylene carbonate (EC) is more compatible with graphite anodes because of a peculiar protective SEI layer formed under its sacrificial reduction decomposition.<sup>29-33</sup> However, EC has some undesirable features such as high melting point ( $36\text{ }^\circ\text{C}$ ) and high viscosity (about  $1.9\text{ mPa s}$  at  $25\text{ }^\circ\text{C}$ ), so the electrolyte usually contains EC and other carbonate solvents to satisfy the diverse requirements which can hardly be met by any individual compound.<sup>27</sup> Lithium salt, another essential component in the electrolyte, is the source of lithium ions. Its anion can directly influence the structure and stability of electrolyte.<sup>34-36</sup> There are various Li salts to be used in the battery applications, such as lithium perchlorate ( $\text{LiClO}_4$ ),<sup>36, 37</sup> lithium hexafluoroarsenate ( $\text{LiAsF}_6$ ),<sup>38</sup> lithium hexafluorophosphate ( $\text{LiPF}_6$ ),<sup>39</sup> lithium tetrafluoroborate ( $\text{LiBF}_4$ )<sup>40-42</sup> and lithium bis(trifluoromethanesulfonyl)imide ( $\text{LiTFSI}$ ).<sup>43-46</sup> Each lithium salt mentioned has its advantages and disadvantages. For instance,  $\text{LiAsF}_6$  is deemed to be better than  $\text{LiClO}_4$  as an electrolyte for lithium metal batteries. However, the application of  $\text{LiAsF}_6$  is fairly limited because of its toxicity and high price. As for  $\text{LiBF}_4$ , the low ionic conductivity limits its practical application.  $\text{LiPF}_6$ , without any single outstanding property is eventually commercialized because of its combination of many well-balanced features, such as good ionic conductivity and electrochemical stability.<sup>27</sup> In liquid electrolyte, lithium ions of lithium salts are always solvated by solvents or anions to form solvated ions and then the solvated ions migrate through solvents.<sup>27, 47</sup> The reason of solvation is that positive charge is located on lithium ions while electron charge is mainly located on solvents and solvation can form a coordination between positive charge and electron charge.<sup>48</sup> Donor number is a measure of the ability of a solvent to solvate cations. Specifically, lithium ions will be strongly coordinated by the solvents with high donor number.<sup>49</sup> There are several methods to determine the solvation behavior of lithium ions such as spectroscopic and computation,<sup>50</sup> IR,<sup>51</sup> raman,<sup>52</sup> and NMR.<sup>53</sup> For example, Watanabe used  $^{13}\text{C}$  NMR measurements to investigate the solvation behavior of lithium ions. Solvation of lithium ions causes deshielding  $^{13}\text{C}$  NMR signals of carbon atoms next to oxygen atoms of solvents, which can be detected by the change in chemical shift values. And the chemical shift change of C in  $\text{C}=\text{O}$  shows a large value of  $+1.6\text{ ppm}$  when the concentration of lithium salts  $\text{LiBF}_4$  is  $1\text{ M}$ . This result suggests that most lithium ions are solvated by oxygen atom of polar carbonyl group of ethyl acetate.<sup>48</sup> Furthermore, the solvation

sheath is one of the determining factors to the SEI components on electrodes. And the solvation behavior of lithium ions is different in different solvents. However, the debates about the preferential solvation and coordination numbers have not solved yet.<sup>54</sup> Nowadays, Most of the electrolytes used in lithium-based batteries are made of  $1\text{ M}$  lithium hexafluorophosphate ( $\text{LiPF}_6$ ) dissolved in organic carbonate solvents, especially as the mixture of ethylene carbonate (EC), diethyl carbonate (DEC), dimethyl carbonate (DMC), propylene carbonate (PC) or ethyl methyl carbonate (EMC).<sup>10</sup> However, the high flammability of these solvents can cause a major safety issue. In addition, their high reactivity towards the electrodes above  $50\text{ }^\circ\text{C}$  is an issue that further retards the application of lithium-based batteries in the vehicle industry.

In this review, recent progresses in LIBs are summarized in conformity with the electrolytes evolution, including finding diversified high voltage solvents and additives, superconcentrated salt strategy etc. Although these ways towards real industries still have many problems to overcome, recent progresses in electrolyte technology creat a promising picture of the on-going LIBs revolution.

### 2.1. High voltage solvents

The interfacial stability between the high voltage cathode and the electrolyte is very crucial to the performance of high voltage batteries. As a result, the solvents should fulfill the following requirements: (1) They should have a high solubility and ionizability to lithium salts; (2) They should exhibit high chemical and physical stability, namely, they should have high flash point and low electrode reaction activity; (3) They should possess a wide electrochemical window; (4) They should reveal stable interfacial chemistry, i.e., they should be able to form protective SEI layers on the electrode surfaces; and finally (5) They should be environment friendly. Generally, the traditional electrolytes can meet most of the above requirements. But they are prone to oxidative decomposition under high voltage ( $> 4.3\text{ V}$  vs.  $\text{Li/Li}^+$ ), resulting in the failure of high voltage batteries. Substantial efforts have been made to solve the problem, such as the surface coating of cathodes, high voltage additives and high voltage solvents, etc. Among them, the development of high voltage solvents is very meaningful because high voltage solvents can make the interface stable at high voltage and solve the problem essentially.<sup>55, 56</sup> Herein, we present several high voltage solvents in detail.

#### 2.1.1. Sulfone-based solvents

As we mentioned above, even though widely adopted, the use of  $\text{LiPF}_6$ , together with carbonate molecular solvents, is also restricted in some aspects, e.g. the safety issue and the oxidation decomposition at a high voltage ( $>4.5\text{ V}$  vs.  $\text{Li/Li}^+$ ).<sup>57</sup> Thus it is fairly urgent to explore new solvents with high voltage stability to address these problems.<sup>58, 59</sup> Among various high voltage solvents, sulfone-based electrolytes have frequently been investigated for lithium-based batteries owing to their strong resistance to burning and exceptional electrochemical stability.<sup>60-65</sup> Obviously, the stronger electron-withdrawing sulfonyl group compared to carbonyl in carbonate molecules can lower the energy level of the highest occupied molecular orbital (HOMO), leading to higher stability of an electrolyte/cathode interface. To demonstrate the possibility of the sulfone-based solvents in the lithium based batteries, Abouimrane et al. evaluated  $\text{Li}_4\text{Ti}_5\text{O}_{12}/\text{LiMn}_2\text{O}_4$  and

$\text{Li}_4\text{Ti}_5\text{O}_{12}/\text{LiNi}_{0.5}\text{Mn}_{1.5}\text{O}_4$  in several sulfone-based electrolytes. The results of cyclic voltammetry indicate that tetramethyl sulfone (TMS) and ethyl methyl sulfone (EMS) show the highest anodic potentials, above 5.0 V vs.  $\text{Li}/\text{Li}^+$ . So TMS- and EMS-based electrolytes can be selected for the  $\text{LiNi}_{0.5}\text{Mn}_{1.5}\text{O}_4$ . Cycling tests also validate the possibility of using these two sulfone-based solvents for the high voltage condition.<sup>62</sup> However, the sulfone-based solvents have problems associated with the complexity of the synthesis,<sup>66</sup> the high melting points (usually higher than room temperature),<sup>63</sup> high viscosity<sup>67</sup> and the inability to form a stable and protective film at the graphite-based anodes,<sup>68</sup> these severely restrict their applications. Introducing additives to the electrolytes or mixing the sulfone-based solvents with the high fluidity carbonate solvents can be the most efficient methods to solve these problems. Wu and co-workers introduced p-Toluenesulfonyl isocyanate (PTSI) as film-forming additive into the electrolyte based on tetramethylene sulfone (TMS).<sup>69</sup> The composite electrolyte shows lower melting points, better wettability and superior anodic stability up to 5.0V vs.  $\text{Li}/\text{Li}^+$ , meanwhile, this electrolyte can improve the cycling stability of  $\text{Li}/\text{MCMB}$  owing to the SEI layer formed by PTSI. From another point of view, Xue and co-workers tested a series of sulfone or sulfone-carbonate binary electrolytes with a variety of cathodes and anodes. They found that sulfone-carbonate mixed electrolytes can improve the Coulombic efficiency, capacity retention and safety of the batteries under high voltage

operations owing to the synergic effect of the sulfone and carbonate.<sup>67, 70</sup>

### 2.1.2. Fluorinated solvents

As is known to us, the HOMO and LUMO energies of the fluorinated molecules are lower than their nonfluorinated counterparts due to the strong electro-withdrawing ability of the fluorine which has strong electronegativity.<sup>71, 72</sup> Thus the fluorinated molecules have higher oxidation potentials, while higher reduction potentials. Based on the significant oxidation-tolerant stability and low reduction-tolerant stability, the fluorinated molecules can be applied in the high voltage battery applications and may be used as SEI film-forming additives for the anodes. Zhang et al. validated the superior oxidation stability of fluorinated solvents by using  $\text{LiNi}_{0.5}\text{Mn}_{1.5}\text{O}_4/\text{Li}$  and  $\text{LiNi}_{0.5}\text{Mn}_{1.5}\text{O}_4/\text{Li}_4\text{Ti}_5\text{O}_{12}$  electrochemical couples.<sup>73</sup> Wang and co-workers utilized a new fluorinated 3-(1,1,2,2-tetrafluoroethoxy)-1,1,2,2-tetrafluoropropane (F-EPE) as solvent to improve the cycling stability of a full cell based on  $\text{LiNi}_{1/3}\text{Co}_{1/3}\text{Mn}_{1/3}\text{O}_2/\text{graphite}$  cycled in a voltage range of 3.0-4.5 V (vs.  $\text{Li}/\text{Li}^+$ ).<sup>74</sup> The improved performance can be ascribed to a fact that F-EPE can not only greatly improve the oxidation-tolerant ability of electrolyte, but also take part in the formation of SEI film on the graphite anode, indicating the positive effect of F-EPE on the performances of the full cells. As shown in **Fig. 2a**, there is no obvious distinction in the reduction peaks between the electrolyte with and without F-EPE. This implies that the electrolyte with F-EPE can also be compatible with the anode of LIBs. Meanwhile, the electrolyte without F-EPE is decomposed at about 4.7 V, while the electrolyte with 20 wt % F-EPE is stable until over 5.4 V. Moreover, the floating test shows that the addition of F-EPE can significantly improve the stability of the electrolyte (**Fig. 2e**). The discharge capacity retention of the full cells with 20 wt % F-EPE is obviously increased from 12.3% to 85.0% after 100 cycles compared with the counterpart without F-EPE in the electrolyte (**Fig. 2b**). As shown in **Fig. 2c**, depicting TEM images of  $\text{LiNi}_{1/3}\text{Co}_{1/3}\text{Mn}_{1/3}\text{O}_2$  electrodes at different stages: (a) fresh, (b-d) with 0%, 10% and 20% F-EPE after 100 cycles, the addition of 20% F-EPE makes the SEI layer thinner, which is beneficial for the  $\text{Li}^+$  intercalation into the cathode materials. Luo and co-workers applied F-EPE in a high voltage cathode  $\text{LiNi}_{0.5}\text{Mn}_{1.5}\text{O}_4$ . The physical characterization results showed that there was a thin and uniform layer on the cathode surface with the addition of F-EPE (**Fig. 2d**).<sup>25</sup>

### 2.1.3. Nitriles

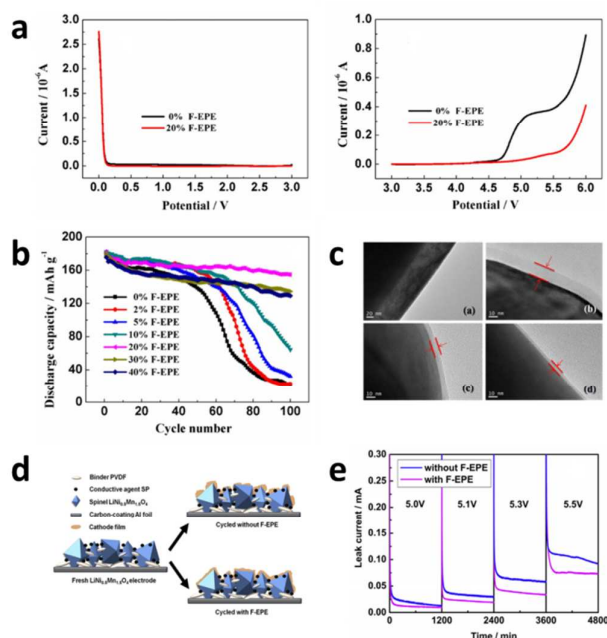


**Fig. 2** (a) The profiles of linear sweep voltammetry at Pt electrode in traditional electrolyte with and without 20% F-EPE. (b) Discharge capacity of the cells based on a  $\text{LiNi}_{1/3}\text{Co}_{1/3}\text{Mn}_{1/3}\text{O}_2/\text{graphite}$  charged to 4.5V. (c) TEM images of  $\text{LiNi}_{1/3}\text{Co}_{1/3}\text{Mn}_{1/3}\text{O}_2$  electrodes after 100 cycles. Reproduced with permission.<sup>74</sup> Copyright 2015, the Electrochemical Society. (d) Schematic illustrations of  $\text{LiNi}_{0.5}\text{Mn}_{1.5}\text{O}_4$  electrodes cycling with and without F-EPE. (e) The floating test of the electrolytes with and without F-EPE. Reproduced with permission.<sup>25</sup> Copyright 2016, Elsevier B.V.

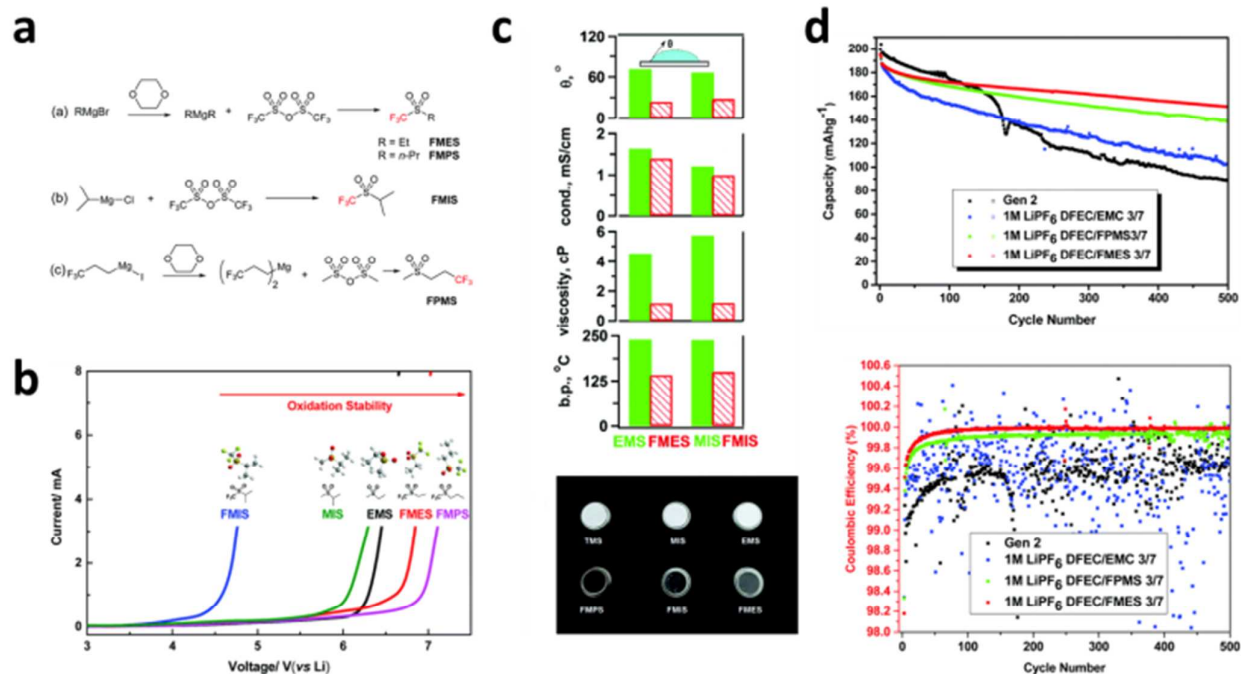


**Fig. 3** (a) Synthetic routes for FMES, FMPS, FMIS and FPMS; (b) Profiles of linear sweep voltammograms of the various sulfones; (c) Comparison of physical properties for EMS and FMES; (d) Electrochemical performance of LiNi<sub>0.5</sub>Mn<sub>0.3</sub>Co<sub>0.2</sub>O<sub>2</sub>/graphite full cells. Reproduced with permission.<sup>80</sup> Copyright 2017, the Royal Society of Chemistry.

In recent years nitrile-based compounds have increasingly gained attention in the battery application because of their excellent physiochemical and thermodynamic stability.<sup>75-77</sup> Particularly,

nitrile-based electrolytes have better thermal stability and high oxidative-tolerant ability. For example, many dinitriles have been reported as additives or cosolvents for high energy LIBs and the

**Table 1** Characteristics of high voltage solvents used for lithium-based batteries

Solvent	Advantages	Limitations
Sulfone-based solvents	higher oxidation potential (>5.5 V), high dielectric constant (>40)	high viscosity, high melting point, cannot reduce the flash point of carbonate solvent when using sulfone-based solvents with carbonate solvents, resulting in unsafety of electrolyte
Fluorinated solvents	higher oxidation potential (>8 V), low melting point, good impregnation of the separator, the ability to form a stable SEI on the graphite-based anode	high viscosity, low ionic conductivity
Nitriles	high flash point, higher oxidation potential (generally >7 V)	Low solubility to lithium salts, low reductive stability and the decomposition products cannot form a stable SEI layer on anodes
Ionic liquids	Negligible vapour pressure, high flash point and inflammable, wide electrochemical stability window (4~6V), outstanding designability characteristic	expensive for large-scale production, high viscosity, poor impregnation of the electrodes and separator

results demonstrate that they can improve the stability of the cathode/electrolyte surface. Nagahama et al. indicated that a sebaconitrile-containing electrolyte (carbonate solvents: sebaconitrile 50:50 vol.%) possessed a good electrochemical stability above 6 V vs.  $\text{Li}^+/\text{Li}$  at a glassy carbon electrode.<sup>77</sup> Additionally, Elise et al. analyzed the influence of sebaconitrile at a lower volume ratio (0-50 vol.%) and also found that adding sebaconitrile allowed reaching a higher oxidation potential limit at the inert electrode glassy carbon.<sup>78</sup> However, dinitriles cannot form an efficient SEI layer on the graphite or lithium metal-based anode surfaces. For example, Xu et al. demonstrated that for  $\text{LiNi}_{0.5}\text{Mn}_{1.5}\text{O}_4/\text{Li}$  cells with 10 wt% glutaronitrile (GLN), in the traditional carbonate-based electrolyte, the discharge capacity retention of the cell after 50 cycles rapidly decreased, reaching to 29.09% after 150 cycles at 1 C rate, owing to incompatibility of GLN with Li anode, especially at a high current density.<sup>79</sup> Fortunately, this incompatibility can be circumvented by adding SEI-forming compounds, such as ethylene carbonate (EC) and other functional additives to protect the interface between the anode and the electrolyte.

#### 2.1.4. Others

Apart from the high voltage solvents mentioned above, there are also many other kinds of solvents which combine various functional groups together developed in recent years. For example, Su et al. synthesized new fluorinated sulfones (**Fig. 3a**) and tested the electrochemical performances in full cells based on  $\text{LiNi}_{0.5}\text{Mn}_{0.3}\text{Co}_{0.2}\text{O}_2/\text{graphite}$  chemistry.<sup>80</sup> The fluorination can lower the HOMO and LUMO energy levels and thus improve the oxidation-tolerant ability of the sulfone compounds (**Fig. 3b**). Additionally, the results suggest that fluorinated sulfones are characterized by low viscosity, great separator wetting and improved safety characteristics (**Fig. 3c**). The cell based on trifluoromethyl ethyl sulfone (FMES)/difluoroethylene carbonate (DFEC) is reported to deliver >80% capacity retention after 500 cycles owing to the excellent oxidative stability of FMES on the charged cathode, whereas the traditional electrolyte-based cell suffers from intensive capacity decay with cycling (**Fig. 3d**).

Herein, we have provided an overview of high voltage solvents for lithium-based batteries. The characteristics of these solvents are summarized in **Table 1** and the ionic liquids will be discussed in detail in **2.3. Ionic liquids**.

## 2.2. Additives

Since the commercialization of LIBs, one of the main issues is the intercalation and de-intercalation of the  $\text{Li}^+$  in the graphite anode. The potential of intercalation and de-intercalation of  $\text{Li}^+$  is far below the stability limits of the most available organic solvents. And, therefore, the interface between the electrolyte and graphite anode is thermodynamically unstable.<sup>6</sup> Thus suppressing the interfacial reaction dynamically by forming an effective solid

electrolyte interface layer (SEI layer) can solve this problem.<sup>81</sup> SEI layer is formed by the reductive decomposition of the electrolyte and it is nonconductive to the electrons, but conductive to  $\text{Li}$  ions.<sup>27</sup> SEI layer is essential to protect the interfacial stability. Without any changes of the main components in electrolytes, additives can improve the battery performance; this way is economical and convenient. Thus intensive efforts have been put to develop the electrolyte additives for better interfacial protection. The energy levels of HOMO and LUMO can be calculated in theory to smartly select additives. Additives used for anode are expected to have the lower unoccupied molecular orbital (LUMO) than traditional organic solvents to initiate the reduction at a higher potential and the products of the reductive decomposition should be stable enough to prevent the continuous decomposition of the electrolytes. For example, Zheng et al. introduced a new solid electrolyte interphase (SEI) forming additive, di(2,2,2-trifluoroethyl) sulfite (DTFES), which can dramatically enhance the performance of LIBs based on the MCMB anode.<sup>82</sup> Despite the organic additives, there are also inorganic additives developing for improving the cycling performance of the batteries. For example, in 1994, Aurbach et al. firstly proposed to use  $\text{CO}_2$  as additive for the graphite anodes.<sup>83</sup> The reason behind is that  $\text{CO}_2$  can improve the performance of graphite electrodes while reacting at a low potential and forming  $\text{Li}_2\text{CO}_3$  on the carbon surface.

Apart from the progress made for the anode additives, there are also many developments for the high voltage cathode additives.<sup>84-86</sup> To pursue high energy density in lithium-based batteries, researchers have made intensive efforts to 5 V-class cathode materials such as  $\text{LiNi}_{0.5}\text{Mn}_{1.5}\text{O}_4$  (4.6 V),<sup>87-90</sup>  $\text{LiNiPO}_4$ <sup>91, 92</sup> and  $\text{LiCoPO}_4$  (4.8 V).<sup>93-95</sup> Among these promising high voltage cathodes,  $\text{LiNi}_{0.5}\text{Mn}_{1.5}\text{O}_4$  has recently attracted prime attention owing to its high working potential of 4.8 V (vs.  $\text{Li}/\text{Li}^+$ ), excellent structural stability and low price. However, the continuous decomposition of  $\text{LiPF}_6$  and conventional organic molecular carbonate-based electrolytes above 4.5 V vs.  $\text{Li}^+/\text{Li}$  severely hampers the application of these materials. In addition to the aforementioned development of new high-voltage solvents, the evolution of the high-voltage additives is also a blooming subject in recent years.<sup>96-99</sup> Many attempts to select additives have been performed via computational approaches on the basis of the HOMO and LUMO energies.<sup>100-103</sup> Higher HOMO energy level means lower oxidation potentials, while lower LUMO energy level means higher reductive potential. So the substances with higher HOMO energy than traditional carbonate electrolytes are prone to oxidize in advance and can serve as high voltage additives in theory.<sup>104</sup> In addition to the oxidative decomposition type additives, there are HF scavenger type additives.<sup>105</sup> Herein we will conclude several kinds of additives which will decompose at a lower potential than the oxidation potential of the electrolyte to form a protective layer on the cathode surface.

#### 2.2.1. Boron-containing additives

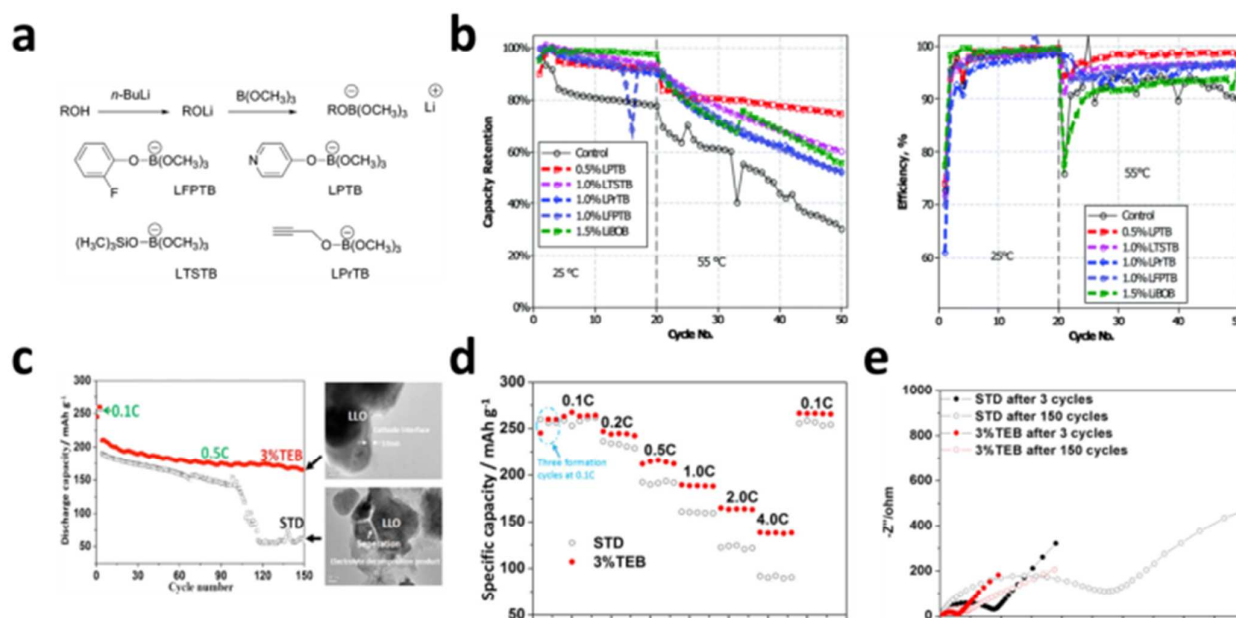


**Fig. 4** (a) The procedure and structure of the boron-based additives; (b) Cycling performance of graphite/  $\text{LiNi}_{0.5}\text{Mn}_{1.5}\text{O}_4$  cells at 25 and 55 °C. Reproduced with permission.<sup>112</sup> Copyright 2016, the Royal Society of Chemistry. (c) Cycling performance of  $\text{Li}[\text{Li}_{0.2}\text{Mn}_{0.54}\text{Ni}_{0.13}\text{Co}_{0.13}]\text{O}_2/\text{Li}$ ; (d) Rate capability of  $\text{Li}[\text{Li}_{0.2}\text{Mn}_{0.54}\text{Ni}_{0.13}\text{Co}_{0.13}]\text{O}_2/\text{Li}$ ; (e) Electrochemical impedance spectra of the  $\text{Li}[\text{Li}_{0.2}\text{Mn}_{0.54}\text{Ni}_{0.13}\text{Co}_{0.13}]\text{O}_2$ . Reproduced with permission.<sup>113</sup> Copyright 2016, American Chemical Society.

Besides the successful application on the graphite anode, boron-containing additives are also investigated as cathode additives.<sup>106–108</sup> Lithium bis(oxalate)borate (LiBOB) is one of the most investigated B-containing additives.<sup>109, 110</sup> Nayak et al. applied LiBOB as additive to high-voltage cathode material  $\text{Li}_{1.2}\text{Ni}_{0.16}\text{Mn}_{0.56}\text{Co}_{0.08}\text{O}_2$  and observed clear enhancement in both capacity retention and lower impedance.<sup>111</sup> Ex situ analysis such as Raman and transmission electron microscopy (TEM) showed that the cathode surface chemistry had been changed and passivated by BOB<sup>-</sup>. More recently, Xu et al. synthesized and reported the behaviors of lithium organoborate additives in the traditional electrolytes.<sup>112</sup> The additives were synthesized via the procedure shown in Fig. 4a. These Li aryl trimethyl borates and Li alkyl trimethyl borates were designed to decompose and then form a borate rich surface with designed function on the  $\text{LiNi}_{0.5}\text{Mn}_{1.5}\text{O}_4$  surface at high voltage and elevated temperature to protect the cathode materials and the electrolytes. The electrochemical results showed that the addition of these borate-based compounds, especially lithium 4-pyridyl trimethyl borate (LPTB) in the traditional electrolytes, could enhance the cycling performance of graphite/ $\text{LiNi}_{0.5}\text{Mn}_{1.5}\text{O}_4$  (Fig. 4b). Meanwhile, Li et al. used triethyl borate (TEB) as high voltage additive to the Li-rich layered oxide,  $\text{Li}[\text{Li}_{0.2}\text{Mn}_{0.54}\text{Ni}_{0.13}\text{Co}_{0.13}]\text{O}_2$ .<sup>113</sup> Electrochemical performance tests showed that when 3% TEB was introduced, the capacity retention had been increased from 30% in the traditional carbonate electrolyte to 79% in the TEB-containing electrolyte owing to the protective SEI layer formed by the preferential oxidation of TEB (Fig. 4c). And the rate capability tests indicated that the addition of TEB significantly had improved the rate property of  $\text{Li}[\text{Li}_{0.2}\text{Mn}_{0.54}\text{Ni}_{0.13}\text{Co}_{0.13}]\text{O}_2/\text{Li}$  (Fig. 4d). From the electrochemical impedance spectroscopy, one can see that the SEI layer formed in the TEB-containing electrolyte can prevent the

electrolyte from continuous oxidative decomposition and reduce the interfacial impedance, whereas the film formed in the standard electrolyte cannot do so (Fig. 4e). These breathtaking findings show that B-based additives are promising for the application of high voltage electrolyte.

### 2.2.2. Benzene derivatives and heterocyclic compounds

Abe et al. found that benzene derivatives and heterocyclic

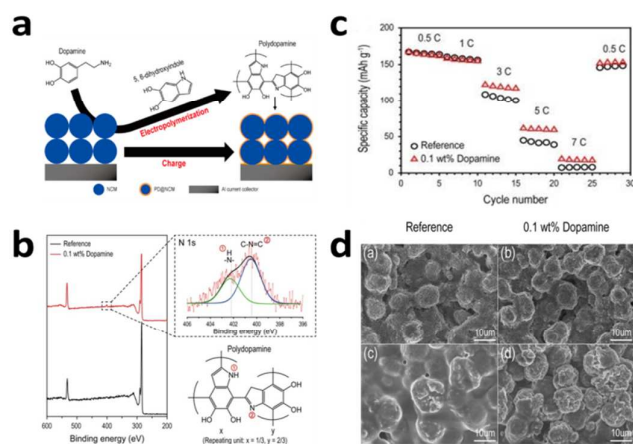


**Fig. 5** (a) Mechanism of the electrochemical polymerization of dopamine. (b) XPS of the cathodes with and without dopamine after precycling, and expected polydopamine chemical structure. (c) The rate performance of the  $\text{LiNi}_{1/3}\text{Co}_{1/3}\text{Mn}_{1/3}\text{O}_2/\text{graphite}$  cells charged to 4.5 V. (d) SEM images of the cathodes with and without dopamine. Reproduced with permission.<sup>115</sup> Copyright 2016, American Chemical Society.

aromatics can serve as electrolyte additives in LiCoO<sub>2</sub>/graphite batteries through improving the cathode cycling stability performance.<sup>114</sup> The monomers usually oxidize at a potential above the 4 V vs. Li/Li<sup>+</sup>. Except for LiCoO<sub>2</sub>, the other cathodes usually require charging to 4.0 V or higher, which is ideal for the polymerization of heterocyclic aromatic monomers. So, polymer film formation is always proceeded successfully. For example, Lee and co-workers introduced a new benzene-based additive, dopamine, into the high voltage LIBs. Dopamine can be electrochemically oxidized to polydopamine on cathode surface to protect both the electrode and electrolyte from destruction (Fig. 5a).<sup>115</sup> The results from XPS that new peak of N 1s indicated that dopamine had already been decomposed after pre-cycling (Fig. 5b). And the results from SEM showed that the cathode material cycled in the blank electrolyte was no longer porous. In addition, the counterpart cycled in the dopamine-containing electrolyte was similar to its original morphology (Fig. 5d). All these findings implied that the SEI layer formed by dopamine could protect the cathode surface. Therefore, the cycling and rate performance was significantly improved by addition of dopamine (Fig. 5c). Abouimrane et al. applied 3-hexylthiophene (3HT) as additive to high capacity Li<sub>1.2</sub>Ni<sub>0.15</sub>Co<sub>0.1</sub>Mn<sub>0.55</sub>O<sub>2</sub> and high voltage LiNi<sub>0.5</sub>Mn<sub>1.5</sub>O<sub>4</sub> cathodes and observed significant enhancement in the discharge capacity retention owing to the ability of 3HT to form a conductive, conjugated polymer film on the cathode surface.<sup>116</sup> And Chen et al. used N-methylpyrrole (MPL) as the additive to high voltage cathode.<sup>117</sup> By adding 0.3 wt % MPL into electrolyte, the discharge

capacity retention of Li/LiNi<sub>0.5</sub>Mn<sub>1.5</sub>O<sub>4</sub> cell after 200 cycles is increased from 83.2% to 89.5% at room temperature and from 59.1% to 87.4% at elevated temperature (55 °C). The reason why the cycling performance had been enhanced is electrochemical polymerization of MPL during the initial charge process and consequent formation of a thin and protective film on the LiNi<sub>0.5</sub>Mn<sub>1.5</sub>O<sub>4</sub> surface.

### 2.2.3. Ethers

According to the molecular orbital energy calculation, the HOMO level of ethers is relatively high among a variety of aprotic solvents. As a result, they are usually susceptible to oxidation decomposition and have been considered to high voltage additives.<sup>16</sup> Extensive efforts have been dedicated to confirm this point. For example, Wang and co-workers demonstrated that for LiNi<sub>1/3</sub>Co<sub>1/3</sub>Mn<sub>1/3</sub>O<sub>2</sub>/Graphite pouch cells with 0.5 wt% 3,3'-(Ethyleneedioxy)dipropionitrile (EDPN) in the traditional carbonate-based electrolyte, the discharge capacity retention of the cell was improved from 32.5% to 83.9% after 100 cycles at 1C rate in the range 3.0-4.5 V.<sup>76</sup> The reason for the improved electrochemical performance is the stable protective interphase film formed on the LiNi<sub>1/3</sub>Co<sub>1/3</sub>Mn<sub>1/3</sub>O<sub>2</sub> electrode surface due to the sacrificial oxidative decomposition of EDPN in the electrolyte.

### 2.2.4. Others

Apart from the additives aforementioned, there have been many other additives for high voltage electrolytes, such as phosphorus-based additives, some special functional carbonate additives and so on. For example, the HOMO energy of N-(triphenylphosphoranylidene) aniline (TPPA) is higher than those of conventional electrolyte solvents. And TPPA contains the electron-donating benzene and aniline derivatives, thus TPPA is speculated to be a proper candidate as a high voltage additive in the electrolyte. To conform this, Lee et al applied TPPA to the flagship cathode lithium cobalt oxide (LiCoO<sub>2</sub>) and reported that capacity retention after 200 cycles increased by 10%, benefiting from the surface films that TPPA formed on the cathode surface.<sup>118</sup> XPS data validated that a modified film was formed at the cathode surface and prevented the solvent from decomposition under high voltage. Wang et al. demonstrated that the addition of 0.5% fumaronitrile (FN) into the blank electrolyte (1.0 mol L<sup>-1</sup> LiPF<sub>6</sub> in EC/EMC/DEC (3:5:2 by weight) can maintain the structural integrity of lithium cobalt oxide (LiCoO<sub>2</sub>) through a protective cathode interphase film formed by the sacrificial oxidative decomposition when it was charged to 4.5 V (vs. Li/Li<sup>+</sup>).<sup>75</sup> Zhang et al. used tris(trimethylsilyl)phosphate (TMSP) as an additive to form a solid electrolyte interface on lithium-rich cathode material Li[Li<sub>0.2</sub>Ni<sub>0.13</sub>Mn<sub>0.54</sub>Co<sub>0.13</sub>]O<sub>2</sub> to improve the electrochemical performances.<sup>119</sup> Furthermore, Zheng et al. demonstrated that adding 0.1 wt% di(methylsulfonyl) methane (DMSM) into the blank electrolyte can significantly improve the discharge capacity retention of the LiNi<sub>1/3</sub>Co<sub>1/3</sub>Mn<sub>1/3</sub>O<sub>2</sub>/graphite full cell cycled in a voltage range of 3.0-4.6V from 61.0% to 80.1% after 100 cycles owing to the protective film formed by the sacrificial oxidation of the DMSM.<sup>120</sup>

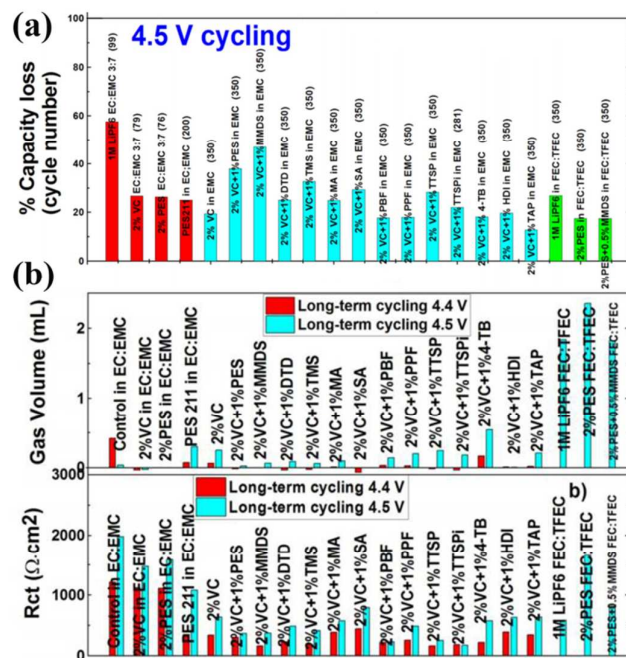


**Fig. 6** (a) % capacity loss at cycle 350 for NMC442/graphite pouch cells containing the different electrolyte formulations cycled to 4.5 V. (b) Summary of gas volume  $R_{ct}$  measured after long-term constant current-constant voltage cycling at 40 °C for cells cycled to 4.4 V (red bars) and 4.5 V (cyan bars) for NMC442/graphite cells with different electrolytes. Reproduced with permission<sup>123</sup>. Copyright 2017, Electrochemical Society.

In the end, as mentioned above, the electrolyte additive is one of the most effective and economical ways to enhance electrochemical performance of lithium-based batteries. Dahn et al. proposed three key parameters to evaluate the impact of an additive on the performance of lithium-based batteries: (1) coulombic efficiencies; (2) discharge capacity retention at both electrodes; (3) cell impedance. A wide range of additives have been available nowadays. However, there are very limit research that have been done on the performance comparison of them. Some additives like LiBOB and LiDFOB have positive effect not only on the cathode but also on the anode. Some additives like phosphazene can not only sever as high voltage additive but also can improve the thermal stability of electrolyte. But there are additives that can significantly decrease the ionic conductivity of the electrolyte. So the work to compare different additives must have been done to evaluate the effectiveness of additives. Xia and co-workers have done a series of research work to compare different additives.<sup>65, 121, 122</sup> For example, as shown in Fig. 6, Xia et al. studied some electrolyte additives such as prop-1-ene,1,3-sultone (PES), methylene methanedisulfonate (MMDS), propanediol cyclic sulfate (trimethylene sulfate-TMS), 1,3,2-dioxathiolan-2,2-oxide (ethylene sulfate -DTD), tris(trimethylsilyl) phosphite (TTSPi).etc in the NMC442/graphite pouch cells.<sup>123</sup> Different additives with different solvents have different influence on the performance of NMC442/graphite. And the capacity retention versus cycle number could be a particular illumination to the researchers when they choose and compare the additives.

### 2.3. Ionic liquids

Ionic liquids, namely room temperature molten salts, are characterized by wide electrochemical window, low volatility and non-flammability, which make them attractive alternatives of traditional carbonate solvents.<sup>61, 124</sup> Recently the scientific community has been driven to apply the LIBs in electric and hybrid vehicle industry, so the concern on battery safety has particularly been raised.<sup>125, 126</sup> From this perspective, as the conventional carbonate electrolyte is flammable, ionic liquids which are non-flammable, have been considered as the safest electrolytes and have been extensively investigated in recent years.<sup>127-129</sup> These ionic liquids are mainly employed with respect to three aspects LIBs: as the solvents or co-solvents in an electrolyte, as additives, and as components for a polymer electrolyte which will be discussed further. Ionic liquids possess great electrochemical anodic stability, usually 5-5.5 V vs. Li/Li<sup>+</sup>.<sup>124, 130</sup> For example, Santosh and co-workers synthesized two novel ionic liquids made of functional imidazolium cations in amalgamation with bis(trifluoromethanesulfonyl)imide (TFSI) anion and studied their physicochemical and electrochemical stability.<sup>131</sup> 1 mol kg<sup>-1</sup> LiTFSI in the ether-ether ionic liquid possessed a wide electrochemical window of 5.9 V and good conductivity of 2.2 mS cm<sup>-1</sup>. We assume that ILs are suitable for the high voltage conditions, but the main challenge for the application of ionic liquids is the unstable electrolyte/anode interface. As for usual ionic liquids, for example, ionic liquids based on imidazoliums, cations always intercalate into the graphite layers and decompose before the lithium intercalation, resulting in the irreversible capacity of the batteries. The

introduction of new chemical structure, such as pyrrolidinium and piperidinium, has advanced the development of ionic liquids in LIBs because they are stable to lithium.<sup>132</sup> Owing to their wide electrochemical windows, many researchers have performed detailed investigations to verify a possibility of using these in high voltage rechargeable LIBs. However, one of the main drawbacks of pure ILs used as solvents for electrolyte is their high viscosity, which implies a poor electrochemical capability. From this perspective, ionic liquids used as electrolyte additives may be the optimal method to enhance the cell performance.

#### 2.3.1. Imidazoliums

Among ionic liquids, imidazolium-based ILs are characterized by a relative ease in synthesis, rather cheap price, low viscosity and decent electrical conductivity, thus they have intensively been investigated.<sup>10, 133-135</sup> Ethylmethyl imidazolium bis(trifluoromethanesulfonyl-imide) (EMITFSI) is the most popular agent owing to its desirable features such as low melting point and high thermal stability. However, this class of ionic liquid has its own drawbacks. Because of the three acidic protons of EMI<sup>+</sup>, especially the protons of C(2) which has strong reducibility, this kind of system is prone to reduce at about 1.0 vs. Li/Li<sup>+</sup>, which is higher than the potential of Li deposition.<sup>136, 137</sup> As a result, this kind of ionic liquid was initially excluded from the applications in LIBs. When this kind of ionic liquid is used with the graphite anode, the reduction products cannot form a stable and protective film on the graphite surface to retard successive reduction decomposition of the electrolyte. Extensive investigations have been conducted to improve the reduction-tolerant ability of imidazolium-based ILs. Searching for new anions and substituent groups, mixing with traditional organic molecular carbonate solvents are the two

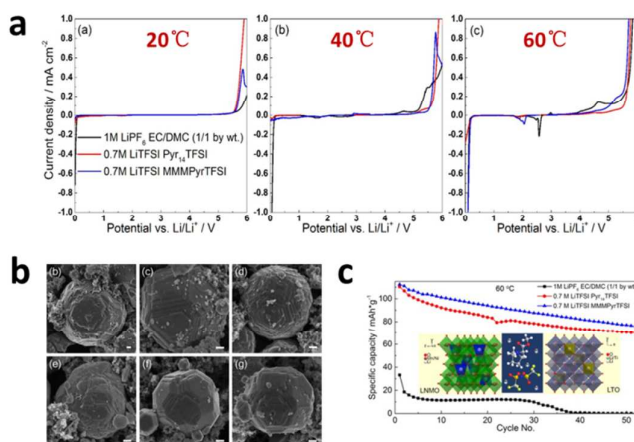


**Fig. 7** (a) Linear sweep voltammetry profiles of the investigated electrolytes at different temperatures. (b) SEM images of LNMO electrode after cycling in different electrolyte and at different temperatures: b-d is at 40 °C and e-g is at 60 °C; b,e are in traditional electrolyte; c,f are in PYR<sub>14</sub>TFSI-based electrolyte; d,g are in MMMPyrTFSI-based electrolyte. (c) Discharge capacity of LNMO/LTO full cells. Reproduced with permission.<sup>125</sup> Copyright 2016, American Chemical Society.

## REVIEW

## Journal of Materials Chemistry A

possible solutions proposed by recent works. Masashi and co-workers firstly used a pure ionic liquid to achieve the reversible lithium intercalation/de-intercalation at the graphitized negative electrode without any additives.<sup>138</sup> An exchange from TFSI to FSI, as a counter anion, cosignificantly improve the interfacial stability. The reason is that SEI layer (formed in the electrolyte containing FSI) is stable. The second method is replacing the protons of C (2) by other groups, like alkyl groups.<sup>126, 139</sup> This method can improve the electrochemical stability of imidazolium ring, and thereby they can become possible electrolytes for LIBs. Seki et al. applied a modified imidazolium cation-based ionic liquid as an electrolyte solvent for half cells based on  $\text{LiCoO}_2/\text{Li}$ .<sup>140</sup> The cells achieved a stable charge-discharge running of more than 100 cycles at a current density of 1/8 C. Another method to apply this kind of ionic liquid into the practical batteries is the usage of co-solvents, such as VC.

### 2.3.2. Pyrrolidiniums

In addition to imidazolium-based ionic liquids, pyrrolidiniums-based and piperidinium-based ionic liquids are also reported.<sup>141-143</sup> According to extensive investigations on the properties of pyrrolidiniums-based ionic liquids, it can be concluded that a wide electrochemical window, rather high conductivity ( $>1 \text{ mS cm}^{-1}$ ), high  $\text{Li}^+$ -transference number, safety, and low viscosity are available from this kind of ionic liquid.<sup>144</sup> To demonstrate its high voltage and high temperature-tolerant ability, Cao and co-workers conducted a contrastive analysis between traditional electrolyte and two pyrrolidiniums-based ILs (Figure 7).<sup>125</sup> The results from linear sweep voltammetry at different temperatures indicated that the electrochemical window had been dependent on the temperature and when the temperature was increased, the electrochemical window became narrow. Fortunately, the ILs-based electrolytes have a wider electrochemical window than the traditional electrolyte at elevated temperatures (Fig. 7a). SEM images showed a clean cathode surface in the ILs-based electrolytes, whereas rough cathode surface in the traditional electrolyte (Fig. 7b). This implies less decomposition in the ILs-based electrolytes. And the constant current charge/discharge cycling at elevated temperature demonstrated the superior cycling properties of ILs-based electrolytes (Fig. 7c). Agostini et al used  $\text{LiPF}_6$  dissolved in a mixture of carbonate solvents and N-*n*-butyl-N-methylpyrrolidinium hexafluorophosphate ( $\text{PYR}_{14}\text{PF}_6$ ) ionic liquid as an electrolyte in the full cells based on  $\text{LiNi}_{0.5}\text{Mn}_{1.5}\text{O}_4/\text{TiO}_2$ .<sup>145</sup> Compared to commercial electrolytes, this new configuration for high voltage electrolyte was able to provide an intrinsically higher safety and prolonged cycling life. It was generally recognized that pyrrolidinium-based ionic liquids can provide superior cathodic-tolerant ability than imidazolium-based ionic liquids. Thus pyrrolidinium-based ionic liquids can serve as electrolytes with a Li anode, whereas imidazolium-based ionic liquids cannot. Anand and co-workers applied 1-propyl-1-methyl-pyrrolidinium bis(fluorosulfonyl)imide (C3mpyrFSI) as electrolyte solvent to investigate the morphological changes of Li surfaces.<sup>146, 147</sup> The results indicates that electrolyte based on the C3mpyrFSI (containing either LiFSI or LiTFSI) is compatible with Li metal electrodes, as was evident by the

reversible deposition and stripping of lithium. Yang et al. reported a mixture electrolyte based on N-propyl-N-methylpyrrolidiniumbis (trifluoromethanesulfonyl) imide ( $\text{PYR}_{13}\text{TFSI}$ ), EC/DMC-5% VC, and lithium bis (trifluoromethanesulfonyl) imide (LiTFSI). The results indicated that the addition of 65%  $\text{PYR}_{13}\text{TFSI}$  by volume led to the best overall properties, such as high safety, lower viscosities of about 30 mPa s at room temperature, a wide electrochemical window of 4.8 V, and thus high reversible discharge capacities of  $\text{LiFePO}_4/\text{Li}$  cells.<sup>148</sup>

### 2.3.3. Piperidiniums

Like pyrrolidinium-based ionic liquids, piperidinium-based ionic liquids are also promising candidates for the electrolyte application owing to their excellent physicochemical properties, such as their high voltage stability (up to 5.0 V), high thermal-tolerant stability (up to 385 °C), and commercially acceptable  $\text{Li}^+$  conductivity at room temperature ( $1.4 \text{ mS cm}^{-1}$ ).<sup>149-155</sup> Madhulata et al. studied the molecular structure in details by infrared (IR), Raman spectroscopies and density functional theory (DFT). They concluded that the H-bonding interaction along with constituents largely controlled the physical state of the salt.<sup>156</sup> Dong and co-workers synthesized N-methylpiperidinium-N-acetate bis(trifluoromethyl-sulfonyl)imide ([MMEPip][TFSI]), a piperidinium-based ionic liquid and applied it as an additive to the blank electrolyte (LiTFSI (0.6 mol  $\text{kg}^{-1}$ ) into the mixture of ethylene carbonate and diethyl carbonate) in the  $\text{LiFePO}_4$  half cells to improve the cycling stability.<sup>157</sup> Andrzej and co-workers demonstrated that with 10% VC the cells based on  $\text{LiMn}_2\text{O}_4$  in the piperidinium-based electrolyte may be cycled with small capacity decay and high Coulombic efficiency.<sup>158</sup>

### 2.3.4. Others

Apart from three main kinds of ionic liquids, other ionic liquids can also be applied for LIBs. For example, Bucher et al. synthesized and characterized the properties of N,N,N',N'-tetramethyl-N'',N''-pentamethyleneguanidinium bis(trifluoromethyl-sulfonyl)imide (PipGuan-TFSI) which combined the advantages of guanidinium and piperidinium structural elements.<sup>159</sup> Navarra et al. prepared and characterized two different ionic liquids based on morpholinium and piperidinium cations and TFSI anions.<sup>160</sup> Substitution of a  $\text{CH}_2$  group in the cation ring with an ether bond in the side chain could restrain the crystallization of the ILs and consequently enhanced ion transport properties.<sup>161, 162</sup>

Although ionic liquids possess intensive desirable properties mentioned above, they have not yet been commercialized owing to their high viscosities, poor wettability with separator and electrodes, and co-intercalation into graphitized carbon-based anode. Recent literatures have proposed some possible methods to solve these problems. However, challenges still remain, such as exploring new kinds of separators which can be wetted well by the ionic liquids.

## 2.4. Superconcentrated electrolytes

The traditional electrolyte in LIBs may have infinite variations of aprotic solvents, lithium salts and their concentration.<sup>16</sup> However, restrictions remain when choosing the solvents, lithium salts and their concentration. In fact, before the group of Dahn<sup>163-167</sup> found that removing ethylene carbonate (EC) from the traditional electrolyte and adding additives could create better cells than the traditional electrolyte and Yamada et al.<sup>168</sup> found that reversible lithium intercalation reaction into graphite without EC could happen in superconcentrated electrolytes (The reason will be discussed later in Section 2.4.2.), EC is almost the essential component because of its SEI layer formation ability. In addition, because other lithium salts, such as LiTFSI, LiFSI, LiBOB, and LiDFOB, have their own limitations, LiPF<sub>6</sub> has dominated the market owing to its superb and comprehensive properties. The concentration of the electrolyte is optimized at around 1 M to obtain the maximum ionic conductivity. However, the traditional electrolytes suffer from severe oxidation decomposition under high voltage. This leads to the eventual failure of batteries. Thus, designing a superior electrolyte is imperative to meet the requirements of high voltage and high energy density batteries. Considerable efforts have been dedicated to invent and develop new classes of solvents, additives, and solid state electrolytes.<sup>6</sup> However, intrinsic disadvantages remain in these new electrolytes. For example, solid state electrolytes are always characterized by low conductivities. New high voltage solvents are always along with high viscosities and incompatibility with the graphite anode. Thus, optimizing physical and chemical properties of traditional electrolytes is necessary. Herein, we intend to popularize a new strategy named superconcentrated salt strategy. This strategy has recently been developed by the University of Tokyo.<sup>16, 168-172</sup> Superconcentrated salt strategy is to use more than 1 M lithium salt to obtain unusual properties of the electrolytes, such as high reductive and oxidative stability, Al anti-corrosion, high thermal stability, fast electrode reactions and low volatility with some compromise in ionic conductivity and viscosity. So the superconcentrated salt strategy is very promising. To better understand the correlation between the structure of superconcentrated electrolyte, the ionic conductivity and the concentration of lithium salts within a wide concentration

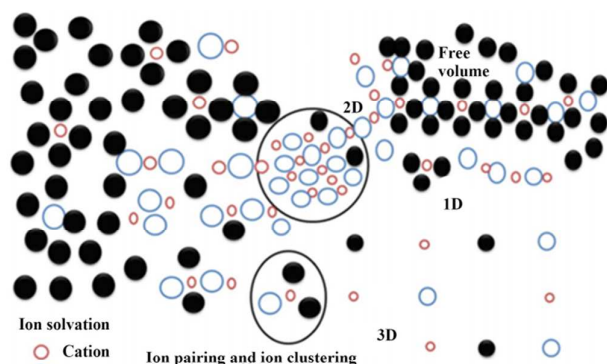


**Fig. 8** A model for change in solution structure and mechanism from vehicular to Grotthuss-type as a function of concentration. Reproduced with permission.<sup>173</sup> Copyright 2017, The Electrochemical Society.

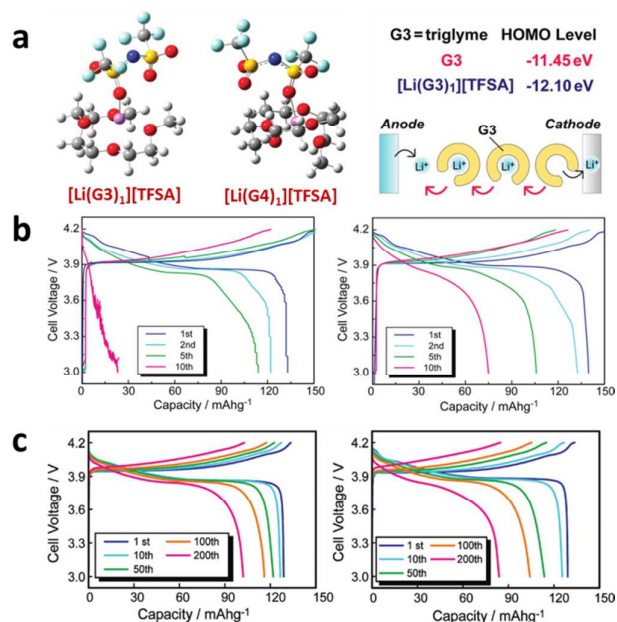


**Fig. 9** (a) Optimized structures of [Li(G3 or G4)<sub>1</sub>][TFSA]; (b) Charge and discharge profiles of LiCoO<sub>2</sub>/Li based on [Li(G3)<sub>4</sub>][TFSA] (left) and [Li(G4)<sub>4</sub>][TFSA] (right); (c) Charge and discharge profiles of LiCoO<sub>2</sub>/Li based on [Li(G3)<sub>1</sub>][TFSA] (left) and [Li(G4)<sub>1</sub>][TFSA] (right). Reproduced with permission.<sup>174</sup> Copyright 2011, American Chemical Society.

range, Yim et al.<sup>173</sup> proposes a semi-empirical equation based on free volume theory,

$$K = AC \exp\left[-\frac{\gamma V_0}{V_f} C\right]$$

where  $V_0$  and  $V_f$  are the occupied and unoccupied free volume;  $C$  is molar concentration;  $\gamma$  is a correction factor;  $A$  is a constant. It is a common feature in liquid electrolyte that with increase of the concentration of lithium salts, the ionic conductivity increases first and then decreases, which means the presence of the concentration of highest conductivity ( $C_{max}$ ). Yim et al. proposes that the variation of ionic conductivity can not be simply attributed to the polyloid ions in superconcentrated electrolyte. As shown in Fig. 8, there is less free solvents in the electrolyte with the increase of the concentration and the most-stable solvated ions, ion pairs and ionic clusters associate into multi-dimensional networks. And the mechanisms of conduction in superconcentrated electrolyte contains ion hopping along networks. All the exploration of electrolyte solution structures can lay a solid foundation for the better understanding of the superior properties of superconcentrated electrolyte. Subsequently the details of superior properties of superconcentrated electrolyte is carried on the elaboration.

#### 2.4.1. High oxidative stability

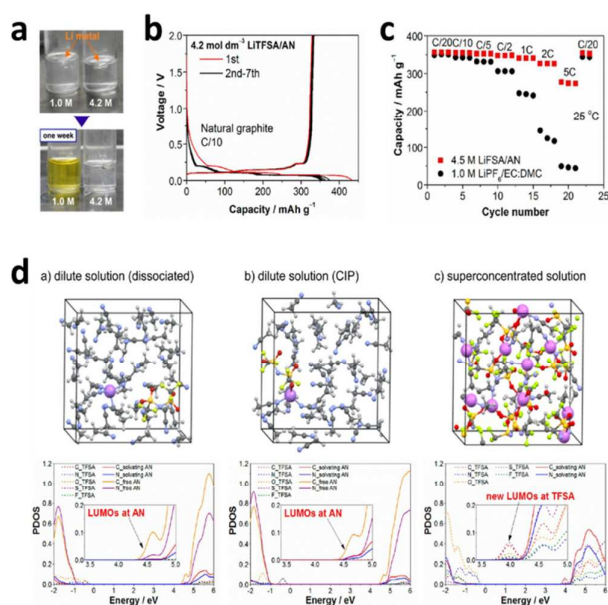


**Fig. 10** (a) Reactivity of lithium metal and LiTFSA/AN solutions; (b) Charge-discharge profiles of natural graphite/lithium metal cell based on  $4.2 \text{ mol dm}^{-3}$  LiTFSA/AN electrolyte; (c) Rate capacity test of natural graphite/lithium metal cell based on traditional electrolyte and superconcentrated electrolyte; (d) Supercells used and projected density of states (PDOS) obtained with quantum mechanical DFT-MD simulations. Reproduced with permission.<sup>171</sup> Copyright 2014, American Chemical Society.

As we mentioned above, the ethers are susceptible to oxidation decomposition and are considered to be used as high voltage additives owing to their high HOMO levels. Despite their inferior oxidative-tolerant ability at  $>4.0 \text{ V vs. Li/Li}^+$ , a pronounced advantage of ethers is their significant solvation ability for salt dissociation. To take full advantage of their solvation ability, Kazuki et al. used the superconcentrated salt strategy in order to improve the oxidative stability as solvents in LIBs.<sup>174</sup> The results of linear sweep voltammograms showed that oxidative stability of Li salt-glyme equimolar solutions  $[\text{Li}(\text{G}3 \text{ or } \text{G}4)_1][\text{TFSa}]$  ( $[\text{Li}(\text{glyme})_x][\text{TFSa}]$ , where the molar ratio of glyme:Li[TFSa]= $x$ :1), was enhanced to 4.5 V vs.  $\text{Li}^+/\text{Li}$ . Current constant charge/discharge curves revealed that the cells based on  $[\text{Li}(\text{G}3 \text{ or } \text{G}4)_4][\text{TFSa}]$  failed rapidly (**Fig. 9b**). As a comparison, the cells based on  $[\text{Li}(\text{G}3 \text{ or } \text{G}4)_1][\text{TFSa}]$  both had reversible charge and discharge behaviors cycled from 3.0 to 4.2 V. The initial discharge capacity of the  $\text{LiCoO}_2$  cathode was  $130 \text{ mA h g}^{-1}$  in both electrolytes and the Coulombic efficiencies were higher than 95% at the first cycle. The discharge capacity after 200 cycles was 100 and  $85 \text{ mA h g}^{-1}$ , respectively, for  $[\text{Li}(\text{G}3)_1][\text{TFSa}]$  and  $[\text{Li}(\text{G}4)_1][\text{TFSa}]$  (**Fig. 9c**). Through the superconcentrated salt strategy, ether was the firstly used as solvent for the LIBs thanks to the improved oxidative stability. From this view, superconcentrated salt strategy proposes a feasible method to improve the oxidative-tolerant ability of solvents.

#### 2.4.2. High reductive stability

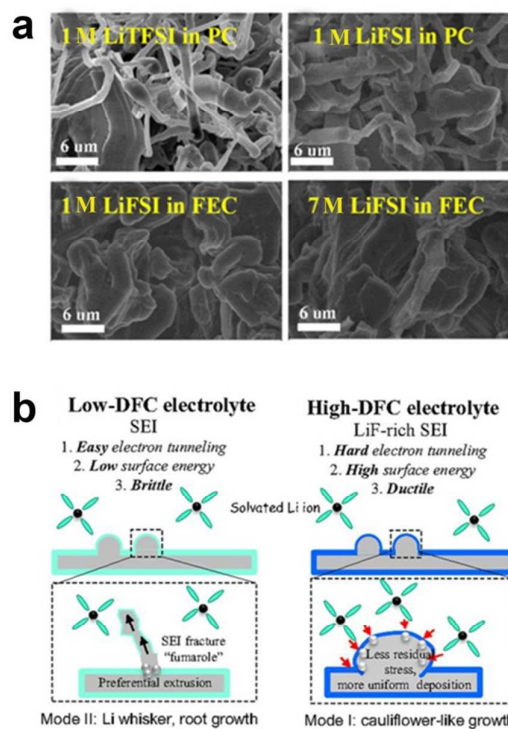


**Fig. 11** (a) Morphologies of Li deposition on Cu foil in different electrolytes; (b) Principle scheme of Li growth mechanism in different electrolytes. Reproduced with permission.<sup>178</sup> Copyright 2018, PNAS.

Recently, aprotic solvents have been successfully used to achieve the reversible intercalation/de-intercalation on the graphite-based anode without EC at a high concentration.<sup>16, 168, 171, 172, 175</sup> For example, Yamada et al. found that acetonitrile (AN), one of the most oxidation-tolerant organic molecular solvents with high dielectric constant (to easily dissolve lithium salts) but poor reductive stability (ease in reaction with metal lithium), can serve as electrolyte when the concentration of lithium salt LiTFSI is above 4.2 M because of the improved reductive stability.<sup>171</sup> As shown in **Fig. 10a**, 1 M LiTFSI in AN easily dissolve the metal lithium, whereas the 4.2 M counterpart does not. This result indicates that the superconcentrated electrolyte can overcome the inherent poor stability towards reduction of AN solvent. To confirm the practical validity of this superconcentrated electrolyte, the electrochemical tests of half cells, with the natural graphite and metal lithium as electrodes, have been conducted and the results are shown in **Fig. 10b** and **Fig. 10c**. One can clearly observe the reversible lithium intercalation/de-intercalation reaction at the natural graphite electrode. Moreover, the half cell in the superconcentrated electrolyte displays a superior rate capacity than that in the traditional electrolyte. The successful application of superconcentrated AN electrolyte validates that superconcentrated salt strategy is a powerful and feasible method to expand the variety of electrolyte other than EC. To explore the mechanism of enhanced reductive stability in a superconcentrated solution, the solution structure was investigated by Roman tests. And the results showed that there is no free solvent in the superconcentrated

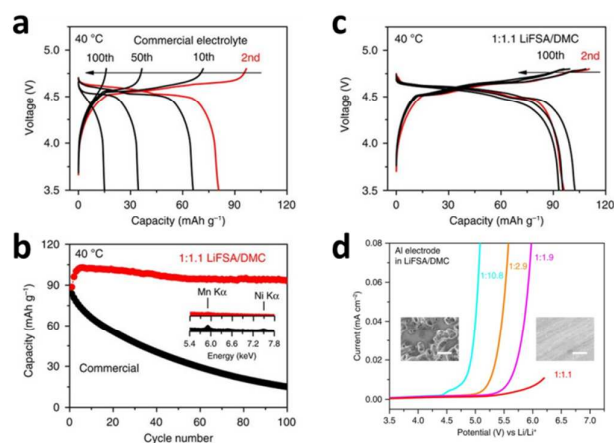


**Fig. 12** (a,b,c) Performance of a high-voltage  $\text{LiNi}_{0.5}\text{Mn}_{1.5}\text{O}_4$ /natural graphite battery; (d) The profiles of LSV of an aluminium electrode in various concentrations of LiFSA/DMC electrolytes. Reproduced with permission.<sup>169</sup> Copyright 2016, Nature Publishing Group.

electrolyte. Thus the reductive stability was significantly improved. To further confirm this consideration, quantum mechanical DFT-MD simulations were conducted and the results are shown in **Fig. 10d**. It can be seen that the energy levels at the lowest energy-level edge of the conduction band of the AN molecular in the dilute electrolyte are lower than those of the TFSI anion. This result is consistent with the experiments confirming that AN is easily reduced. And in the superconcentrated electrolyte, new energy levels of TFSI anion appear and become lower than those of AN molecules. And this is because the lone pair of oxygen of TFSI anion is biased towards the lithium ion.<sup>176</sup> In addition, the components of TFSI anion-derived passivation films have less solubility into the electrolyte in the superconcentrated electrolyte. Thus the reductive-tolerant ability of AN in superconcentrated condition has been improved.

Qian et al applied the superconcentrated electrolyte into the anode-free rechargeable LIBs and found that the superconcentrated electrolyte can improve the reversibility of the Li plating/stripping process. Thus the Coulombic efficiency and cycling life of the battery were improved.<sup>177</sup>

More recently, Suo et al.<sup>178</sup> found that 7 M LiFSI/FEC can not only has a wide stability window but also have the ability to make lithium metal anode more stable and reversible. Firstly, the superconcentration strategy makes the electron ion pairs (C=O in FEC and O=S in FSI<sup>-</sup>) more stable because of its extensive  $\text{Li}^+$  coordination, thus leading to superior oxidation stability. Then, XPS reveals that the SEI layer formed on the lithium metal anode contains mainly LiF and Suo et al proposes that the reduction path of FEC is:  $\text{FEC} + \text{Li}^+ + \text{e}^- \rightarrow \text{poly(VC)} + \text{LiF} + \text{Li}_2\text{CO}_3$ . It can be seen from **Fig. 11a** that the growth of Li in 7 M LiFSI/FEC is not whisker but big grain size ( $>20 \mu\text{m}$ ). In addition, the whisker is leading loss of electrical connection to its rest (dead lithium) and its fracture (lithium flotsam), thus resulting in irreversibility of lithium metal anode. As a contrast, the SEI layer formed in 7 M LiFSI/FEC is ductile because LiF has higher surface energy and small lattice constant, thus leading to high reversibility of lithium metal anode (Principle

scheme of Li growth mechanism is shown in **Fig. 11b**). Charge/discharge tests show that LNMO/Li full cell cycled in 7 M LiFSI/FEC exhibits a capacity retention of 78% after 130 cycles at a current density of 0.5 mA while LNMO/Li full cell cycled in 1 M LiPF<sub>6</sub> in DEC/DMC/EC fails after around 20 cycles.

### 2.4.3. Al-anti corrosion

A LiPF<sub>6</sub> salt is chemically unstable and will form hydrofluoric acid (HF) which accelerates transition metal dissolution of the electrode materials, but, fortunately, HF can react with the Al current collector to form an insoluble layer,  $\text{AlF}_3$ , that can beneficially protect collector from oxidative dissolution. Replacing LiPF<sub>6</sub> with more stable lithium salts may diminish transition metal dissolution, but, unfortunately, encounters severe oxidation of collector. In order to replace the LiPF<sub>6</sub> by more stable lithium salts, the corrosion of Al current collector must be mitigated. The superconcentrated salt strategy can perfectly resolve these problems. Wang and co-workers found that a superconcentrated 1:1.1 LiFSA/DMC electrolytes can suppress the dissolution of metal ions from cathode materials and protect the Al current collector.<sup>169</sup> The linear sweep voltammetry (LSV) of an Al electrode, as indicated in **Fig. 12d**, shows that with the concentration of lithium salts increasing, the potential of anodic dissolution of the aluminium current collector is also increased and when the concentration is 1:1.1 LiFSA/DMC, the oxidation potential becomes up to 6V vs.  $\text{Li/Li}^+$ . The performance tests show that the discharge capacity retention of the cells after 100 cycles with the commercial electrolyte and superconcentrated electrolyte is 18% and 90%, respectively (**Fig. 12b**). From these results, we can conclude that superconcentrated salt strategy may be a key to circumvent the Al corrosion problem without LiPF<sub>6</sub>.

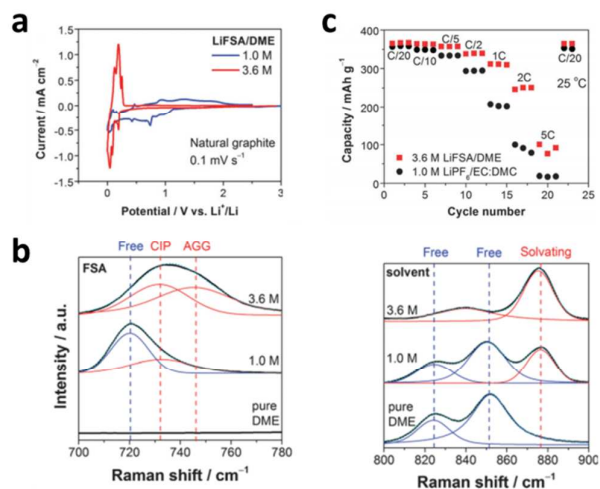


**Fig. 13** (a) Cyclic voltammograms of a natural graphite electrode in LiFSA-DME electrolytes; (b) Raman spectra of LiFSA-DME solutions at various concentrations; (c) Reversible capacity of a natural graphite/Li based on the two electrolytes at different C-rates. Reproduced with permission.<sup>172</sup> Copyright 2013, the Royal Society of Chemistry.

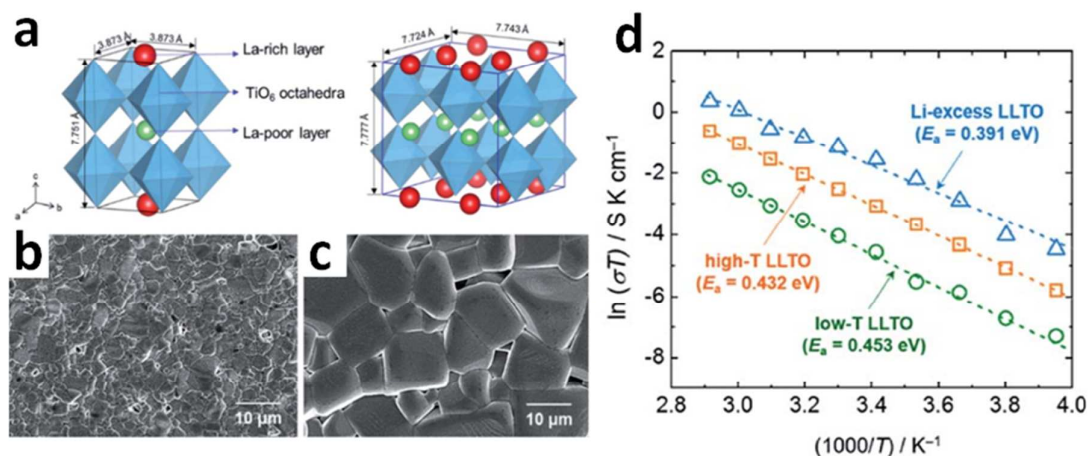


**Fig. 14** (a) Crystal structures of LLTOs; a tetragonal structure (left) and an orthorhombic structure (right). FESEM micrographs of LLTOs sintered at (b) 1200 °C and (c) 1400 °C, respectively. (d) Arrhenius plots of the boundary conductivities for low-T LLTO, high-T LLTO and Li-excess LLTO measured between 20 and 70 °C. Reproduced with permission.<sup>180</sup> Copyright 2017, The Royal Society of Chemistry.

#### 2.4.4. Fast electrode reactions

It is true that superconcentrated electrolytes always have low ionic conductivity and high viscosity. Yamada et al. found that 4.2 mol L<sup>-1</sup> LiTFSI/AN electrolyte suffers from rate capability issue that the discharge capacity of natural graphite/Li cells is close to zero at the current density of 1 C because of its low ionic conductivity (0.98 mS cm<sup>-1</sup>) and high viscosity (138.3 mPa s).<sup>171</sup> However, the rate capability issue can be improved by exploring new solvents and lithium salts. For example, when replacing LiTFSI by LiFSI, 4.5 mol L<sup>-1</sup> LiFSI/AN electrolyte exhibits superb rate property that natural graphite/Li cells cycled in 4.5 mol L<sup>-1</sup> LiFSI/AN electrolyte delivers a discharge capacity of almost 270 mAh g<sup>-1</sup> while cells cycled in traditional electrolyte delivers a discharge capacity of merely 30 mAh g<sup>-1</sup> at the current density of 5 C. This is probably because of the high ionic conductivity (9.7 mS cm<sup>-1</sup>) and low viscosity (23.8 mPa s) of LiFSI-based superconcentrated electrolyte, 4.5 mol L<sup>-1</sup> LiFSI/AN.<sup>171</sup>

In addition, as ethers can easily dissolve lithium salts through strong coordination to Li<sup>+</sup> by the lone pair of oxygen atoms. Because of their high chemical stability, they are deemed as attractive electrolyte solvents. Yamada and co-workers used 3.6 M LiFSI in 1,2-dimethoxyethane (DME) (which has low viscosity as electrolyte) in natural graphite/Li half cells and found that this superconcentrated ether electrolyte not only can achieve reversible Li intercalation/de-intercalation in graphite-based anode, but also can realize a faster Li<sup>+</sup> intercalation into graphite compared with traditional electrolyte (Fig. 13a and 13c).<sup>172</sup> This successful application on the anode has shown that the superconcentrated electrolyte is compatible with the anode side. The reason of this phenomenon is explained by the Raman spectra, i.e. all FSA anions and DME solvents interact with Li<sup>+</sup> to develop a polymeric fluid network of Li<sup>+</sup> and FSA (Fig. 13b). This unique structure amplifies the Li<sup>+</sup> intercalation/de-intercalation in graphite anode for a large variety of organic solvents other than EC. The ultrafast Li<sup>+</sup> intercalation reaction, namely, small polarization, is contributed by

Li<sup>+</sup> de-solvation kinetics, a remarkable surface film and a high Li<sup>+</sup> transference number.<sup>172</sup>

### 3. Solid electrolytes for lithium battery

The most widely used organic liquid electrolytes are low cost and easy to prepare but volatile and flammable. The leakage of the liquid electrolytes, as well as the internal short circuit caused by dendrites on lithium anode, increase the safety risks of a Li battery, which are the main concerns in regard of applications.

Solid electrolytes are solid materials transforming currents by ions, which are different from metals, graphite and conducting polymers by electrons. The technology of solid electrolytes is currently one of the foremost methods to prevent the growth of Li dendrites. Solid electrolytes can be divided into two main groups: solid inorganic electrolytes and solid polymer electrolytes.

To develop a useful solid electrolyte, several requirements should be fulfilled: (1) high mechanical strength to prevent the dendrite deposition on Li metal; (2) considerable Li ionic conductivity; (3) a wide electrochemical window to match more types of cathodes, especially high voltage cathodes (LiNi<sub>0.5</sub>Mn<sub>1.5</sub>O<sub>4</sub>, LiNi<sub>x</sub>Mn<sub>y</sub>Co<sub>2</sub>O<sub>2</sub>); (4) low interfacial resistance and good stickiness between two electrodes and electrolyte, etc.

In this review section, we focus on the functions of solid electrolytes to construct safe and high performance lithium batteries.

#### 3.1. Solid inorganic electrolytes

Lithium solid inorganic electrolytes, also called lithium fast ion conductors, can be divided into two streams, i.e. crystalline electrolytes (or ceramic electrolytes) and amorphous electrolytes (or glassy electrolytes). They show extremely high ionic conductivities (>10<sup>-3</sup> S cm<sup>-1</sup> at room temperature), high lithium ion

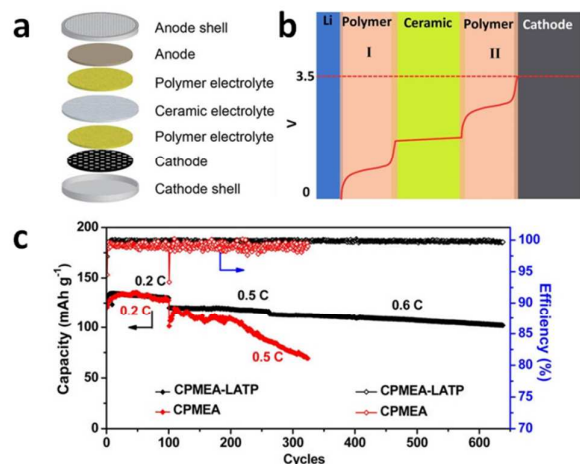


**Fig. 15** (a) Sketch map of an all-solid-state battery design with the PCPSE/LATP/PCPSE sandwich electrolyte. (b) Illustration of the potential profile across the sandwich electrolyte in a Li/LiFePO<sub>4</sub> battery during the charge process. (c) Cycling and C rate performance of the Li/LiFePO<sub>4</sub> cells with sandwich electrolyte. Reproduced with permission.<sup>188</sup> Copyright 2016, American Chemical Society.

transference number ( $\approx 1$ ), and low conductive activation energy ( $E_a < 0.5$  eV). Though somewhat poor mechanical properties, big interfacial resistance when contact with electrodes and narrow electrochemical windows, which suppress widely use.

### 3.1.1. Crystalline electrolytes

Crystalline electrolytes with the structures like perovskite-type, NASICON-type, garnet-type and LISICON-type have mainly been explored. Preparation methods for these ceramic electrolyte include high temperature solid-state synthesis process, sol-gel method, sol precipitation method, spray drying method, pulsed laser deposition, microwave induction method, hydro-thermal synthesis, etc.

Perovskite-type electrolytes with a structure ABO<sub>3</sub> show high bulk conductivity, about  $10^{-3}$  S cm<sup>-1</sup> at room temperature. Li<sub>3-x</sub>La<sub>2/3-x</sub>TiO<sub>3</sub> (LLTO) ( $0.04 < x < 0.17$ ) (LLTO) consists of a mixture of phases, which depends on the product composition and synthesis conditions. Li<sup>+</sup> and La<sup>3+</sup> on A site were randomly distributed in the cubic phase and orderly arranged in a doubled perovskite structure. LLTO exhibits many advantages, such as high electrochemical stability up to 8 V, lithium single ion conduction, and stability in atmosphere.<sup>179</sup> Low grain-boundary conductivity and instability against Li metal anode are the two disadvantages of LLTO electrolytes. Kwon et al.<sup>180</sup> synthesis LLTOs with reduced boundary resistance by a microstructure engineering. A total ionic conductivity as high as  $4.8 \times 10^{-4}$  S cm<sup>-1</sup> was achieved at room temperature by controlling the sintering temperature and Li content (Fig. 14). Recently, anti-perovskite electrolytes have been explored for their increased Li ion conductivity and high decomposition voltages. Hood et al.<sup>181</sup> found that a cold-pressed Li<sub>2</sub>OHCl from fast cooling exhibited the highest ionic conductivity. Li et al.<sup>182</sup> reported that Li<sub>2</sub>(OH)<sub>0.9</sub>F<sub>0.1</sub>Cl showed high stability on

contact with lithium metal anode and had an electrochemical stability window extending to 9 V vs. Li/Li<sup>+</sup>.

Sodium super ionic conductors (NASICON) exhibit good structural stability and fast ionic conductivity, which enables them to be used in metallic based battery system.<sup>183-189</sup> They have a general formula, MA<sub>2</sub>(BO<sub>4</sub>)<sub>3</sub>, where M, A, B stand for metal cations with different valence states. The M position is occupied by Li, Na, K or Ag. Atoms on the position of A are usually occupied by Ti, Zr, Ge or V. The B site is usually taken by P, Si or Mo. Elements on A and B sites can be replaced by other metal cations to form multitudinous NASICONs. In the structure of NASICON, AO<sub>6</sub> octahedra and BO<sub>4</sub> tetrahedra use the same corner angles to form a 3D interconnected structure and two kinds of clearance positions (M I and M II). NASICONs with Ti, LiTi<sub>2</sub>(PO<sub>4</sub>)<sub>3</sub>, exhibit high ionic conductivity, compared with other tetrahedral metal ions. To further increase the ionic conductivity of LiTi<sub>2</sub>(PO<sub>4</sub>)<sub>3</sub>, Ti is partly replaced by cations with larger radius to form Li<sub>1-x</sub>Ti<sub>2-x</sub>M<sub>x</sub>(PO<sub>4</sub>)<sub>3</sub> (M = Al, Sc, La, Cr, In, Ga, etc.) and Li<sub>1.3</sub>Ti<sub>1.7</sub>Al<sub>0.3</sub>(PO<sub>4</sub>)<sub>3</sub>. These demonstrated the highest ionic conductivity of  $7 \times 10^{-4}$  S cm<sup>-1</sup> at room temperature.<sup>190</sup> Besides, NASICON-type electrolytes have a relatively wide electrochemical stability window. The LiGe<sub>2</sub>(PO<sub>4</sub>)<sub>3</sub>-based electrolytes can reach nearly 6 V (vs. Li/Li<sup>+</sup>).<sup>187</sup> In the system of Li<sub>1-x</sub>Al<sub>x</sub>Ti<sub>2-x</sub>(PO<sub>4</sub>)<sub>3</sub>, Al<sup>3+</sup> replaces the larger Ti<sup>4+</sup> cations, which reduces the unit-cell dimensions of NASICONs and develops the ionic conductivity by three orders of magnitude.<sup>190, 191</sup> Li<sub>1-x</sub>Al<sub>x</sub>Ti<sub>2-x</sub>(PO<sub>4</sub>)<sub>3</sub> displays a higher ionic conductivity than Li<sub>1-x</sub>Al<sub>x</sub>Ge<sub>2-x</sub>(PO<sub>4</sub>)<sub>3</sub>, when  $x = 0.2$  or  $0.4$  at room temperature.<sup>192</sup> However, Ti<sup>4+</sup> is not stable enough against lithium metal. Zhou et al.<sup>188</sup> developed a polymer/ceramic/polymer sandwich electrolyte. In their structure, a polymer layer (PCPSE) wets the Li metal surface and makes the Li<sup>+</sup> flux more homogeneous. Li/LiFePO<sub>4</sub> cells showed a high Coulombic efficiency of 99.8-100% over 640 cycles (Fig. 15). Xie et al. developed a solid electrolyte, PEO/LATP, and investigated it in a Li/PEO/LATP/LiCoO<sub>2</sub> battery,

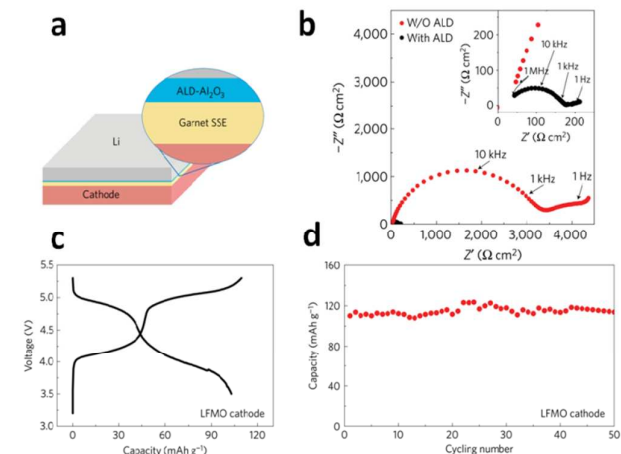


**Fig. 16** (a) Schematic of full cell using ALD-coated LLCZN as electrolyte, Li metal anode and LFMO cathode. (b) Interfacial resistance of the symmetric Li non-blocking cells with/without ALD layer. (c) Charge and discharge profile of the LFMO/ALD-garnet SSE/Li full cell. (d) Cycling performance of the cell at 0.1 C. Reproduced with permission.<sup>202</sup> Copyright 2017, Macmillan Publishers Limited, part of Springer Nature.

## REVIEW

which showed a high operation voltage of 3.8 V.<sup>193</sup> Similarly, Chinnam et al.<sup>189</sup> prepared a hybrid ceramic-polymer electrolyte via interfaces engineering to get an enhanced performance. These inter-layers were used to avoid the reduction of  $Ti^{4+}$  when contacting with Li metal anode. LATP are used as a separator in some other metallic based battery systems or non-aqueous/aqueous hybrid systems.<sup>183-186</sup>

Garnet-type lithium solid electrolytes have a general formula  $Li_5La_3M_2O_{12}$  ( $M = Nb$  or  $Ta$ ). They have recently been used as electrolytes for all solid state Li batteries.<sup>194</sup>  $Li_6BaLa_2Ta_2O_{12}$  exhibited a high ionic conductivity of  $1.69 \times 10^{-5} \text{ S cm}^{-1}$  at 25 °C with an activation energy of 0.40 eV.<sup>195</sup>  $Li_{6.4}La_3Zr_{1.6}Ta_{0.6}O_{12}$  prepared at 1140 °C revealed the highest bulk conductivity ( $10^{-3} \text{ S cm}^{-1}$  at room temperature).<sup>196</sup> Garnet-type  $Li_7La_3Zr_2O_{12}$  (LLZO) has attracted much attention since it had firstly been reported by Murugan et al.<sup>197</sup> In the phase of LLZO, the change occurs from a tetragonal structure to the cubic structure under increase in sintering temperature, these belong to the space groups  $Iad$  and  $I4_1A/cd$ , respectively.<sup>198</sup> Cubic phase possesses a higher ionic conductivity,  $1 \times 10^{-4} \text{ S cm}^{-1}$  at room temperature, which is about two orders of magnitude higher than that of tetragonal phase. So, garnet electrolytes are attractive for their wide electrochemical windows and the most stable interfaces against Li metal. However, large interfacial impedance between garnet electrolyte and electrode becomes one of the major problems. To overcome the impedance growth and capacity fade caused by chemically and electrochemically instabilities on electrode-electrolyte interface, approaches such as coating, alloying and artificial SEI were widely employed in recent years.<sup>199,200</sup> Li et al.<sup>201</sup> introduced 2 wt% LiF to garnet  $Li_{6.5}La_3Zr_{1.5}Ta_{0.5}O_{12}$  (LLZT) to reduce the interfacial resistance against Li metal. Han et al.<sup>202</sup> efficiently reduced the interfacial impedance, from  $1710 \Omega \text{ cm}^2$  to  $1 \Omega \text{ cm}^2$ , between a lithium metal anode and a  $Li_7La_{2.75}Ca_{0.25}Zr_{1.75}Nb_{0.25}O_{17}$  electrolyte with an ultrathin  $Al_2O_3$  film by atomic layer deposition. Li/ALD-garnet SSE/ $Li_2FeMn_3O_8$  full cell shows a stable cycling performance, around 110 mAh  $g^{-1}$  over 50 cycles (Fig. 16).

The typical representative of LISICON-type electrolytes,  $Li_{14}ZnGe_4O_{16}$ , possesses the highest ionic conductivity,  $1.25 \times 10^{-1} \text{ S cm}^{-1}$  at 300 °C, but only  $10^{-7} \text{ S cm}^{-1}$  at room temperature.  $[Li_{11}ZnGe_4O_{16}]^{3-}$  is a strong 3D anionic framework and the three remaining Li ions are located in clearance positions for conduction. Liquid sublattice model can be used to classify the mechanism of  $Li^+$  movement through the frameworks. The average size of channels in  $Li_{14}ZnGe_4O_{16}$  (4.38 Å) is big enough for  $Li^+$  transport. The minimum size of 4.0 Å is required.  $Li_{14}ZnGe_4O_{16}$  is unstable at high temperature and highly reactive to atmospheric  $CO_2$  and Li metal. To improve the ionic conductivity of LISICON-type electrolytes, Kanno et al.<sup>203,204</sup> replaced oxide by sulfur within the framework. Sulfur-based inorganic electrolytes show the best conductivity among inorganic electrolytes till now, and we will emphasize the series in section 3.1.3.

### 3.1.2. Amorphous electrolytes

Amorphous electrolytes have attracted much attention due to the isotropic ionic conduction, zero grain-boundary resistance, easy

## Journal of Materials Chemistry A

fabrication into films and low cost.<sup>194</sup> Amorphous electrolytes can be divided into two categories: oxide and sulfide types. The former exhibit electrochemical and thermal stability, but low conductivity ( $10^{-8} \sim 10^{-6}$  at room temperature),<sup>205</sup> whereas the latter glassy electrolytes show higher conductivity ( $10^{-4} \sim 10^{-3}$  at room temperature), though they are unstable with moisture and  $O_2$ , and difficult to prepare.<sup>206</sup>

The lithium glassy electrolytes can be prepared using a melt quenching technique,<sup>207</sup> high-energy ball-milling,<sup>208,209</sup> and radio frequency magnetron sputtering.<sup>210</sup>

Oxide glassy electrolytes consist of network forming oxides ( $SiO_2$ ,  $B_2O_3$  or  $P_2O_5$ ) and network modifying oxides ( $Li_2O$ ). The structure is a stable system at low temperature. The network forming oxides make strongly interconnected giant molecular chains. Chemical reactions between the network modifying and forming oxides can break the oxygen bridge in macro-molecular chains and reduce the average length of the macro-molecular chains. The above process produces an open structure in which only Li ions are allowed to travel within the material. So, the ionic conductivity of amorphous electrolytes is universal higher than crystalline electrolytes made of the same elements.

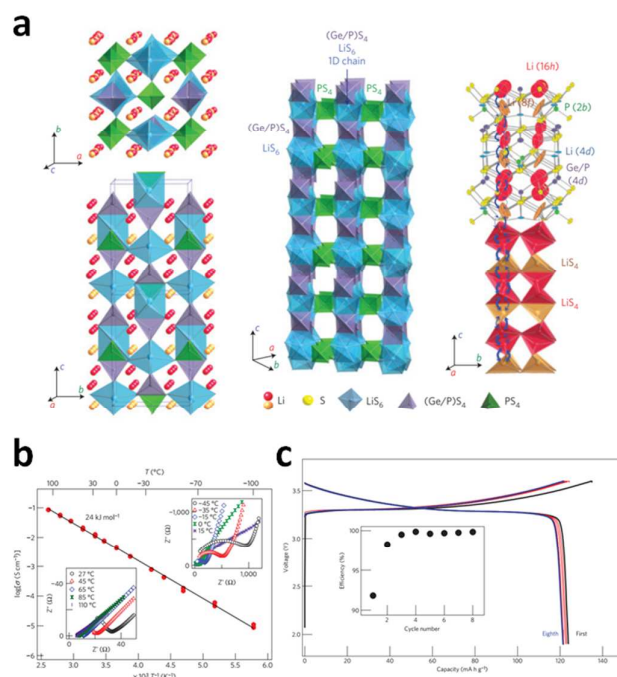


**Fig. 17** (a) Crystal structure of  $Li_{10}GeP_2S_{12}$ . (Left) The framework structure and Li ions that participate in ionic conduction. (Middle) Framework structure of this electrolyte. (Right) Conduction pathways of lithium ions. (b) Li-ion conductivity of  $Li_{10}GeP_2S_{12}$ . (c) Charge-discharge curves of an all-solid-state battery with  $Li_{10}GeP_2S_{12}$  electrolyte. Reproduced with permission.<sup>222</sup> Copyright 2011, Nature Publishing Group.

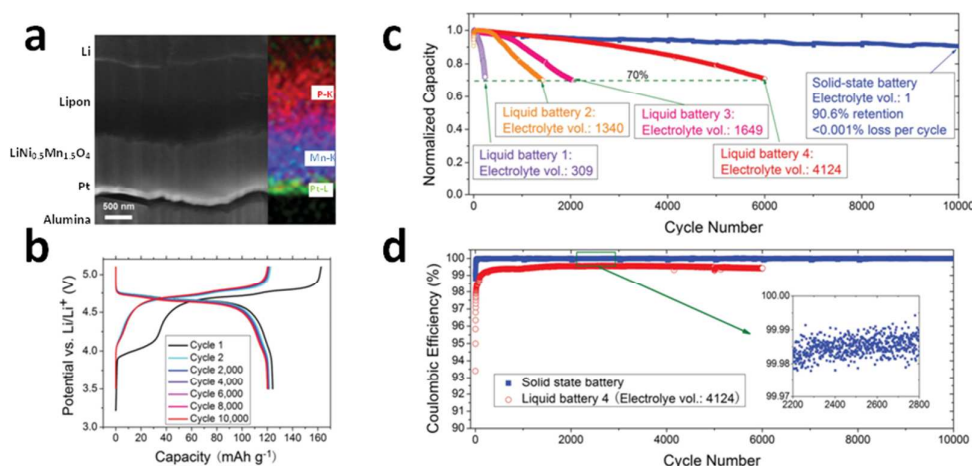


**Fig. 18** (a) SEM image and EDX elemental mapping of the cross section of the solid-state lithium battery after 1000 cycles. (b) Voltage profile of the solid-state battery under C/10 at different cycles. (c) Comparison of capacity retention and (d) Coulombic efficiency of high-voltage solid-state and liquid-electrolyte Li batteries. All cells were cycled under a rate of 5 C. Reproduced with permission.<sup>229</sup> Copyright 2014, WILEY-VCH Verlag GmbH & Co. KGaA, Weinheim.

Binary  $\text{Li}_2\text{O}-\text{B}_2\text{O}_3$  glassy electrolyte has a relatively low ionic conductivity, about  $1.2 \times 10^{-8} \text{ S cm}^{-1}$  at room temperature. Lee et al.<sup>205</sup> increased the ionic conductivity of a  $\text{Li}_2\text{O}-\text{B}_2\text{O}_3$  glassy electrolyte by the addition of  $\text{SeO}_2$  with different ratios to form a new electrolyte,  $0.5\text{Li}_2\text{O}-0.5(\gamma\text{SeO}_2-(1-\gamma)\text{B}_2\text{O}_3)$  ( $\gamma = 0.2 \sim 0.7$ ). When  $\gamma = 0.5$ , the ionic conductivity had a maximum,  $8 \times 10^{-7} \text{ S cm}^{-1}$  at room temperature. In addition, increasing lithium concentration is another approach to enhance the ionic conductivity of glassy electrolytes. Saetova et al.<sup>211</sup> found that the ionic conductivity of the glass,  $\text{Li}_2\text{O}-\text{B}_2\text{O}_3-\text{SiO}_2$ , might sharply be increased above  $\text{Li}_2\text{O}$  concentration more than 62.5 mol%, which was a result from the glass network changes and the formation of boroxol rings and diborate units. Deshpande et al.<sup>212</sup> doped a series of LiCl contents into  $40\text{Li}_2\text{O}-40\text{B}_2\text{O}_3-20\text{SiO}_2$ . The  $40\text{Li}_2\text{O}-30\text{B}_2\text{O}_3-15\text{SiO}_2-15\text{LiCl}$  composition showed the highest ionic conductivity and the lowest activation energy. LIPON is another kind of an oxide amorphous electrolyte fabricated via introducing nitrogen into  $\text{Li}_2\text{O}-\text{P}_2\text{O}_5$ . We will emphasize the series in section 3.1.4.

The structure of sulfide amorphous electrolytes is the same as that of oxide glass electrolytes, only the replacement of oxygen atoms by sulfur atoms is required. The lower electronegativity of  $\text{S}^{2-}$  than  $\text{O}^{2-}$  leads to lowering binding ability with  $\text{Li}^+$ , whereas the larger radius of  $\text{S}^{2-}$  than  $\text{O}^{2-}$  can establish the larger  $\text{Li}^+$  transport channels.<sup>213</sup> Compared with oxide glass electrolytes, sulfide glass electrolytes can achieve a relatively higher ionic conductivity ( $10^{-4} \sim 10^{-3} \text{ S cm}^{-1}$  at room temperature). Therefore,  $\text{Li}_2\text{S}-\text{P}_2\text{S}_5$ ,<sup>214</sup>  $\text{Li}_2\text{S}-\text{SiS}_2$ <sup>215</sup> and  $\text{Li}_2\text{S}-\text{B}_2\text{S}_3$ <sup>216</sup> are excellent electrolytes in all solid state batteries. Ohara et al.<sup>217</sup> found that  $\text{P}_2\text{S}_6^{4-}$  ions, as well as  $\text{PS}_4^{3-}$  and  $\text{P}_2\text{S}_7^{4-}$  ions, are present in  $67\text{Li}_2\text{S}-33\text{P}_2\text{S}_5$ ,  $70\text{Li}_2\text{S}-30\text{P}_2\text{S}_5$ , and  $75\text{Li}_2\text{S}-25\text{P}_2\text{S}_5$  glasses. The structure can be stabilized by P-P correlation in all three glasses. The S-Li-S bond angle distribution at distinct peak around  $100^\circ$  is peculiar to a high  $\text{Li}_2\text{S}$  content, which corresponds to the enhancement in the edge sharing polyhedral connection between  $\text{PS}_x$  and  $\text{LiS}_y$ . The free volume around the  $\text{PS}_x$  polyhedral anion allows for the even distribution of  $\text{Li}^+$  ions. Glassy electrolytes

with  $\text{P}_2\text{S}_5$  show decent electrochemical stability against Li metal anode. Similarly to oxide glassy electrolytes, a mixed network structure can effectively increase the ionic conductivity of sulfide glassy electrolytes.  $95\text{Li}_3\text{PS}_4-5\text{Li}_4\text{GeS}_4$  can reach a high ionic conductivity of  $4 \times 10^{-4} \text{ S cm}^{-1}$  at room temperature and good Li ion transference number close to 1. Takada et al.<sup>218</sup> improved the Li ionic conductivity of  $67\text{Li}_2\text{S}-33\text{P}_2\text{S}_5$  from  $10^{-4} \text{ S cm}^{-1}$  to  $10^{-3} \text{ S cm}^{-1}$  at room temperature by adding 45 wt% of LiI. Rangasamy et al.<sup>219</sup> synthesized a fast Li ion conductor,  $\text{Li}_7\text{P}_2\text{S}_8\text{I}$ , which exhibited high ion conductivity and good electrochemical stability (10 V vs.  $\text{Li}/\text{Li}^+$ ), and revealed the characteristics of a solid solution between LiI and  $\text{Li}_3\text{PS}_4$ . Wei et al.<sup>220</sup> investigated the impact of annealing treatment on the ionic transference and storage stability of  $70\text{Li}_2\text{S}-30\text{P}_2\text{S}_5$ . The ionic conductivity was enhanced from 1 to  $1.5 \times 10^{-3} \text{ cm}^{-1}$ , while the interfacial resistance of  $\text{Li}/70\text{Li}_2\text{S}-30\text{P}_2\text{S}_5/\text{Li}$  cell is reduced by an order of magnitude with increasing annealing temperature up to  $250^\circ\text{C}$ . The higher annealing temperature induced formation of a low conductivity  $\text{Li}_4\text{P}_2\text{S}_6$  phase, which increased both the bulk and interfacial resistances. And the storage stability was also improved after annealing treatments. Glassy electrolytes with  $\text{SiS}_2$  show high ionic conductivity and ease in fabrication under atmospheric pressure. The addition of LiI can enhance ion conductivity to  $1.32 \times 10^{-3} \text{ S cm}^{-1}$ , but reduce its decomposition voltage. By contrast,  $\text{Li}_x\text{MO}_y$  ( $\text{M} = \text{B}, \text{Al}, \text{Ga}, \text{In}$ ) in  $\text{Li}_2\text{S}-\text{SiS}_2$  can increase the conductivity without decreasing the decomposition voltage.<sup>221</sup>  $95(0.6\text{Li}_2\text{S}-0.4\text{SiS}_2)-5\text{Li}_3\text{BO}_3$  shows high ion conductivity ( $2.5 \times 10^{-3} \text{ S cm}^{-1}$ ) and particularly high decomposition voltage (10 V).<sup>213</sup>

### 3.1.3. Thio-LISICON-type electrolytes

Kanno et al.<sup>204</sup> first to synthesize a kind of new LISICON,  $\text{Li}_{4-x}\text{Ge}_{1-x}\text{P}_x\text{S}_4$ , when  $x = 0.75$ , the ionic conductivity could reach up to  $2.2 \times 10^{-3} \text{ S cm}^{-1}$ .  $\text{Li}_{3.25}\text{Ge}_{0.25}\text{P}_{0.75}\text{S}_4$  showed good electrochemical and thermal stability against lithium metal anode without phase transition even at  $500^\circ\text{C}$ . Recently, Kamaya et al.<sup>222</sup> developed a typical thio-LISICON structure,  $\text{Li}_{10}\text{GeP}_2\text{S}_{12}$ , with a very high

## REVIEW

## Journal of Materials Chemistry A

conductivity of  $1.2 \times 10^{-2} \text{ S cm}^{-1}$  at 27 °C (**Fig. 17**).  $\text{Li}_{10}\text{GeP}_2\text{S}_{12}$  was tested in a practical battery which had exhibited a relatively high discharge specific capacity (over  $120 \text{ mAh g}^{-1}$ ) and an excellent discharge efficiency (about 100% after the 2nd cycle). Wenzel et al.<sup>223</sup> monitored the chemical reactions at the  $\text{Li}/\text{Li}_{10}\text{GeP}_2\text{S}_{12}$  interface with the formation of  $\text{Li}_3\text{P}$ ,  $\text{Li}_2\text{S}$ , and  $\text{Li-Ge}$  alloy by in situ XPS combining with time-resolved electrochemical measurements, which is in perfect agreement with theoretical predictions. To achieve a better interfacial process in practical application, an optimized electrode containing both electrolyte and electrode materials was developed.<sup>224</sup> Capacity retention of 80% of the theoretical capacity ( $137 \text{ mAh g}^{-1}$ ) was achieved with 70 wt% of  $\text{LiCoO}_2$  and 30 wt% of LGPS in the cathode. After cycling and measurements, the results demonstrate that a relatively low mass fraction of solid electrolyte is sufficient for high energy density, while a higher fraction of solid electrolyte is required for high power density.<sup>224</sup>  $\text{Li}_{10}\text{SnP}_2\text{S}_{12}$  is another kind thio-LISICON structure where Ge is replaced with Sn, the conductivity reaches to  $4 \times 10^{-3} \text{ S cm}^{-1}$  at room temperature for this case.<sup>225</sup>

### 3.1.4. LiPON-type electrolytes

Adding N in an oxide glassy electrolyte,  $\text{Li}_2\text{O-P}_2\text{O}_5$ , can form the new glassy electrolyte (LiPON).  $\text{Li}_{0.99}\text{PO}_{2.55}\text{N}_{0.30}$  exhibited the highest ionic conductivity,  $3.0 \times 10^{-7} \text{ S cm}^{-1}$  at room temperature. LiPONs are stable with lithium metal and cathode materials, but expensive for the large-scale production. LiPONs can be easily fabricated into films by thermal atomic layer deposition (ALD).<sup>226</sup> Flexible thin film batteries can be developed through layer by layer deposition of LiPONs electrolytes and cathodes onto Li metals.<sup>227, 228</sup> Li et al.<sup>229</sup> assembled a high-voltage solid state Li battery using  $\text{LiNi}_{0.5}\text{Mn}_{1.5}\text{O}_4$  cathode, LiPON, and Li metal anode (**Fig. 18**). The batteries showed an outstanding cycling performance with 90% capacity retention after 10 000 cycles. The requirement of electrolyte amount was thousands of times less than that of liquid electrolyte. Such battery

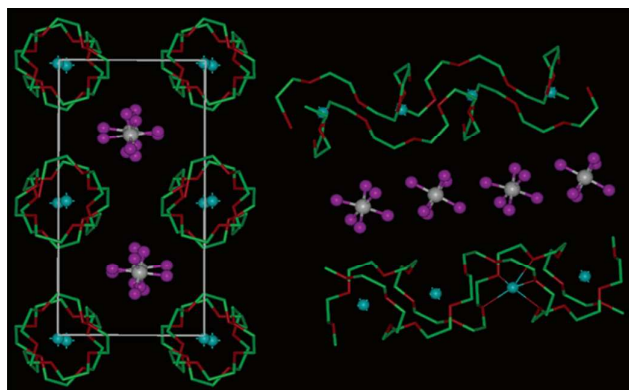


**Fig. 19** Structures of  $\text{PEO}_6:\text{LiAsF}_6$ . (Left) View of the structure along the rows of  $\text{Li}^+$  ions perpendicular to the page. (Right) View of the structure showing the relative position of the chains and their conformation (hydrogen atoms are not shown). Thin lines indicate coordination around the  $\text{Li}^+$  cation. Blue spheres - lithium; white spheres - arsenic; magenta - fluorine; green - carbon; red - oxygen. Reproduced with permission.<sup>239</sup> Copyright 2003, American Chemical Society.

demonstrated the lowest electrolyte decomposition, which contributed to high Coulombic efficiency of 99.98%.

### 3.1.5. Glass-ceramic electrolytes

Crystallization is a useful way to enhance the ionic conductivity of glassy electrolytes. Thus produced electrolytes are called glass-ceramic electrolytes. The glass-ceramic electrolytes usually have lower grain-boundary resistance than their crystalline counterparts.<sup>230</sup> Glass-ceramics, like LATP<sup>231, 232</sup> and LAGP,<sup>233, 234</sup> have been most studied and their ionic conductivities could reach up to  $10^{-4} \sim 10^{-3} \text{ S cm}^{-1}$  at room temperature. Xu et al.<sup>235</sup> reported a  $\text{MoS}_2$ -doped  $\text{Li}_2\text{S-P}_2\text{S}_5$  glass-ceramic electrolyte ( $\text{Li}_7\text{P}_{2.9}\text{S}_{10.85}\text{Mo}_{0.01}$ ) prepared via combining high-energy ball milling and annealing.  $\text{Li}_7\text{P}_{2.9}\text{S}_{10.85}\text{Mo}_{0.01}$  exhibited a high ionic conductivity of  $4.8 \times 10^{-3} \text{ S cm}^{-1}$  at room temperature, and a wide electrochemical window up to 5 V (vs.  $\text{Li}/\text{Li}^+$ ). Eom et al.<sup>236</sup> enhanced the conductivity  $\text{Li}_2\text{S-P}_2\text{S}_5$  glass-ceramic electrolyte by the adding  $\text{Li}_3\text{BO}_3$  in  $\text{Li}_2\text{S-P}_2\text{S}_5$ . The  $97(0.78\text{Li}_2\text{S}-0.22\text{P}_2\text{S}_5)-3\text{Li}_3\text{BO}_3$  glass-ceramic exhibited the highest conductivity of  $1.03 \times 10^{-3} \text{ S cm}^{-1}$  at room temperature. In addition, a  $\text{Li}_3\text{PO}_4$ -doped  $\text{Li}_7\text{P}_3\text{S}_{11}$  glass-ceramic,  $70\text{Li}_2\text{S}-29\text{P}_2\text{S}_5-1\text{Li}_3\text{PO}_4$ , possessed the highest total conductivity of  $1.87 \times 10^{-3} \text{ S cm}^{-1}$  at 25 °C and the lowest activation energy of  $18 \text{ kJ mol}^{-1}$ .<sup>237</sup> Nuernberg et al.<sup>238</sup> proposed a series of NASICON based on  $\text{Li}_{1-x}\text{Cr}_x(\text{Ge}_y\text{Ti}_{1-y})_{2-x}(\text{PO}_4)_3$  (LCGTP) system. The LCGTP glasses show internal nucleation and relatively stable compared to other self-nucleating glasses. The  $\text{LiTi}_2(\text{PO}_4)_3$ -type phase was crystallized and the cell parameters of the structure were in the range of other general systems. This indicated that the composition formed a solid solution and the octahedral sites were shared by Cr, Ge, Ti. The ionic conductivity of this glass-ceramic is more than 5 orders of magnitude higher than that of the precursor glass. Meanwhile, the highest total ionic conductivity was reached  $6.6 \times 10^{-5} \text{ S cm}^{-1}$ , as revealed by the glass-ceramic heat-treated at 900 °C.

## 3.2. Solid polymer electrolytes

The use of polymers in LIBs can enhance mechanical properties and improve safety performance during producing and operating. Polymer electrolytes could be classified into three categories: solid polymer electrolytes, gel polymer electrolytes and quasi solid electrolytes.

### 3.2.1. PEO-based solid polymer electrolytes

Researchers have made much effort toward the development of novel polymer electrolytes for LIBs. Among those poly (ethylene oxide) (PEO) is the most commonly used. The mixture of PEO and alkali metal salts displays a conductive behavior. Polymer structures with oligoether  $(-\text{CH}_2-\text{CH}_2-\text{O}-)_n$  can effectively dissolve Na salts and Li salts. The mechanism of the  $\text{Li}^+$  motivation in polymer chain segments was proposed by Armand decades later. Flexible ethylene oxide segments and ether oxygen atoms were found to be good donors for  $\text{Li}^+$  transport. However, the electrolytes exhibit low ionic conductivities due to their high crystallinity. In 2003, Stoeva et al.<sup>239</sup> reported that the ionic conductivity in a PEO crystalline phase is greater than that in amorphous phase (**Fig. 19**). However,

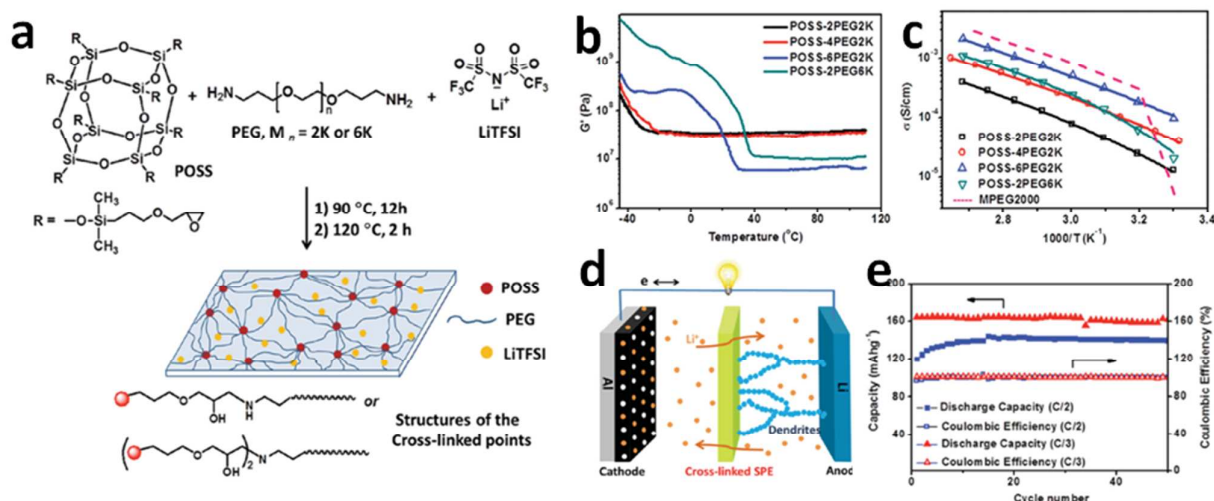


**Fig. 20** (a) Synthetic route of the POSS-PEO cross-linked SPE ( $\text{EO}/\text{Li}^+ = 16$ ) and its ideal network structure. (b) The storage modulus  $G'$  and (c) ionic conductivity of the POSS-PEO solid polymer electrolytes at different temperatures. (d) Schematic illustration of a LMB with this SPE as separator/electrolyte to block the growth of Li dendrites. (e) Capacity and Coulombic efficiency of the LMBs during charge-discharge cycling at C/2 and C/3 rates at 90 °C. Reproduced with permission<sup>244</sup>. Copyright 2015, WILEY-VCH Verlag GmbH & Co. KGaA, Weinheim.

Henderson et al.<sup>240</sup> opposed that an amorphous phase in polymer electrolytes predominates in ionic conductivity.

There are three main ways to improve ionic conductivity. First, adding novel and suitable lithium salts can efficiently improve it.<sup>10</sup> Lithium salts like  $\text{LiClO}_4$ ,  $\text{LiBF}_4$ ,  $\text{LiPF}_6$ ,  $\text{LiAsF}_6$ ,  $\text{LiCF}_3\text{SO}_3$  and  $\text{LiN}(\text{CF}_3\text{SO}_2)_2$  are widely used in polymer electrolytes. While combining with the compound action between polymer chains and salt cations, the ability to form polymer electrolytes depends on the solvation energy of polymers on cations and the salt lattice energy (usually less than  $850 \text{ J mol}^{-1}$ ) merge better with PEO and make a good solid electrolyte. On the other hand, the dissociation constant determines the conductivity by forming ion pairs and ion aggregates in polymers. Lithium salts with higher dissociation constant form less ion pairs and ion aggregates and exhibit better ionic conductivity. Among these lithium salts, lattice energies and dissociation constants are in the following sequence:

Lattice energies ( $\text{J mol}^{-1}$ ):  $\text{LiBF}_4$  (699)  $\sim$   $\text{LiAsF}_4$  <  $\text{LiClO}_4$  (723)  $\sim$   $\text{LiCF}_3\text{SO}_3$  <  $\text{LiSCN}$  (807) <  $\text{LiI}$  (757) <  $\text{LiBr}$  (807) <  $\text{LiCl}$  (853) <  $\text{LiF}$  (1036)

Dissociation constants:  $\text{LiN}(\text{CF}_3\text{SO}_2)_2$  >  $\text{LiAsF}_6$  >  $\text{LiPF}_6$  >  $\text{LiClO}_4$  >  $\text{LiBF}_4$  >  $\text{LiCF}_3\text{SO}_3$ .<sup>9</sup>

Among these lithium salts, Li trifluoromethanesulfonate (LiTFSI), Li bis(trifluoromethanesulfonimide) (LiTFSI), Li bis(oxalato)borate (LiBOB) and Li difluoro(oxalato)borate (LiDFOB) have been used to improve the ionic conductivity. The negative charges have a large degree of delocalization in anionic group, and strong electron withdrawing group such as  $-\text{CF}_3$  makes the charge more dispersed. The electrochemical window of Li salt can reach above 3.8 V vs.  $\text{Li}/\text{Li}^+$ . Recently, Yang et al.<sup>241</sup> reported a novel super-molecular PEO/ $\text{Li}^+$  based solid electrolyte, which contains PEO,  $\text{LiAsF}_6$  and  $\alpha$ -cyclodextrin and exhibits high ionic conductivity.

Secondly, inhibiting the formation of crystalline phase is another useful way to enhance the performance of PEO-based solid polymer electrolytes. In general, researchers achieve it by physical modification (blending) and chemical (copolymerization and cross-linking) modification. Inspired by the concept of “rigid-flexible” in Chinese Tai-chi, Cui et al.<sup>242</sup> developed a new class of rigid-flexible coupling solid polymer electrolyte (CCPL). They blended PEO, poly (cyano acrylate) (PCA) and LiBOB according to the mass ratio of 10:2:1 and casted the homogeneous solution on a home-made cellulose nonwoven membrane. The electrolyte film possessed high mechanical strength, sufficient ionic conductivity ( $3.0 \times 10^{-4} \text{ S cm}^{-1}$  at 60 °C) and improved dimensional thermostability (up to 160 °C).  $\text{Li}/\text{CCPL}/\text{LiFePO}_4$  cells exhibited excellent rate performance at 25 °C, and they could achieve capacities of 153, 148, 134, 118, 102, 74.4 and  $58.1 \text{ mAh g}^{-1}$  at various current rates of 0.1 C, 0.2 C, 0.5 C, 1 C, 2 C, 4 C and 6 C, respectively. Luca et al.<sup>243</sup> added tetraglyme, photoinitiator (MBP) and LiTFSI in PEO to obtain a highly flexible PEO based electrolyte. Under UV irradiation, the *in-situ* polymerized tetraglyme oligomers can easily crosslink with PEO backbones to reduce the crystalline phase. The electrolyte demonstrated a high ionic conductivity ( $10^{-4} \text{ S cm}^{-2}$ ) and good electrochemical stability up to 5 V. Pan et al.<sup>244</sup> synthesized a hybrid electrolyte based on POSS with controlled network structures (Fig. 20). The solid polymer electrolytes exhibited high room temperature ionic conductivity ( $\approx 1 \times 10^{-4} \text{ S cm}^{-1}$ ) and high storage modulus (33.6 MPa at 105 °C), which makes them good electrolyte/separator to block the growth of lithium dendrites.  $\text{Li}/\text{LiFePO}_4$  batteries using POSS-2PEG6K as electrolytes showed improved cycling stability and rate capability. Charge/discharge capacity (above  $160 \text{ mAh g}^{-1}$ ) for  $\text{LiFePO}_4$  was delivered at C/5 and C/3, and decreased to 144 and  $135 \text{ mAh g}^{-1}$  when increasing the rates to C/2 and 1 C, respectively. Zeng et al.<sup>245</sup> developed a bifunctional solid polymer electrolyte with interconnected “cages” formed by branched acrylate to spatially restrain PEO crystallization

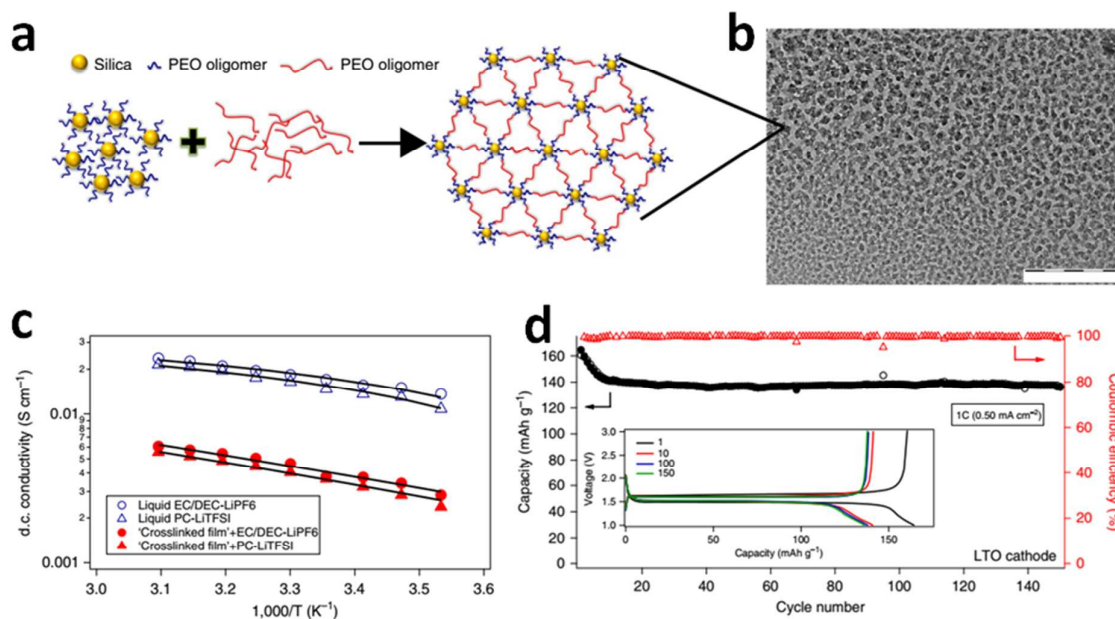


**Fig. 21** (a) Synthetic route of a free-standing crosslinked nanoparticle-polymer composite. (b) TEM image of the crosslinked membrane. Scale bar, 200nm. (c) DC conductivity as a function of inverse absolute temperature. (d) Cycling performance for Li/composite electrolyte/LTO at 1C. The inset shows the voltage profiles. Reproduced with permission.<sup>255</sup> Copyright 2015, Nature Publishing Group.

effectively, and the electrolyte reached relatively high room temperature conductivity ( $2.2 \times 10^{-4}$  S cm<sup>-1</sup>). The Li/SPE/LiFePO<sub>4</sub> batteries exhibited specific capacities of 141 and 66 mA h g<sup>-1</sup> at 0.5 and 5 C, respectively.

Thirdly, the addition of inorganic fillers to form a composite polymer electrolyte (CPE) has been a widely used strategy for decades. Inorganic fillers can be classified into two parts: active fillers and inactive fillers. Active fillers, such as Li<sub>1+x</sub>Al<sub>x</sub>Ti<sub>2-x</sub>(PO<sub>4</sub>)<sub>3</sub>, Li<sub>7</sub>La<sub>3</sub>Zr<sub>2</sub>O<sub>12</sub>, Li<sub>0.5</sub>La<sub>0.5</sub>TiO<sub>3</sub> and Li<sub>3</sub>N, are fast Li ion conductors. They generally exhibit high ionic conductivities and lithium ion transference numbers. Inactive fillers, like Al<sub>2</sub>O<sub>3</sub>, TiO<sub>2</sub>, ZrO<sub>2</sub> and SiO<sub>2</sub>, cannot directly offer a pathway for Li<sup>+</sup> ions in electrolytes but can facilitate Li<sup>+</sup> transport via the amorphization of PEO and the creation of space-charge regions. An electrolyte with low degree of crystallinity, low glass transition temperature ( $T_g$ ), and high melting point ( $T_m$ ) is extremely important. Inert ceramic fillers, like Lewis acid or Al<sub>2</sub>O<sub>3</sub>, can improve the ionic conductivity of PEO/LiClO<sub>4</sub> based polymer electrolytes through reducing the degree of crystallinity.<sup>246</sup> The charged state on the surface of nano-Al<sub>2</sub>O<sub>3</sub> particle can result in different performances of the PEO<sub>20</sub>-LiCF<sub>3</sub>SO<sub>3</sub> system, as studied by Croce et al.<sup>247</sup> Nano-Al<sub>2</sub>O<sub>3</sub> particle with basic groups cannot improve the ionic conductivity, but with Lewis acid groups or neutral groups the ionic conductivity can rise to  $8 \times 10^{-6}$  S cm<sup>-1</sup> and  $1 \times 10^{-6}$  S cm<sup>-1</sup> at room temperature, respectively. In addition, the content and particle size of inert ceramic fillers are also important parameters to control the filler functions and corresponding composite polymer electrolytes. It seems that nano-Al<sub>2</sub>O<sub>3</sub> is much better in increasing ionic conductance than micrometer-sized particles, as was concluded by Dissanayake et al.<sup>248</sup> An appropriate content of Al<sub>2</sub>O<sub>3</sub> in composite electrolyte,

(Al<sub>2</sub>O<sub>3</sub>)<sub>x</sub>(PEO)<sub>12.5-x</sub>(LiClO<sub>4</sub>), was researched by Masoud et al.<sup>249</sup> When containing 1.25 mol of Al<sub>2</sub>O<sub>3</sub>, the electrolyte exhibits the highest value of conductivity ( $8.3 \times 10^{-5}$  S cm<sup>-1</sup> at 20 °C). Other inert ceramic oxides, such as TiO<sub>2</sub><sup>250, 251</sup>, SiO<sub>2</sub><sup>252, 253</sup> can also enhance conductance of polymer electrolytes. For example, Lin et al.<sup>254</sup> added nanoscale TiO<sub>2</sub> with a size of 3.7 nm into PEO/LiClO<sub>4</sub> and the electrolyte demonstrated a high Li ion transference number (0.51) and high ionic conductivity ( $1.40 \times 10^{-4}$  S cm<sup>-1</sup> at 30 °C). Choudhury et al.<sup>255</sup> developed a solid electrolyte based on crosslinked hairy silica nanoparticles (**Fig. 21**). The strategy of using hairy nanoparticles can go well along with crosslinking of rigid PEO matrixes and the ion-conducting membranes and lead to good mechanical properties ( $G_N=1$  MPa) and liquid-like ionic conductivity ( $\sigma = 5 \times 10^{-3}$  S cm<sup>-1</sup>) at room temperature. The materials can efficiently work in LMBs based on LTO cathodes with high discharge capacity (~140 mAh g<sup>-1</sup>) for over 150 cycles at 1 C.

Mostly, polymer matrixes possess low dielectric constant, which suppresses the dissociation of Li salts in a polymer. Ferroelectric ceramics are generally polar particles. Doping into the polymer matrixes can efficiently improve the ionic conductivity and Li ion transference number. Itoh et al.<sup>256</sup> prepared a composite polymer electrolyte containing PEO, LiTFSI and BaTiO<sub>3</sub>. The ionic conductivity of the electrolyte was  $2.6 \times 10^{-4}$  S cm<sup>-1</sup> at 30 °C and the electrochemical stability window reached of 4.0 V at 30 °C. Recently, a novel composite electrolytes composed of PEO/PVP/LiClO<sub>4</sub>/PC with different ratios of BaTiO<sub>3</sub> has been developed by Kesavan et al.<sup>257</sup> The highest ionic conductivity of  $1.2399 \times 10^{-3}$  S cm<sup>-1</sup> at 30 °C documented after addition of 10 wt% BaTiO<sub>3</sub>. Batteries assembled as Li/PEO-LiTFSI-BaTiO<sub>3</sub>/C exhibited an excellent charging/discharging specific capacity, more than 330

mAh g<sup>-1</sup> after 20 cycles. Other ferroelectric ceramic such as PbTiO<sub>3</sub>, LiNbO<sub>3</sub>, can also enhance the conductance of polymer electrolytes, reduce the interfacial resistance and enhance mechanical properties of polymer electrolytes.<sup>258, 259</sup>

Metal-organic frameworks (MOFs) are compounds consisting of metal ions or clusters coordinated to organic ligands to form one-, two-, or three-dimensional structures. They are a subclass of coordination polymers; often they are porous. Due to their high surface areas, regular and porous channels and ease to modifying, MOFs have been used in many fields, including catalysis, gas storage and separation, and sensors. In recent years, they have been applied as fillers in composite polymer electrolytes.<sup>11</sup> Liu et al.<sup>260</sup> prepared an electrolyte containing PEO, LiTFSI and MOF-5 by *in situ* method. The ionic conductivity and electrode/ electrolyte interface stability of polymer electrolytes were improved by the addition of MOF-5. The highest ionic conductivity was 3.16×10<sup>-5</sup> S cm<sup>-1</sup> at 25 °C for an optimized content of 10 wt% MOF-5 with EO: Li = 10: 1. The Lewis sites in MOF-5 can inhibit the crystallization of PEO and build up pathways for conducting Li<sup>+</sup> on the surface of MOF-5 fillers. Besides, charging/discharging specific capacities of LiFePO<sub>4</sub> half cells using the electrolytes in different rates were enhanced by MOF-5 fillers, 118 to 138 mAh g<sup>-1</sup> at 0.5 C and 107 to 132 mAh g<sup>-1</sup> at 1 C. The electrolyte can be applied in LIBs operated at < 4.57 V at 60 °C. To further improve the rate performance and ionic conductivity, Liu's group altered MOF-5 by MIL-53(Al) in the above electrolyte system.<sup>261</sup> The electrolytes showed a high oxidation potential of 5.10 V at 120 °C and a high ionic conductivity of 3.39×10<sup>-3</sup> S cm<sup>-1</sup> at 120 °C. All solid state batteries assembled by Li/CPE/LiFePO<sub>4</sub> possessed a high discharge capacity of 136.4 mAh g<sup>-1</sup> at 5 C and 120 °C in the first cycle, 129.2 mAh g<sup>-1</sup> in the 300th cycles and remained at 83.5 mAh g<sup>-1</sup> after 1400th cycles. Kumar et al.<sup>262</sup> prepared a CPE compose of PEO/LiTFSI/Cu-BDC (copper benzene dicarboxylate) by using an electrochemical method. Between 0 to 70 °C, the ionic conductivity ranged from 10<sup>-6</sup> to 10<sup>-3</sup> S cm<sup>-1</sup>. The Li/CPE/LiFePO<sub>4</sub> cells displayed high discharge specific capacity, good rate capacity and high Coulombic efficiency. At rate of 1 C, the cell delivered 120 mAh g<sup>-1</sup> with 98% Coulombic efficiency. Besides, MOFs can not only provide pathways for Li<sup>+</sup>, but also work as adsorbents to trap trace amount of impurities, like O<sub>2</sub> and H<sub>2</sub>O, during cells operation.

In addition to inert ceramics, ferroelectric ceramics and MOFs, application of strong acid oxides (e.g., Zr-O-SO<sub>4</sub><sup>263</sup>) and molecular sieves (e.g., MCM-41<sup>264</sup>, SBA-15<sup>265-267</sup>, ZSM-5<sup>268, 269</sup>, etc.) in solid polymer electrolytes was analyzed. In general, the above inactive fillers can more or less improve ionic conductivity, but not significantly.

Inactive fillers, that are not involved in Li ion conduction process, and active ones can directly participate in Li ion transport. Nanoscale ceramic fillers have large specific surface area and can drastically enhance the ionic conductivity. Li<sub>3</sub>N exhibits ion conductivity of the order of 10<sup>-3</sup> S cm<sup>-1</sup> at ambient temperature<sup>270</sup>. Masoud et al.<sup>271</sup> synthesized nano-LiAlO<sub>2</sub> fillers by sol-gel method. The addition of nano-LiAlO<sub>2</sub> can reduce the crystallization of PEO and promote the growth of a passive layer on lithium metal anode.

Wang et al.<sup>272</sup> prepared a PEO-based solid CPE film with different Li<sub>1.3</sub>Al<sub>0.3</sub>Ti<sub>1.7</sub>(PO<sub>4</sub>)<sub>3</sub> content by a solution-cast technique. With LAMP acting as both fillers and ion conductors, the PEO/LAMP film showed the highest ionic conductivity of 1.185×10<sup>-4</sup> S cm<sup>-1</sup> at 100 °C and 2.631×10<sup>-6</sup> S cm<sup>-1</sup> at room temperature, at an EO/Li molar ratio of 16. Meanwhile, the PEO/LiClO<sub>4</sub>/LAMP film delivered the highest ionic conductivity of 1.161×10<sup>-3</sup> S cm<sup>-1</sup> at 100 °C and 7.985×10<sup>-6</sup> S cm<sup>-1</sup> at room temperature, at a LAMP content of 15 wt%. Recently, Wang et al.<sup>273</sup> prepared a composite solid electrolyte compose of Li<sub>1.5</sub>Al<sub>0.5</sub>Ge<sub>1.5</sub>(PO<sub>4</sub>)<sub>3</sub> (LAGP)-PEO-LiTFSI for the suppression of lithium dendrite formation. The ratio of PEO in the composite polymer electrolyte was reduced to become lower, at a level of 1 wt%, and PEO remained stable even at a high potential of 5.12 V (vs Li/Li<sup>+</sup>). The molar ratios and integrating modes of polymer and inorganic ceramic particles strongly affect properties and performances of composite electrolytes. The all-solid-state Li-PEO-500000(LiTFSI)/LAGP-PEO1/LiMn<sub>0.8</sub>Fe<sub>0.2</sub>PO<sub>4</sub> cell shows a high initial discharge capacity of 160.8 mAh g<sup>-1</sup> at 50 °C. Zheng et al.<sup>274</sup> probed Li<sup>+</sup> diffusion pathway in a Li<sub>7</sub>La<sub>3</sub>Zr<sub>2</sub>O<sub>12</sub>-PEO (LiClO<sub>4</sub>) composite electrolyte by 1D high-resolution <sup>6</sup>Li NMR. The evidence showed that Li ions mainly pass through LLZO particles, not through the interface or polymer phase. Choi et al.<sup>275</sup> demonstrated that the combination of the organic matrix (PEO) and the inorganic filler (Li<sub>7</sub>La<sub>3</sub>Zr<sub>2</sub>O<sub>12</sub>) in the solid electrolyte membranes synergistically enhances their ionic conductivities. The composite membrane containing 52.5% LLZO exhibited the highest ionic conductivity, 4.42×10<sup>-4</sup> S cm<sup>-1</sup> at 55 °C. Fu et al.<sup>276</sup> built up a 3D Li<sup>+</sup>-conducting ceramic network based on garnet-type Li<sub>6.4</sub>La<sub>3</sub>Zr<sub>2</sub>Al<sub>0.2</sub>O<sub>12</sub> (LLZAO) lithium-ion conductor to provide continuous Li<sup>+</sup> transfer channels in a PEO-based electrolyte. The flexible electrolyte membrane revealed an ionic conductivity of 2.5×10<sup>-4</sup> S cm<sup>-1</sup> at room temperature. It could also effectively suppress lithium dendrite growth in a symmetric Li/CPE/Li cell during multiple lithium stripping/plating measurement at room temperature, at a current density of 0.2 mA cm<sup>-2</sup> for about 500 hrs and a current density of 0.5 mA cm<sup>-2</sup> for more than 300 hrs. Recently, Liu et al.<sup>277</sup> reported on a composite polymer electrolyte with well-aligned inorganic Li<sup>+</sup>-conductive nanowires. The latter exhibited an ionic conductivity of

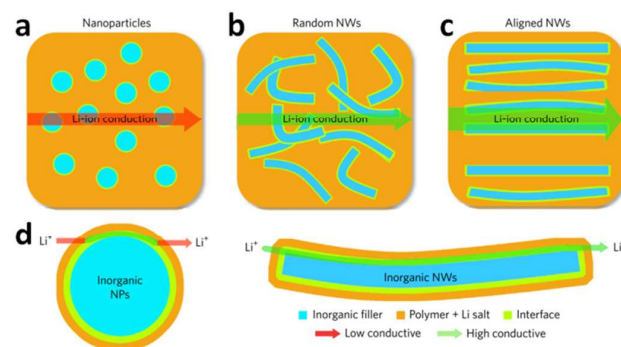


**Fig. 22** The comparison of possible Li-ion conduction pathways. Li-ion conduction pathways in composite polymer electrolytes with (a) Nanoparticles, (b) Random nanowires and (c) Aligned nanowires. (d) The surface region of inorganic nanoparticles and nanowires as an expressway for Li-ion conduction. Reproduced with permission.<sup>277</sup> Copyright 2017, Nature Publishing Group.

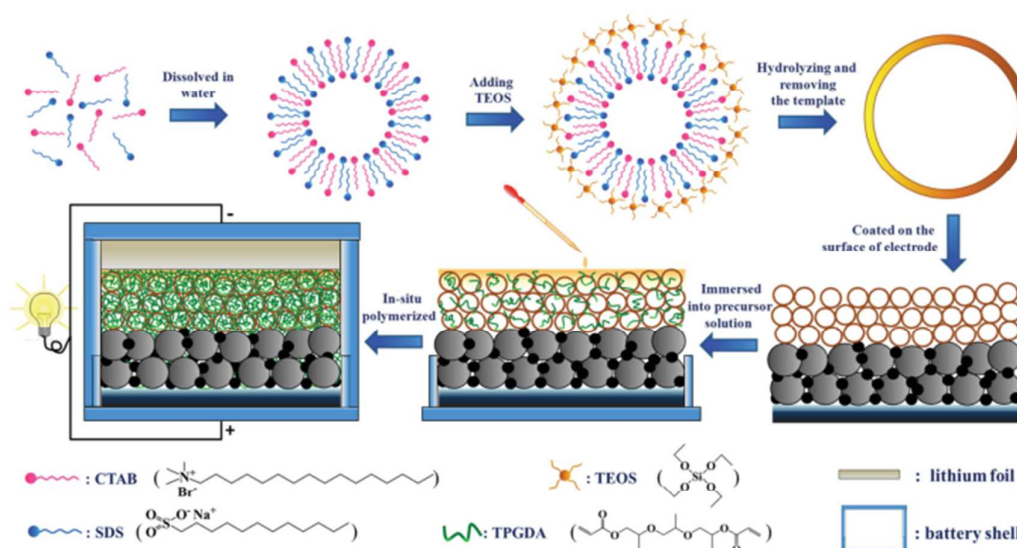


**Fig. 23** The preparation route of SiO<sub>2</sub> hollow nanosphere-based composite solid electrolyte. Reproduced with permission.<sup>284</sup> Copyright 2016, WILEY-VCH Verlag GmbH & Co. KGaA, Weinheim.

$6.05 \times 10^{-5} \text{ S cm}^{-1}$  at 30 °C, which is one order of magnitude higher than for previous polymer electrolytes with randomly aligned nanowires. Their further study confirmed that random nanowires could supply a more continuous fast conduction pathway for Li ions than isolated nanoparticles. Also the absence of crossing junctions makes conducting for ion diffusion (**Fig. 22**).

### 3.2.2. Others

Though PEO-based electrolytes were researched the most, several drawbacks, like low dielectric constant and ion aggregation phenomenon, are detrimental to the migration of Li<sup>+</sup>. Different from PEO-based electrolytes, polycarbonate-based electrolytes have strong polar groups, [–O–(C=O)–O–], which can increase dielectric constant and improve ionic conductivity.<sup>278</sup> Cui et al.<sup>279</sup> studied poly(propylene carbonate)/cellulose nonwoven membrane/LiTFSI based electrolyte. The ionic conductivity of the electrolyte was  $3.0 \times 10^{-4} \text{ S cm}^{-1}$  at 20 °C, which was much higher than PEO-based electrolyte ( $2.1 \times 10^{-6} \text{ S cm}^{-1}$ ). The Li/LiFe<sub>0.2</sub>Mn<sub>0.8</sub>PO<sub>4</sub> cell exhibited superior charge/discharge and rate performance at 120 °C. Li/LiFePO<sub>4</sub> cells using the electrolytes could deliver capacities of 138.7, 128.7, 113.9, 97.6, and 73.6 mAh g<sup>-1</sup> at varied rates of 1 C, 2 C, 3 C, 4 C, and 5 C, respectively. Later on, Cui's group prepared a poly(vinylene carbonate) based solid polymer through *in situ* polymerization. The electrolyte possess a high ionic conductivity of  $9.82 \times 10^{-5} \text{ S cm}^{-1}$  at 50 °C and a considerable electrochemical stability window up to 4.5 V vs. Li/Li<sup>+</sup>.<sup>280</sup> Besides, polysiloxane-based electrolytes demonstrated the low glass transition temperature and high room temperature ionic conductivity. In general, low glass transition temperature results in

reduced mechanical properties. Forming a network by blending, grafting and crosslinking can enhance comprehensive performance of these electrolytes. Lim et al.<sup>281</sup> reported a ceramic based composite solid electrolyte composed of 80 wt% Li<sub>1.3</sub>Ti<sub>1.7</sub>Al<sub>0.3</sub>(PO<sub>4</sub>)<sub>3</sub> (LTAP) as a lithium ion conducting ceramic, 10 wt% of poly(vinylidene fluoride) (PVDF) as a binder, and 10 wt% 1 M LiPF<sub>6</sub>/EC+DMC. The composite electrolyte demonstrated a lithium ionic conductivity of  $8.9 \times 10^{-4} \text{ S cm}^{-1}$  at room temperature without leakage. Li et al.<sup>282</sup> developed a novel polysiloxane by grafting ethylene oxide oligomer on the side chain of polymethylhydrosiloxane, then the polymer was blended with PVDF and certain amount of LiTFSI. The electrolyte showed the highest ionic conductivity of  $7.9 \times 10^{-5} \text{ S cm}^{-1}$  at 25 °C and  $8.7 \times 10^{-4} \text{ S cm}^{-1}$  at 80 °C with 30 wt% LiTFSI. The electrolyte exhibited excellent mechanical properties and compatibility with the lithium metal anode with 20 wt% LiTFSI. The decomposition temperature of the electrolyte was 275 °C, and the electrochemical stability windows of 25 °C and 60 °C is up to 5.17 V and 5.05 V, respectively. Horowitz et al.<sup>283</sup> created a PDMS-supported IL gel electrolyte with 80 wt% IL loadings via a sol-gel reaction at room temperature. The electrolytes displayed favorable ionic conductivity ( $\sim 3 \times 10^{-3} \text{ S cm}^{-1}$  at room temperature) and excellent mechanical behavior. Zhou et al.<sup>284</sup> prepared a SiO<sub>2</sub> hollow nanosphere-based composite solid electrolyte by *in situ* interpenetrating polymerization of the tripropylene glycol diacrylate (TPGDA) monomers with SiO<sub>2</sub> hollow nanospheres. The composite polymer electrolytes had high room temperature ionic conductivity ( $1.74 \times 10^{-3} \text{ S cm}^{-1}$ ) due to the large liquid electrolyte uptake of SiO<sub>2</sub> hollow nanospheres (**Fig. 23**). Li/LiFePO<sub>4</sub> cells achieved an acceptable discharge capacity of 119.5 mAh g<sup>-1</sup> at a high rate of 5 C (73.6% of the capacity at 0.1 C).

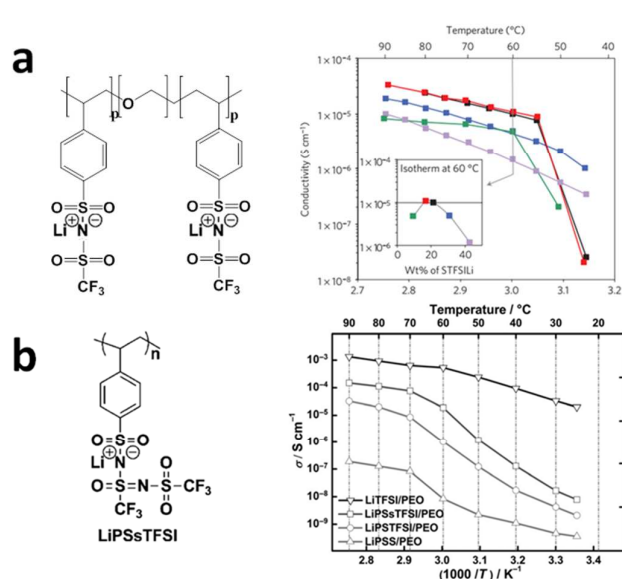


**Fig. 24** (a) (Left) Chemical structure of the single-ion conductor, triblock copolymer P(STFSiLi)-b-PEO-b-P(STFSiLi). (Right) Ionic conductivity for several P(STFSiLi)-PEO-P(STFSiLi) A-BCEs at different temperatures. Reproduced with permission<sup>285</sup>. Copyright 2013, Macmillan Publishers Limited. (b) (Left) Chemical structure of the single-ion conductor, LiPsTsFSI. (Right) Ionic conductivities for the LiX/PEO (X=PSS, PSTFSI, PSsTFSI, TFSI) blended polymer electrolytes (EO/Li<sup>+</sup>=20) at different temperatures. Reproduced with permission.<sup>286</sup> Copyright 2016, Wiley-VCH Verlag GmbH & Co. KGaA, Weinheim.

In traditional electrolyte system, anions and cations migrate together, and the transference of anions results in concentration polarization within the system, which reduces the cycle performance of the battery. Single-lithium-ion conducting polymer electrolyte can achieve single-ion conduction. Anions cannot migrate in electrolyte system and the Li ion transference number is close to 1. Bouchet et al.<sup>285</sup> synthesized a triblock polyanion (LiPSTFSI-*b*-PEO-*b*-LiPSTFSI) electrolyte by copolymerization (**Fig. 24a**). The EO chains enhanced the flexibility of LiPSTFSI main chains and provided pathways for migration of Li<sup>+</sup>. The electrolyte delivered the highest ionic conductivity of  $1.3 \times 10^{-5}$  S cm<sup>-1</sup> at 60 °C with 20 wt % LiPSTFSI (EO/Li ≈ 30). The Li/LiFePO<sub>4</sub> cells displayed good discharge specific capacity and rate capacity between 60 °C to 80 °C. Ma et al.<sup>286</sup> synthesized a novel single-lithium-ion conductor composed of a polyanion, PsTsFSI<sup>-</sup>, and then blended it with PEO to fabricate a composite polymer electrolyte (**Fig. 24b**). LiPsTsFSI ionomer displays a low glass transition temperature (44.3 °C), which can make up for the shortcomings of PEO. The LiPsTsFSI/PEO composite membrane exhibited a high lithium ion transference number (0.91) and an ionic conductivity as high as  $1.35 \times 10^{-4}$  S cm<sup>-1</sup> at 90 °C. Villaluenga et al.<sup>287</sup> prepared a glass-polymer hybrid single

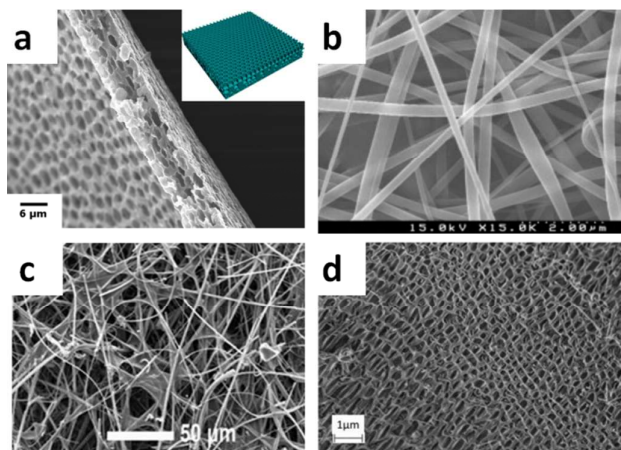


**Fig. 25** SEM of a PVDF membrane obtained by different methods: (a) Breath-Figureure method. Reproduced with permission.<sup>289</sup> Copyright 2014, Nature Publishing Group. ; (b) Electrospinning. Reproduced with permission.<sup>290</sup> Copyright 2003, WILEY-VCH Verlag GmbH & KGaA, Weinheim.; (c) Casting PVDF on glass fiber mats. Reproduced with permission.<sup>291</sup> Copyright 2013, Nature Publishing Group. ; (d) Casting PVDF-HFP on nanoporous alumina layer. Reproduced with permission.<sup>292</sup> Copyright 2013, WILEY-VCH Verlag GmbH & Co. KGaA, Weinheim.

ion-conducting electrolyte in which inorganic sulfide glass particles were covalently bonded to perfluoropolyether polymer chains. The electrolyte showed an ionic conductivity of  $10^{-4}$  S cm<sup>-1</sup> at room temperature, a lithium ion transference number close to 1, and an electrochemical stability window up to 5 V vs. Li/Li<sup>+</sup>.

### 3.3. Gel polymer electrolytes and quasi solid electrolytes

#### 3.3.1. Gel polymer electrolytes

Polymer gels are a special form, between solid and liquid phases, which possesses both the strong mechanical properties of solid polymers and super diffusion ability of ions in liquids. Gel polymer electrolytes can be formed by adding one or more plasticizers into solid polymer electrolyte.

In general, gel polymer electrolytes create three main domains: polymer crystalline phases, swollen amorphous phases and interconnected electrolyte phases in pores. The transport of Li ions is mainly contributed by solvation of plasticizers. Polymers mainly play a supporting role in gel polymer electrolytes. Polymer matrices, such as polyethylene (PEO), polyacrylonitrile (PAN), polyvinyl chloride (PVC), poly(methyl methacrylate) (PMMA), polyvinylidene fluoride (PVDF), poly(vinylidene fluoride-hexafluoropropylene) (PVDF-HFP), polyvinyl acetate (PVAC), polystyrene (PS), polyvinylpyrrolidone (PVP), etc., are widely used as frameworks in gel polymer electrolytes.

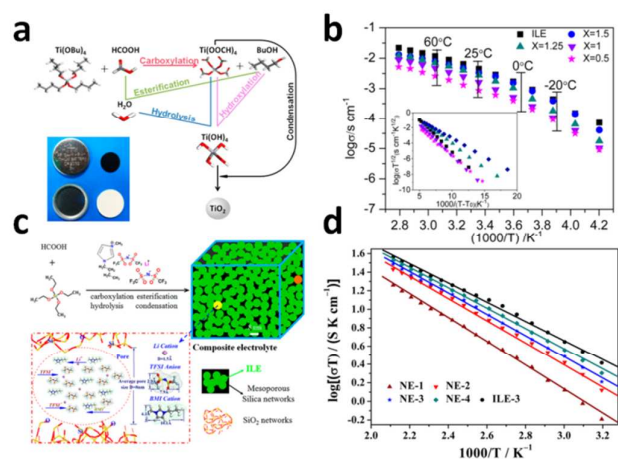


**Fig. 26** (a) Sol-gel reaction of tetrabutyl titanate (TBOT) with formic acid in the solution of 1 M LiTFSI-EMITFSI, (b) Arrhenius plots of the ionic conductivity of ILE (1 M LiTFSI-[EMI][TFSI]) and IGE containing different molar ratios of EMITFSI/TBOT ( $X = 0.5$ ,  $X = 1$ ,  $X = 1.25$ , and  $X = 1.5$ ) as a function of temperature. Inset: VTF fitting curves. Reproduced with permission.<sup>298</sup> Copyright 2016, American Chemical Society. (c) The synthetic route and structural composition of the  $\text{SiO}_2$ /BMITFSI/LiTFSI nanocomposite electrolytes. (d) Arrhenius plots of ionic conductivity of the ILE-3 and NEs containing different molar ratios of BMITFSI/TEOS ( $X = 0.5$ ,  $X = 1$ ,  $X = 1.5$ , and  $X = 2$ ) as a function of temperature. Reproduced with permission.<sup>299</sup> Copyright 2016, American Chemical Society.

Among these polymer matrixes, PVDF-based gel polymer

electrolytes have been applied to the practical production of lithium batteries because of their large dielectric constant 8.4,<sup>10</sup> high glass transition temperature ( $-40^\circ\text{C}$ )<sup>9</sup>, good chemical and electrochemical stability and the easiness in the fabrication of spacioius films. Plasticizers can increase the content of amorphous phase and promote segment motion. Li et al.<sup>288</sup> prepared a highly porous polymer membrane based on PVDF-HFP by means of a simple process using urea as the foaming agent. The obtained membrane was soaked in 1 M LiPF<sub>6</sub>/EC+DMC (1:1:1, wt %). The ionic conductivity of the resultant porous gelled polymer electrolyte arrived at  $1.43 \times 10^{-3} \text{ S cm}^{-1}$  at room temperature, showing a promising application in rechargeable Li batteries. Zhang et al.<sup>289</sup> fabricated a honeycomb-like porous gel polymer electrolyte membrane with  $\sim 78\%$  porosity, which resulted in the high electrolyte uptake of 86.2 wt% for 1 M LiPF<sub>6</sub>/EC+DMC (1:1, wt %) (**Fig. 25a**). The electrolyte membranes exhibited a high ionic conductivity of  $1.03 \times 10^{-3} \text{ S cm}^{-1}$  at room temperature, much higher than commercial separator. Moreover, the gel polymer electrolyte was also thermally stable up to  $350^\circ\text{C}$ ; and the electrochemical stability was up to 5 V. The Li/LiFePO<sub>4</sub> batteries with PVDF-HFP polymer electrolyte could operate at least 50 cycles with a reversible capacity of  $145 \text{ mAh g}^{-1}$  at 0.2 C and no obvious capacity degradation. Such good performance is related to porous structure of PVDF or PVDF-HFP matrix. This enhances the ability of electrolyte uptake for a lithium battery. On the other hand, a large amount of electrolytes absorption may lead to poor mechanical strength. Choi et al.<sup>290</sup> produced a PVDF membrane by electrospinning. The latter exhibited high porosity, large surface area, fully interconnected pore structure, and sufficient mechanical strength (**Fig. 25b**). After soaking it in the electrolyte

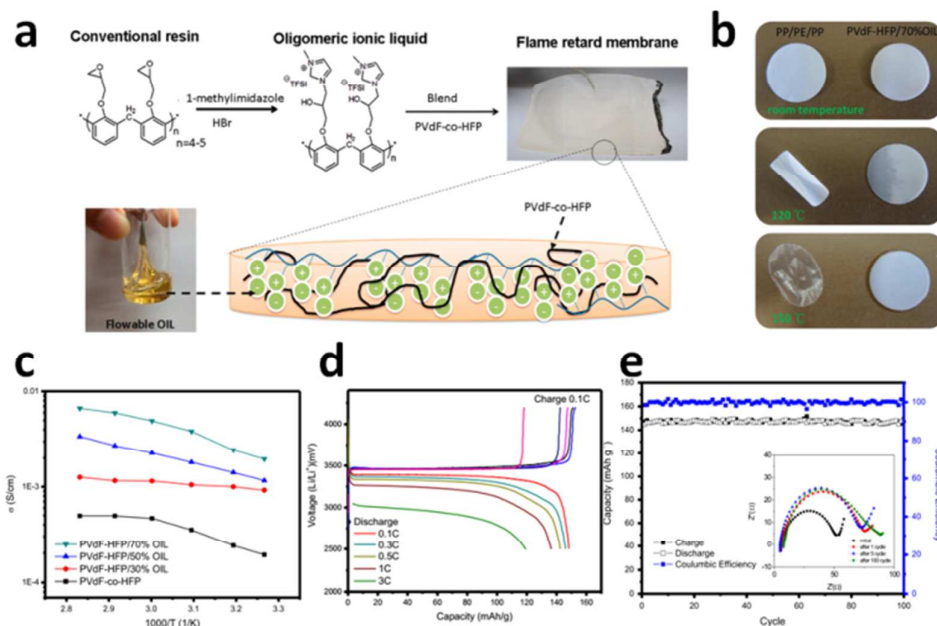


**Fig. 27** (a) Preparation of PVDF-HFP/X%OIL membrane and its scheme. (b) Thermal and dimensional stability of the PVDF-HFP/70%OIL tested at various temperatures. (c) Ionic conductivity of the electrolyte membrane at different OIL contents tested at various temperatures. (d) Charge-discharge profiles of Li/PVDF-HFP/70%OIL/LiFePO<sub>4</sub> battery tests at various C rates. (e) Cyclic performance of Li/PVDF-HFP/70%OIL/LiFePO<sub>4</sub> at a constant current density of 0.5 C. The inset is EIS before and after charge-discharge. Reproduced with permission.<sup>310</sup> Copyright 2016, Elsevier B.V.

solution, 1 M LiPF<sub>6</sub>/EC+DMC (1:1, wt %) mixture, they got a PVDF-based gel electrolyte membrane. The electrolyte showed a high ionic conductivity of  $1 \times 10^{-3}$  S cm<sup>-1</sup> at room temperature and a broad electrochemical stability window of 4.5 V. The mechanical strength was further enhanced by electrospinning technology. To the same purpose, Zhu et al.<sup>291</sup> developed an economic gel composite membrane based on glass fiber mats; these displayed high safety and good mechanical strength (**Fig. 25c**). The maximum stress and strain came to 14.3 MPa and 1.8%, respectively. The gelled membrane exhibits high ionic conductivity ( $1.13 \times 10^{-3}$  S cm<sup>-1</sup>), high Li ion transference number (0.56) and wide electrochemical window. Similarly, researchers added inorganic fillers such as SiO<sub>2</sub>, Al<sub>2</sub>O<sub>3</sub>, TiO<sub>2</sub> or MgO, etc. to improve mechanical strength and electrochemical properties. Tu et al.<sup>292</sup> prepared a dendrite-free polymer/ceramic composite electrolyte using porous Al<sub>2</sub>O<sub>3</sub> films and PVDF (**Fig. 25d**). The electrolyte demonstrated excellent mechanical strength and good ionic conductivity. Electrolyte membranes with strong shear modulus can suppress lithium dendrite growth.<sup>12</sup> In addition to the mechanical strength, another problem of PVDF or PVDF-HFP electrolyte is the interfacial instability against Li metal anode. Generally, electrolyte membranes with high storage modulus can suppress lithium dendrite growth to achieve stable Li metal anodes.<sup>12</sup> However, in recent years this

statement has proved to be insufficient.<sup>293, 294</sup> It is reported that dendrite suppression via inducing plastic deformation will be much efficiency than developing polymer electrolytes with high shear modulus.<sup>293</sup> But developing polymer electrolytes is still one of the best choices to pave the way for high energy density Li-based batteries.

PMMA, PVC and PAN also can be used to prepare gel polymer electrolytes. Each polymer matrix has its advantage, but cannot fulfill all the requirements for the best cell performance. Blending, copolymerization and crosslinking are strategies to fabricate an electrolyte with all needed advantages.

### 3.3.2. Quasi solid electrolytes

Besides inorganic-based, polymer-based and gel polymer-based electrolytes, some composite systems with liquid electrolytes have also been used as solid electrolytes in batteries. These systems can be designated as quasi-solid electrolytes.

Gong et al.<sup>295</sup> developed an electrolyte membrane fabricated by biopolymer of lignin, then activated it by immersion in liquid electrolytes. Before 100 °C, the electrolyte did not loss any weight and was thermally stable. It shows a high ionic conductivity of

**Table 2** Characteristics of solid state electrolytes used for lithium batteries

Electrolyte	Typical example	Ionic conductivity (S cm <sup>-1</sup> )	Advantages	Limitations
Crystalline	Perovskite, NASICON, LISICON, garnet	$10^{-5} \sim 10^{-3}$	High chemical and electrochemical stability, high oxidation voltage, high mechanical strength	Inelastic, expensive for large-scale production
Amorphous	Li <sub>2</sub> S-P <sub>2</sub> S <sub>5</sub>	$10^{-8} \sim 10^{-3}$	High ionic conductivity	Sensitive to moisture
Thio-LISICON	Li <sub>10</sub> GeP <sub>2</sub> S <sub>12</sub>	$10^{-3}$	High Li <sup>+</sup> transference numbers, stable against lithium metal anode and thermal stability	High operation temperature, low conductivity, poor rate capability,
LIPON	Li <sub>0.99</sub> PO <sub>2.55</sub> N <sub>0.3</sub>	$10^{-7}$	Stable with lithium metal anode and cathode materials	Expensive for large-scale production
Glass-ceramic	LATP, LAGP	$10^{-4} \sim 10^{-3}$	Lower grain-boundary resistance	low oxidation stability
Solid polymer	PEO	$10^{-4} \sim 10^{-3}$ (elevated temperature)	Flexible, stable with lithium anode, easy to be fabricated	unstable at elevated temperature, low oxidation voltage
Gel polymer	PVDF, PVDF-HFP	$10^{-3}$	Higher conductivity than solid polymer electrolytes, mechanically stable	evaporation, still leakage, poorer battery performance than organic liquid electrolytes
Ionic liquid & polymerized ionic liquid	EMimTFSI, PYR <sub>13</sub> TFSI, PPYR <sub>11</sub> TFSI	$10^{-6} \sim 10^{-3}$	High conductivity, large capacity, no vapor pressure and non-flammability of electrolytes	expensive for large-scale production

$3.73 \times 10^{-3} \text{ S cm}^{-1}$  at room temperature and a high Li ion transference number of 0.85. The electrolyte was compatible with lithium metal anode and had a wide electrochemical window of up to 7.5 V. Li et al.<sup>296</sup> reported a solid electrolyte based on nanoporous graphene-analogues g-BN nanosheets confining ionic liquids. The amount of ILs was as much as 10 times of the host's weight. These nanosheets demonstrated high ionic conductivity of  $3.85 \times 10^{-3} \text{ S cm}^{-1}$  at 25 °C, even  $2.32 \times 10^{-4} \text{ S cm}^{-1}$  at -20 °C. Similarly, ILs electrolytes were filled in mesoporous silica, and the materials could also exhibit good Li ion transference number of > 0.8 and an electrochemical window of > 5 V.<sup>297</sup> Wu et al.<sup>298</sup> presented a  $\text{Ti}(\text{OH})_4$  sol electrolyte prepared via a nonaqueous self-assembly sol-gel process, in which ionic liquid electrolyte was immobilized within an inorganic gel (**Fig. 26a,b**). Batteries using  $\text{LiFePO}_4$  cathodes and ionogel electrolytes offered a capacity of 150 mAh  $\text{g}^{-1}$  for over 300 cycles, and even at a 2 C rate, the capacity still stayed above 98 mAh  $\text{g}^{-1}$ . The electrolyte exhibited a liquid-like ionic conductivity above  $1 \times 10^{-3} \text{ S cm}^{-1}$  at room temperature. Later, Wu's group<sup>299</sup> developed a silica sol electrolyte and a solid-state Li-ion full cell technology. Solid-state full cells ( $\text{LiFePO}_4$ ,  $\text{LiCoO}_2$ ,  $\text{LiCo}_{1/3}\text{Ni}_{1/3}\text{Mn}_{1/3}\text{O}_2$  as cathodes, and MCMB as anode) all delivered high specific capacities (144.6 mAh  $\text{g}^{-1}$  for over 100 cycles), long cycling stability, and excellent high-temperature performances (**Fig. 26c,d**). The silica sol electrolyte can also be synthesized by organically modified silica.<sup>300</sup>

### 3.4. Ionic Liquids in solid electrolytes

#### 3.4.1. Ionic liquids in solid electrolytes

Polymer electrolytes usually possess low ionic conductivity at room temperature. The addition of plasticizer and solvent can enhance their room temperature ionic conductivity. Ionic liquids can be used as a kind of plasticizer or solvent in solid/gel electrolyte systems, with no volatile and no flammable properties. Interactions between PEO and different ionic liquids can be characterized by hard and soft acid and base theory.<sup>301</sup> EO segments in PEO matrix are hard base. ILs with hard cations show good miscibility with PEO, such as imidazolium groups; conversely, pyrrolidinium groups show poor miscibility. Shin et al.<sup>302</sup> added  $\text{PYR}_{13}\text{TFSI}$  into  $\text{PEO}_{20}\text{-LiTFSI}$  to form an IL-based solid polymer electrolyte. The composite electrolyte had an ionic conductivity of  $\sim 10^{-4} \text{ S cm}^{-1}$  at 20 °C. Fisher et al.<sup>303</sup> prepared a solid polymer electrolyte by adding triethyl sulfonium bis(trifluorosulfonyl)imide ( $\text{S}_2\text{TFSI}$ ) into  $\text{PEO}_{20}\text{-LiTFSI}$ . The hybrid electrolyte possessed a sufficient ionic conductivity,  $1.17 \times 10^{-4} \text{ S cm}^{-1}$  at 0 °C, and  $1.20 \times 10^{-3} \text{ S cm}^{-1}$  at 25 °C. At the temperature of the human body (37 °C), ionic conductivity of the hybrid electrolyte system approached to  $1 \times 10^{-2} \text{ S cm}^{-1}$ . The system demonstrated reversible cathodic stability, up to 4.5 V, and long term cycling stability against metallic lithium. Susan et al.<sup>304</sup> exploited a high ionic conductivity of ionic liquid-based gel polymer electrolyte. *In situ* free radical polymerization of compatible vinyl monomers at room temperature ionic liquid, 1-ethyl-3-methyl imidazolium bis(trifluoromethane sulfonyl)imide (EMITFSI), afforded a novel series of polymer electrolytes. Polymer gels obtained by the polymerization of methyl methacrylate (MMA) in EMITFSI with a small amount of a cross-linker could give a self-standing, flexible, and optically-clear film. And the ionic conductivity reached a value about  $10^{-2} \text{ S cm}^{-1}$  at ambient temperature.

#### 3.4.2. Poly ionic liquid based solid electrolytes

Polymerized or poly(ionic liquids) are polymers derived from ionic liquids. In the structure of poly(ionic liquids), either the cations or anions are participated within the backbone of matrix.<sup>301</sup> Poly(diallyldimethylammonium)TFSI ( $\text{PPYR}_{11}\text{TFSI}$ ) cooperated with  $\text{PYR}_{14}\text{TFSI}$  and  $\text{LiTFSI}$  was exploited by Pont et al.<sup>305,306</sup> The research showed that higher ionic liquid content had led to higher ionic conductivity. The highest ionic conductivity of  $5 \times 10^{-4} \text{ S cm}^{-1}$  was found at the ionic liquid content of 60 wt % and temperature of 40 °C. A series of guanidinium polymeric ionic liquid (PIL) electrolyte membranes combining different anions, such as  $\text{BF}_4^-$ ,  $\text{PF}_6^-$ ,  $\text{ClO}_4^-$  and TFSI, were synthesized through copolymerization or anion exchange processes.<sup>307</sup> Specifically, the  $\text{BF}_4^-$  anode possessed the best thermal stability; the TFSI anode showed the lowest  $T_g$  and enhanced the ionic conductivity. Pyrrolidinium based poly(ionic liquid) (PIL) electrolytes with poly (ethylene glycol) (PEG) side chains was reported by Döbbelin et al.<sup>308</sup> The obtained electrolyte displayed very good ionic conductivities, in the optimal case of up to  $2.4 \times 10^{-3} \text{ S cm}^{-1}$  at 25 °C and  $1.02 \times 10^{-2} \text{ S cm}^{-1}$  at 100 °C. A PIL- $\text{LiTFSI-PYR}_{13}\text{TFSI-SiO}_2$  electrolyte membrane was found to be chemically stable even at 80 °C in contact with lithium metal anode and thermally stable up to 320 °C.<sup>309</sup> Particularly, LMBs using the quaternary polymer electrolytes exhibit high lithium ion conductivity at high temperature, wide electrochemical stability window, low time-storage interfacial resistance values and good lithium stripping/plating performance. Even at 80 °C, LMBs were capable to deliver 140 mAh  $\text{g}^{-1}$  at 0.1 C with good capacity retention. Kuo et al.<sup>310</sup> used an oligomeric ionic liquid (OIL) to synthesize a PVDF-HFP based based gel polymer electrolyte (**Fig. 27**). The gel polymer electrolyte showed a low interfacial resistance. The electrolyte possessed high ionic conductivities of  $2.0 \times 10^{-3} \text{ S cm}^{-1}$  at 30 °C and  $6.6 \times 10^{-3} \text{ S cm}^{-1}$  at 80 °C, respectively, though the liquid electrolyte uptake was low (< 50%). These two factors result in high cell capacity under different charge/discharge rates.

Thus, we have provided a extensive overview of solid state electrolytes for lithium batteries. The characteristics of these electrolytes are summarized in **Table 2**.

## 4. Challenges and Perspectives

The principal issues facing the development of lithium-based batteries for the vehicle industry are safety, rate capacity and energy density. To improve the safety of an electrolyte, the inflammable solvents like ionic liquids and sulfone-based solvents, have been developed. To improve the energy density, high voltage electrolytes have been designed through the inclusion of new high voltage solvents and additives. In this review, four aspects of electrolytes of current investigations including (i) high voltage solvents, (ii) additives, (iii) ionic liquids, and (iv) superconcentrated salt strategy have been discussed. These new components always have one or more desirable functions toward the improvement of battery performance. However, they may simultaneously introduce some negative impacts. For example, the completely new electrolyte solvents, like sulfone-based solvents and the ionic liquids with high anodic stability and inflammability, still confront

severe capacity fading and inferior rate performance because of their high viscosity, poor wettability with a separator and poor SEI forming ability on the graphite anode. Blending the traditional carbonate solvents with the new high voltage solvents can mitigate these restrictions. A working mechanism of the high voltage additives is their sacrificial decomposition to form a protective film on the electrode surface which can inhibit the dissolution of the cathode materials and the oxidative decomposition of the solvents. A small amount of additive can significantly improve the battery performance, so the development of additives is essential for the next generation high voltage LIBs.

The superconcentrated salt strategy is a new route combining various useful functionalities, such as improved reductive and oxidative stability owing to the peculiar structure at a high salt concentration. For example, the superconcentrated salt strategy can improve the reductive and oxidative stability of acetonitrile and the ethers, respectively, to expand the stable range of solvents in lithium-based batteries. In addition, the superconcentrated salt strategy can also improve the Al-anti corrosion ability and the electrode reaction kinetics to allow the electrolyte not to rely on  $\text{LiPF}_6$  salt for the passivation of aluminum current collector and attaining the fast charging process. As a result, a lot of lithium salts and aprotic solvents can be used in LIBs to diversify the electrolyte design. Noticeably high rate capability and high voltage tolerant ability have been demonstrated in the laboratories worldwide. However, there are still several problems to be overcome before the practical application of the superconcentrated salt. These are high viscosity, poor wettability with the separator and high cost (mostly because of large requirements for lithium salts). Thus these studies still have a long way to go before their final practical accomplishment. Nonetheless, such fundamental studies are still significantly meaningful. They can give a guide to rebuild the composition of the electrolyte through optimization, such as smart selection of solvents, lithium salts and concentration.

The solid state electrolyte is the key component in advanced solid state lithium batteries. High ionic conductivity, good charging/discharging performance, decent mechanical strength to suppress lithium dendrite growth, high chemical and thermal stability are important properties that should be highlighted.

Inorganic solid electrolytes include NASICON-type, LISICON-type, perovskite-type, garnet-type and sulfide-based glass-ceramics. Among these electrolytes, sulfides have the highest ionic conductivities, but they are sensitive to humidity and chemically unstable. Garnet-type and perovskite-type inorganic solid electrolytes are particularly becoming attractive in recent years due to their high ionic conductivities and chemical stabilities, but these electrolytes show poor interfacial compatibility with electrodes. To overcome these challenges, three possible directions are proposed: (1) increasing the conductivity of the solid electrolytes; (2) optimizing their structures; (3) using interfacial engineering to decrease the interfacial resistance and to stabilize the lithium metal anode.

Solid polymer electrolytes comprise polymer organic frameworks, lithium salts and fillers. PEO-based polymer electrolytes possess low ionic conductivity at room temperature, which is attributed to the crystallization of PEO phase. Strategies of blending, crosslinking, copolymerization and adding fillers can suppress crystallization and increase ionic conductivity at different levels. Even so, the ionic conductivities of solid polymer electrolytes are still two orders of magnitude lower than those of solid inorganic electrolytes. Meanwhile, PEO-based polymer electrolytes show instabilities at elevated temperature and low oxidation voltage. Further research should be focused on the modification of PEO chains and the development of new structures.

Gel polymer electrolytes are formed by adding plasticizers or solvents in solid polymer electrolytes. The plasticizers or solvents can be ether solvents, liquid oligomers, ionic liquids. PVDF and PVDF-HFP are elite candidates as polymer matrixes for gel polymer electrolytes. These electrolytes exhibit good performance in electrochemical measurements and cell operations, which is due to the predominant liquid phase. On the one hand, organic liquids are inflammable and they increase the safety risk of lithium batteries in operation. On the other hand, too much organic liquids can decrease mechanical strength of gel polymer matrices and cause short circuiting under lithium dendrite penetration through the gel polymer electrolytes. The addition of fillers can enhance the mechanical strength of the electrolytes and nonflammable solvents, like ionic liquids, and to ensure the safe use of lithium batteries.

Polymer electrolytes, based on ionic liquids and polymerized ionic liquids, exhibit high ionic conductivity and high interfacial stability against lithium metal anode. The good properties make these electrolytes promising polymer electrolytes in future LIBs.

Overall, researchers have achieved a great progress in the design of solid electrolytes and development of solid state lithium batteries. In the future, the inorganic solid electrolytes may be applied in power batteries for vehicles and large scale power grids. In addition, the polymer electrolytes may be assembled in flexible batteries for flexible screens, wearable devices and other 3C products.

## Conflicts of interest

There are no conflicts to declare.

## Acknowledgements

This work was supported by National Natural Science Foundation of China (No. 91534109 and 21276257), the "Strategic Priority Research Program" of the Chinese Academy of Sciences (No. XDA09010103), National Key Projects for Fundamental Research and Development of China (No. 2016YFB0100104), Beijing Municipal Science and Technology Project (D171100005617001) and Henan province science and technology cooperation project (172106000061). D. Golberg is grateful to the Australian Research Council for granting a Laureate Fellowship.

## References

- 1 B. L. Ellis, P. Knauth and T. Djenizian, *Adv. Mater.*, 2014, **26**, 3368.
- 2 J. B. Goodenough and K. S. Park, *J. Am. Chem. Soc.*, 2013, **135**, 1167.
- 3 J.-W. Jung, W.-H. Ryu, J. Shin, K. Park and I.-D. Kim, *Acs Nano*, 2015, **9**, 6717.
- 4 N. Liu, Z. D. Lu, J. Zhao, M. T. McDowell, H. W. Lee, W. T. Zhao and Y. Cui, *Nat. Nanotechnol.*, 2014, **9**, 187.
- 5 X. Su, Q. Wu, J. Li, X. Xiao, A. Lott, W. Lu, B. W. Sheldon and J. Wu, *Adv. Energy Mater.*, 2014, **4**, 1300882.
- 6 K. Xu, *Chem. Rev.*, 2014, **114**, 11503.
- 7 A. Manthiram, X. Yu and S. Wang, *Nat. Rev. Mater.*, 2017, **2**, 16103.
- 8 C. Sun, J. Liu, Y. Gong, D. P. Wilkinson and J. Zhang, *Nano Energy*, 2017, **33**, 363.
- 9 L. Long, S. Wang, M. Xiao and Y. Meng, *J. Mater. Chem. A*, 2016, **4**, 10038.
- 10 Q. Li, J. Chen, L. Fan, X. Kong and Y. Lu, *Green Energy & Environment*, 2016, **1**, 18.
- 11 X. Fu, D. Yu, J. Zhou, S. Li, X. Gao, Y. Han, P. Qi, X. Feng and B. Wang, *Crystengcomm*, 2016, **18**, 4236.
- 12 M. D. Tikekar, S. Choudhury, Z. Tu and L. A. Archer, *Nat. Energy*, 2016, **1**, 16114.
- 13 L. Fan, S. Wei, S. Li, Q. Li and Y. Lu, *Adv. Energy Mater.*, 2018, **8**, 1702657.
- 14 V. Etacheri, R. Marom, R. Elazari, G. Salitra and D. Aurbach, *Energy Environ. Sci.*, 2011, **4**, 3243.
- 15 B. Scrosati, J. Hassoun and Y. K. Sun, *Energy Environ. Sci.*, 2011, **4**, 3287.
- 16 Y. Yamada and A. Yamada, *J. Electrochem. Soc.*, 2015, **162**, A2406.
- 17 Y. Liu, S. Fang, P. Shi, D. Luo, L. Yang and S.-i. Hirano, *J. Power Sources*, 2016, **331**, 445.
- 18 Y. Liu, S. Fang, D. Luo, L. Yang and S.-i. Hirano, *J. Electrochem. Soc.*, 2016, **163**, A1951.
- 19 Z. Zeng, B. Wu, L. Xiao, X. Jiang, Y. Chen, X. Ai, H. Yang and Y. Cao, *J. Power Sources*, 2015, **279**, 6.
- 20 Y. Wang and W.-H. Zhong, *Chemelectrochem*, 2015, **2**, 22.
- 21 X. Sun, X. Zhu, X. Yang, J. Sun, Y. Xia and D. Yang, *Green Energy & Environment*, 2017, **2**, 160.
- 22 X. Zhang, X.-G. Wang, Z. Xie and Z. Zhou, *Green Energy & Environment*, 2016, **1**, 4.
- 23 Y. Lu, *Green Energy & Environment*, 2016, **1**, 3.
- 24 W. Li, S. Chen, J. Yu, D. Fang, B. Ren and S. Zhang, *Green Energy & Environment*, 2016, **1**, 91.
- 25 Y. Luo, T. L. Lu, Y. X. Zhang, L. Q. Yan, J. Y. Xie and S. S. Mao, *J. Power Sources*, 2016, **323**, 134.
- 26 A. Manthiram, *J. Phys. Chem. Lett.*, 2011, **2**, 176.
- 27 K. Xu, *Chem. Rev.*, 2004, **104**, 4303.
- 28 G. M. Zhou, F. Li and H. M. Cheng, *Energy Environ. Sci.*, 2014, **7**, 1307.
- 29 M. D. Bhatt and C. O'Dwyer, *Chem. Phys. Lett.*, 2015, **618**, 208.
- 30 H. Zhao, S.-J. Park, F. Shi, Y. Fu, V. Battaglia, P. N. Ross, Jr. and G. Liu, *J. Electrochem. Soc.*, 2014, **161**, A194.
- 31 M. D. Bhatt, M. Cho and K. Cho, *J. Solid State Electr.*, 2012, **16**, 435.
- 32 C. X. Wang, H. Nakamura, H. Komatsu, H. Noguchi, M. Yoshio and H. Yoshitake, *Denki Kagaku*, 1998, **66**, 286.
- 33 M. D. Bhatt, M. Cho and K. Cho, *Appl. Surf. Sci.*, 2010, **257**, 1463.
- 34 B. Jiang, V. Ponnuchamy, Y. N. Shen, X. M. Yang, K. J. Yuan, V. Vetere, S. Mossa, I. Skarmoutsos, Y. F. Zhang and J. R. Zheng, *J. Phys. Chem. Lett.*, 2016, **7**, 3554.
- 35 D. Ortiz, I. J. Gordon, S. Legand, V. Dauvois, J. P. Baltaze, J. L. Marignier, J. F. Martin, J. Belloni, M. Mostafavi and S. Le Caer, *J. Power Sources*, 2016, **326**, 285.
- 36 S. Das and A. Ghosh, *Journal of Physics D-Applied Physics*, 2016, **49**, 235601.
- 37 J. Inamoto, T. Fukutsuka, K. Miyazaki and T. Abe, *Chemistryselect*, 2017, **2**, 2895.
- 38 E. G. Leggesse, R. T. Lin, T.-F. Teng, C.-L. Chen and J.-C. Jiang, *J. Phys. Chem. A*, 2013, **117**, 7959.
- 39 M. J. Boyer, L. Vilčiauskas and G. S. Hwang, *Phys. Chem. Chem. Phys.*, 2016, **18**, 27868.
- 40 S. S. Zhang, K. Xu and T. R. Jow, *J. Electrochem. Soc.*, 2002, **149**, A586.
- 41 T. Doi, Y. Shimizu, M. Hashinokuchi and M. Inaba, *J. Electrochem. Soc.*, 2017, **164**, A6412.
- 42 H. Zhou, K. Xiao and J. Li, *J. Power Sources*, 2016, **302**, 274.
- 43 M. Dahbi, F. Ghamouss, F. Tran-Van, D. Lemordant and M. Anouti, *J. Power Sources*, 2011, **196**, 9743.
- 44 D. Enslin, M. Stjerndahl, A. Nyten, T. Gustafsson and J. O. Thomas, *J. Mater. Chem.*, 2009, **19**, 82.
- 45 Y. Xie, H. Xiang, P. Shi, J. Guo and H. Wang, *J. Membrane Sci.*, 2017, **524**, 315.
- 46 M. Iliku, A. Khetan, S. Yang, U. Simon, H. Pitsch and D. U. Sauer, *ACS Appl. Mater. Interfaces*, 2017, **9**, 19319.
- 47 X. Q. Zhang, X. Chen, X. B. Cheng, B. Q. Li, X. Shen, C. Yan, J. Q. Huang and Q. Zhang, *Angew. Chem. Int. Ed.*, 2018, **57**, 5301.
- 48 Y. Watanabe, S. I. Kinoshita, S. Wada, K. Hoshino, H. Morimoto and S. I. Tobishima, *J. Power Sources*, 2008, **179**, 770.
- 49 C. S. Kim, S. M. Oh, *Electrochim. Acta*, 2000, **45**, 2101.
- 50 O. O. Postupna, Y. V. Kolesnik, O. N. Kalugin and O. V. Prezhdo, *J. Phys. Chem. B*, 2011, **115**, 14563.
- 51 C. M. Burba, R. Frech, *J. Phys. Chem. B*, 2005, **109**, 15161.
- 52 H. Tsunekawa, A. Narumi, M. Sano, A. Hiwara, M. Fujita and H. Yokoyama, *J. Phys. Chem. B*, 2003, **107**, 10962.
- 53 V. P. Reddy, M. C. Smart, K. B. Chin, B. V. Ratnakumar, S. Surampudi, J. Hu, P. Yan and G. K. Surya Prakash, *Electrochem. Solid State Lett.* 2005, **8**, A294.
- 54 Y. Y. Zhang, M. Su, X. F. Yu, Y. F. Zhou, J. G. Wang, R. G. Cao, W. Xu, C. M. Wang, D. R. Baer and O. Borodin, *Anal. Chem.*, 2018, **90**, 3341.
- 55 N. S. Choi, J. G. Han, S. Y. Ha, I. Park and C. K. Back, *Rsc Adv.*, 2015, **5**, 2732.
- 56 S. Tan, Y. J. Ji, Z. R. Zhang and Y. Yang, *Chemphyschem*, 2014, **15**, 1956.
- 57 J. Hassoun and B. Scrosati, *J. Electrochem. Soc.*, 2015, **162**, A2582.
- 58 X. R. Lin, M. Salari, L. M. R. Arava, P. M. Ajayan and M. W. Grinstaff, *Chem. Soc. Rev.*, 2016, **45**, 5848.
- 59 B. Flamme, G. R. Garcia, M. Weil, M. Haddad, P. Phansavath, V. Ratovelomanana-Vidal and A. Chagnes, *Green Chemistry*, 2017, **19**, 1828.
- 60 L. Xue, S.-Y. Lee, Z. Zhao and C. A. Angell, *J. Power Sources*, 2015, **295**, 190.
- 61 M. Hu, X. L. Pang and Z. Zhou, *J. Power Sources*, 2013, **237**, 229.
- 62 A. Abouimrane, I. Belharouak and K. Amine, *Electrochem. Commun.*, 2009, **11**, 1073.
- 63 K. Xu and C. A. Angell, *J. Electrochem. Soc.*, 2002, **149**, A920.
- 64 N. Shao, X. G. Sun, S. Dai and D. E. Jiang, *J. Phys. Chem. B*, 2011, **115**, 12120.
- 65 J. Xia and J. R. Dahn, *J. Power Sources*, 2016, **324**, 704.
- 66 C. C. Su, M. N. He, P. Redfern, L. A. Curtiss, C. Liao, L. Zhang, A. K. Burrell and Z. C. Zhang, *Chemelectrochem*, 2016, **3**, 790.
- 67 L. G. Xue, S. Y. Lee, Z. F. Zhao and C. A. Angell, *J. Power Sources*, 2015, **295**, 190.
- 68 X.-G. Sun and C. A. Angell, *Electrochem. Commun.*, 2005, **7**, 261.
- 69 F. Wu, J. Xiang, L. Li, J. Z. Chen, G. Q. Tan and R. J. Chen, *J. Power Sources*, 2012, **202**, 322.
- 70 L. G. Xue, K. Ueno, S. Y. Lee and C. A. Angell, *J. Power Sources*, 2014, **262**, 123.
- 71 T. Achiha, T. Nakajima, Y. Ohzawa, M. Koh, A. Yamauchi, M.

- Kagawa and H. Aoyama, *J. Electrochem. Soc.*, 2009, **156**, A483.
- 72 G. Q. Ma, L. Wang, J. J. Zhang, H. C. Chen, X. M. He and Y. S. Ding, *Prog. Chem.*, 2016, **28**, 1299.
- 73 Z. C. Zhang, L. B. Hu, H. M. Wu, W. Weng, M. Koh, P. C. Redfern, L. A. Curtiss and K. Amine, *Energy Environ. Sci.*, 2013, **6**, 1806.
- 74 C. Y. Wang, S. H. Tang, X. X. Zuo, X. Xiao, J. S. Liu and J. M. Nan, *J. Electrochem. Soc.*, 2015, **162**, A1997.
- 75 X. S. Wang, X. W. Zheng, Y. H. Liao, Q. M. Huang, L. D. Xing, M. Q. Xu and W. S. Li, *J. Power Sources*, 2017, **338**, 108.
- 76 C. Y. Wang, L. Yu, W. Z. Fan, J. W. Liu, L. Z. Ouyang, L. C. Yang and M. Zhu, *ACS Appl. Mater. Interfaces*, 2017, **9**, 9630.
- 77 M. Nagahama, N. Hasegawa and S. Okada, *J. Electrochem. Soc.*, 2010, **157**, A748.
- 78 E. Nanini-Maury, J. Swiatowska, A. Chagnes, S. Zanna, T. V. Pierre, P. Marcus and M. Cassir, *Electrochim. Acta*, 2014, **115**, 223.
- 79 Y. Xu, L. Y. Wan, J. L. Liu, L. C. Zeng and Z. G. Yang, *J. Alloys Compd.*, 2017, **698**, 207.
- 80 C. C. Su, M. He, P. C. Redfern, L. A. Curtiss, I. A. Shkrob and Z. C. Zhang, *Energy Environ. Sci.*, 2017, **10**, 900.
- 81 S. S. Zhang, *J. Power Sources*, 2006, **162**, 1379.
- 82 X. Z. Zheng, W. G. Wang, T. Huang, G. H. Fang, Y. Pan and M. X. Wu, *J. Power Sources*, 2016, **329**, 450.
- 83 D. Aurbach, Y. Eineli, O. Chusid, Y. Carmeli, M. Babai and H. Yamin, *J. Electrochem. Soc.*, 1994, **141**, 603.
- 84 W. N. Huang, L. D. Xing, Y. T. Wang, M. Q. Xu, W. S. Li, F. C. Xie and S. G. Xia, *J. Power Sources*, 2014, **267**, 560.
- 85 S. J. Lee, J. G. Han, Y. Lee, M. H. Jeong, W. C. Shin, M. Ue and N. S. Choi, *Electrochim. Acta*, 2014, **137**, 1.
- 86 R. Zheng, W. Wang, Y. Dai, Q. Ma, Y. Liu, D. Mu, R. Li, J. Ren and C. Dai, *Green Energy & Environment*, 2017, **2**, 42.
- 87 X. Zhang, F. Cheng, J. Yang and J. Chen, *Nano Lett.*, 2013, **13**, 2822.
- 88 D. Aurbach, B. Markovsky, Y. Talyossef, G. Salitra, H.-J. Kim and S. Choi, *J. Power Sources*, 2006, **162**, 780.
- 89 J. Liu and A. Manthiram, *J. Electrochem. Soc.*, 2009, **156**, A833.
- 90 X. L. Xu, S. X. Deng, H. Wang, J. B. Liu and H. Yan, *Nano-Micro Letters*, 2017, **9**, 19.
- 91 Y. Zhang, Y. Pan, J. Liu, G. Wang and D. Cao, *Chemical Research in Chinese Universities*, 2015, **31**, 117.
- 92 M. K. Devaraju, T. Quang Duc, H. Hyodo, Y. Sasaki and I. Honma, *Sci. Rep.*, 2015, **5**, 11041.
- 93 J. Ni, H. Wang, L. Gao and L. Lu, *Electrochim. Acta*, 2012, **70**, 349.
- 94 V. Aravindan, Y. L. Cheah, W. C. Ling and S. Madhavi, *J. Electrochem. Soc.*, 2012, **159**, A1435.
- 95 J. L. Allen, T. R. Jow and J. Wolfenstine, *J. Power Sources*, 2011, **196**, 8656.
- 96 P. Dong, D. Wang, Y. Yao, X. Li, Y. J. Zhang, J. J. Ru and T. Ren, *J. Power Sources*, 2017, **344**, 111.
- 97 T. Yim, K. S. Kang, J. Mun, S. H. Lim, S. G. Woo, K. J. Kim, M. S. Park, W. Cho, J. H. Song, Y. K. Han, J. S. Yu and Y. J. Kim, *J. Power Sources*, 2016, **302**, 431.
- 98 S. Kim, M. Kim, I. Choi and J. J. Kim, *J. Power Sources*, 2016, **336**, 316.
- 99 W. Lu, J. Zhang, J. Xu, X. Wu and L. Chen, *ACS Appl. Mater. Interfaces*, 2017, **9**, 19313.
- 100 M. D. Bhatt and C. O'Dwyer, *Curr. Appl. Phys.*, 2014, **14**, 349.
- 101 A. M. Haregewoin, E. G. Leggesse, J.-C. Jiang, F.-M. Wang, B.-J. Hwang and S. D. Lin, *J. Power Sources*, 2013, **244**, 318.
- 102 L. J. Miara, W. D. Richards, Y. E. Wang and G. Ceder, *Chem. Mater.*, 2015, **27**, 4040.
- 103 P. Jankowski, W. Wiecek and P. Johansson, *J. Mol. Model.*, 2017, **23**, 9.
- 104 A. von Cresce and K. Xu, *J. Electrochem. Soc.*, 2011, **158**, A337.
- 105 B. W. Deng, H. Wang, W. J. Ge, X. Li, X. X. Yan, T. Chen, M. Z. Qu and G. C. Peng, *Electrochim. Acta*, 2017, **236**, 61.
- 106 X. R. Yang, J. H. Li, L. D. Xing, Y. H. Liao, M. Q. Xu, Q. M. Huang and W. S. Li, *Electrochim. Acta*, 2017, **227**, 24.
- 107 J. H. Li, L. D. Xing, R. Q. Zhang, M. Chen, Z. S. Wang, M. Q. Xu and W. S. Li, *J. Power Sources*, 2015, **285**, 360.
- 108 B. Wang, Q. T. Qu, Q. Xia, Y. P. Wu, X. Li, C. L. Gan and T. van Ree, *Electrochim. Acta*, 2008, **54**, 816.
- 109 L. Imholt, S. Roser, M. Borner, B. Streipert, B. R. Rad, M. Winter and I. Cekic-Laskovic, *Electrochim. Acta*, 2017, **235**, 332.
- 110 S. Dalavi, M. Q. Xu, B. Knight and B. L. Lucht, *Electrochem. Solid State Lett.*, 2012, **15**, A28.
- 111 P. K. Nayak, J. Grinblat, M. Levi and D. Aurbach, *J. Electrochem. Soc.*, 2015, **162**, A596.
- 112 M. Q. Xu, L. Zhou, Y. N. Dong, Y. J. Chen, J. Demeaux, A. D. MacIntosh, A. Garsuch and B. L. Lucht, *Energy Environ. Sci.*, 2016, **9**, 1308.
- 113 J. H. Li, L. P. Zhang, L. Yu, W. Z. Fan, Z. S. Wang, X. R. Yang, Y. L. Lin, L. D. Xing, M. Q. Xu and W. S. Li, *J. Phys. Chem. C*, 2016, **120**, 26899.
- 114 K. Abe, Y. Ushigoe, H. Yoshitake and M. Yoshio, *J. Power Sources*, 2006, **153**, 328.
- 115 H. Lee, T. Han, K. Y. Cho, M. H. Ryou and Y. M. Lee, *ACS Appl. Mater. Interfaces*, 2016, **8**, 21366.
- 116 A. Abouimrane, S. A. Odom, H. Tavassol, M. V. Schulmerich, H. M. Wu, R. Bhargava, A. A. Gewirth, J. S. Moore and K. Amine, *J. Electrochem. Soc.*, 2013, **160**, A268.
- 117 L. Liu, M. Qing, Y. Wang and S. Chen, *J. Mater. Sci. Technol.*, 2015, **31**, 599.
- 118 J.-N. Lee, G.-B. Han, M.-H. Ryou, D. J. Lee, S. Jongchan, J. W. Choi and J.-K. Park, *Electrochim. Acta*, 2011, **56**, 5195.
- 119 J. Zhang, J. L. Wang, J. Yang and Y. N. Nuli, *Electrochim. Acta*, 2014, **117**, 99.
- 120 X. Zheng, T. Huang, Y. Pan, W. Wang, G. Fang and M. Wu, *J. Power Sources*, 2015, **293**, 196.
- 121 J. Xia, J. E. Harlow, R. Petibon, J. C. Burns, L. P. Chen and J. R. Dahn, *J. Electrochem. Soc.*, 2014, **161**, A547.
- 122 J. Xia, N. N. Sinha, L. P. Chen and J. R. Dahn, *J. Electrochem. Soc.*, 2014, **161**, A264.
- 123 J. Xia, S. L. Glazier, R. Petibon and J. R. Dahn, *J. Electrochem. Soc.*, 2017, **164**, A1239.
- 124 E. Markevich, V. Baranchugov and D. Aurbach, *Electrochem. Commun.*, 2006, **8**, 1331.
- 125 X. Cao, X. He, J. Wang, H. D. Liu, S. Roser, B. R. Rad, M. Evertz, B. Streipert, J. Li, R. Wagner, M. Winter and I. Cekic-Laskovic, *ACS Appl. Mater. Interfaces*, 2016, **8**, 25971.
- 126 T. Yim, M. S. Kwon, J. Mun and K. T. Lee, *Isr. J. Chem.*, 2015, **55**, 586.
- 127 G. A. Elia, U. Ulissi, S. Jeong, S. Passerini and J. Hassoun, *Energy Environ. Sci.*, 2016, **9**, 3210.
- 128 F. Wu, Q. Zhu, R. Chen, N. Chen, Y. Chen and L. Li, *Electrochim. Acta*, 2015, **184**, 356.
- 129 H. Nakagawa, *Electrochemistry*, 2015, **83**, 707.
- 130 D. R. MacFarlane, N. Tachikawa, M. Forsyth, J. M. Pringle, P. C. Howlett, G. D. Elliott, J. H. Davis, M. Watanabe, P. Simon and C. A. Angell, *Energy Environ. Sci.*, 2014, **7**, 232.
- 131 S. N. Chavan, A. Tiwari, T. C. Nagaiah and D. Mandal, *Phys. Chem. Chem. Phys.*, 2016, **18**, 16116.
- 132 A. Fericola, F. Croce, B. Scrosati, T. Watanabe and H. Ohno, *J. Power Sources*, 2007, **174**, 342.
- 133 Y. Wang, M. C. Turk, M. Sankarasubramanian, A. Srivatsa, D. Roy and S. Krishnan, *J. Mater. Sci.*, 2017, **52**, 3719.
- 134 X. He, Z. Wang, W. Zhou, X. Jiang, Z. Han and D. Chen, *J. Appl. Polym. Sci.*, 2017, **134**, 44884.
- 135 S. Kazemiabnavi, Z. C. Zhang, K. Thornton and S. Banerjee, *J. Phys. Chem. B*, 2016, **120**, 5691.
- 136 P. Bonhote, A. P. Dias, N. Papageorgiou, K. Kalyanasundaram and M. Gratzel, *Inorg. Chem.*, 1996, **35**, 1168.
- 137 P. A. Z. Suarez, C. S. Consorti, R. F. de Souza, J. Dupont and R. S. Goncalves, *J. Brazil. Chem. Soc.*, 2002, **13**, 106.
- 138 M. Ishikawa, T. Sugimoto, M. Kikuta, E. Ishiko and M. Kono, *J.*

- Power Sources*, 2006, **162**, 658.
- 139 M. H. Kowsari, M. Fakhraee, S. Alavi and B. Najafi, *J. Chem. Eng. Data*, 2014, **59**, 2834.
- 140 S. Seki, Y. Ohno, Y. Kobayashi, H. Miyashiro, A. Usami, Y. Mita, H. Tokuda, M. Watanabe, K. Hayamizu, S. Tsuzuki, M. Hattori and N. Terada, *J. Electrochem. Soc.*, 2007, **154**, A173.
- 141 Y. Shimizu, K. Fujii, M. Imanari and K. Nishikawa, *J. Phys. Chem. B*, 2015, **119**, 12552.
- 142 J. H. Lee, J. B. Ryu, A. S. Lee, W. Na, H. S. Yoon, W. J. Kim and C. M. Koo, *Electrochim. Acta*, 2016, **222**, 1847.
- 143 M. Montanino, M. Moreno, M. Carewska, G. Maresca, E. Simonetti, R. Lo Presti, F. Alessandrini and G. B. Appetecchi, *J. Power Sources*, 2014, **269**, 608.
- 144 S. Yamaguchi, M. Yoshizawa-Fujita, Y. Takeoka and M. Rikukawa, *J. Power Sources*, 2016, **331**, 308.
- 145 M. Agostini, S. Brutti, M. A. Navarra, S. Panero, P. Reale, A. Matic and B. Scrosati, *Sci. Rep.*, 2017, **7**, 1104.
- 146 A. I. Bhatt, P. Kao, A. S. Best and A. F. Hollenkamp, *J. Electrochem. Soc.*, 2013, **160**, A1171.
- 147 A. I. Bhatt, A. S. Best, J. H. Huang and A. F. Hollenkamp, *J. Electrochem. Soc.*, 2010, **157**, A66.
- 148 B. B. Yang, C. H. Li, J. H. Zhou, J. H. Liu and Q. L. Zhang, *Electrochim. Acta*, 2014, **148**, 39.
- 149 K. Ababtain, G. Babu, X. R. Lin, M. T. F. Rodrigues, H. Gullapalli, P. M. Ajayan, M. W. Grinstaff and L. M. R. Arava, *ACS Appl. Mater. Interfaces*, 2016, **8**, 15242.
- 150 A. Lewandowski and A. Swiderska-Mocek, *J. Power Sources*, 2009, **194**, 601.
- 151 V. Baranchugov, E. Markevich, E. Pollak, G. Salitra and D. Aurbach, *Electrochem. Commun.*, 2007, **9**, 796.
- 152 K. Kim, Y.-H. Cho and H.-C. Shin, *J. Power Sources*, 2013, **225**, 113.
- 153 K. Gao and S. D. Li, *J. Power Sources*, 2014, **270**, 304.
- 154 T. Belhocine, S. A. Forsyth, H. Q. N. Gunaratne, M. Nieuwenhuizen, P. Nockemann, A. V. Puga, K. R. Seddon, G. Srinivasan and K. Whiston, *Phys. Chem. Chem. Phys.*, 2015, **17**, 10398.
- 155 L. Fang, Y. F. Hu, J. G. Qi, Y. F. Chen, H. R. Zhang and H. Z. Huang, *Electrochim. Acta*, 2014, **133**, 440.
- 156 M. Shukla, H. Noothalapati, S. Shigeto and S. Saha, *Vib. Spectrosc.*, 2014, **75**, 107.
- 157 T. Dong, L. Zhang, S. M. Chen, X. M. Lu and S. J. Zhang, *Ionics*, 2015, **21**, 2109.
- 158 A. Lewandowski, A. Swiderska-Mocek and I. Acznik, *Electrochim. Acta*, 2010, **55**, 1990.
- 159 N. Bucher, S. Hartung, M. Arkhipova, D. Yu, P. Kratzer, G. Maas, M. Srinivasan and H. E. Hoster, *RSC Adv.*, 2014, **4**, 1996.
- 160 M. A. Navarra, K. Fujimura, M. Sgambetterra, A. Tsurumaki, S. Panero, N. Nakamura, H. Ohno and B. Scrosati, *ChemSusChem*, 2017, **10**, 2496.
- 161 G. B. Appetecchi, M. Montanino, M. Carewska, M. Moreno, F. Alessandrini and S. Passerini, *Electrochim. Acta*, 2011, **56**, 1300.
- 162 F. Trequattrini, O. Palumbo, S. Gatto, G. B. Appetecchi and A. Paolone, *Advances in Chemistry*, 2016, **2016**, 1.
- 163 S. L. Glazier, R. Petibon, J. Xia and J. R. Dahn, *J. Electrochem. Soc.*, 2017, **164**, A567.
- 164 Q. Q. Liu, D. J. Xiong, R. Petibon, C. Y. Du and J. R. Dahn, *J. Electrochem. Soc.*, 2016, **163**, A3010.
- 165 L. Ma, S. L. Glazier, R. Petibon, J. Xia, J. M. Peters, Q. Liu, J. Allen, R. N. C. Doig and J. R. Dahn, *J. Electrochem. Soc.*, 2017, **164**, A5008.
- 166 R. Petibon, J. Xia, L. Ma, M. K. G. Bauer, K. J. Nelson and J. R. Dahn, *J. Electrochem. Soc.*, 2016, **163**, A2571.
- 167 J. Xia, R. Petibon, D. J. Xiong, L. Ma and J. R. Dahn, *J. Power Sources*, 2016, **328**, 124.
- 168 Y. Yamada, K. Usui, C. H. Chiang, K. Kikuchi, K. Furukawa and A. Yamada, *ACS Appl. Mater. Interfaces*, 2014, **6**, 10892.
- 169 J. H. Wang, Y. Yamada, K. Sodeyama, C. H. Chiang, Y. Tateyama and A. Yamada, *Nat. Commun.*, 2016, **7**, 12032.
- 170 Y. Yamada, C. H. Chiang, K. Sodeyama, J. H. Wang, Y. Tateyama and A. Yamada, *Chemelectrochem*, 2015, **2**, 1687.
- 171 Y. Yamada, K. Furukawa, K. Sodeyama, K. Kikuchi, M. Yaegashi, Y. Tateyama and A. Yamada, *J. Am. Chem. Soc.*, 2014, **136**, 5039.
- 172 Y. Yamada, M. Yaegashi, T. Abe and A. Yamada, *Chem. Commun.*, 2013, **49**, 11194.
- 173 C. H. Yim, J. Tam, H. Soboleski and Y. Abu-Lebdeh, *J. Electrochem. Soc.*, 2017, **164**, A1002.
- 174 K. Yoshida, M. Nakamura, Y. Kazue, N. Tachikawa, S. Tsuzuki, S. Seki, K. Dokko and M. Watanabe, *J. Am. Chem. Soc.*, 2011, **133**, 13121.
- 175 K. Sodeyama, Y. Yamada, K. Aikawa, A. Yamada and Y. Tateyama, *J. Phys. Chem. C*, 2014, **118**, 14091.
- 176 Y. Yamada and A. Yamada, *Chem. Lett.*, 2017, **46**, 1056.
- 177 J. Qian, B. D. Adams, J. Zheng, W. Xu, W. A. Henderson, J. Wang, M. E. Bowden, S. Xu, J. Hu and J.-G. Zhang, *Adv. Funct. Mater.*, 2016, **26**, 7094.
- 178 L. M. Suo, W. J. Xue, M. Gobet, S. G. Greenbaum, C. Wang, Y. M. Chen, W. L. Yang, Y. X. Li and J. Li, *Proc. Natl. Acad. Sci. U. S. A.*, 2018, **115**, 1156.
- 179 O. Bohnke, *Solid State Ionics*, 2008, **179**, 9.
- 180 W. J. Kwon, H. Kim, K.-N. Jung, W. Cho, S. H. Kim, J.-W. Lee and M.-S. Park, *J. Mater. Chem. A*, 2017, **5**, 6257.
- 181 Z. D. Hood, H. Wang, A. Samuthira Pandian, J. K. Keum and C. Liang, *J. Am. Chem. Soc.*, 2016, **138**, 1768.
- 182 Y. Li, W. Zhou, S. Xin, S. Li, J. Zhu, X. Lu, Z. Cui, Q. Jia, J. Zhou, Y. Zhao and J. B. Goodenough, *Angew. Chem. Int. Ed.*, 2016, **55**, 9965.
- 183 B. Senthilkumar, Z. Khan, S. Park, I. Seo, H. Ko and Y. Kim, *J. Power Sources*, 2016, **311**, 29.
- 184 Z. Khan, S. Park, S. M. Hwang, J. Yang, Y. Lee, H.-K. Song, Y. Kim and H. Ko, *NPG Asia Mater.*, 2016, **8**, e294.
- 185 Z. Khan, B. Senthilkumar, S. O. Park, S. Park, J. Yang, J. H. Lee, H.-K. Song, Y. Kim, S. K. Kwak and H. Ko, *J. Mater. Chem. A*, 2017, **5**, 2037.
- 186 Z. Khana, N. Parveenb, S. A. Ansari, S. T. Senthilkumara, S. Parka, Y. Kima, M. H. Chob and H. Ko, *Electrochim. Acta*, 2017, **257**, 328.
- 187 X. Xu, Z. Wen, X. Wu, X. Yang and Z. Gu, *J. Am. Ceram. Soc.*, 2007, **90**, 2802.
- 188 W. Zhou, S. Wang, Y. Li, S. Xin, A. Manthiram and J. B. Goodenough, *J. Am. Chem. Soc.*, 2016, **138**, 9385.
- 189 P. R. Chinnam and S. L. Wunder, *ACS Energy Lett.*, 2017, **2**, 134.
- 190 K. Arbi, J. M. Rojo and J. Sanz, *J. Eur. Ceram. Soc.*, 2007, **27**, 4215.
- 191 Z. Jian, Y.-S. Hu, X. Ji and W. Chen, *Adv. Mater.*, 2017, **29**, 1601925.
- 192 K. Arbi, W. Bucheli, R. Jiménez and J. Sanz, *J. Eur. Ceram. Soc.*, 2015, **35**, 1477.
- 193 J. Xie, N. Imanishi, T. Zhang, A. Hirano, Y. Takeda and O. Yamamoto, *J. Power Sources*, 2009, **189**, 365.
- 194 C. Cao, Z.-B. Li, X.-L. Wang, X.-B. Zhao and W.-Q. Han, *Frontiers Energy Res.*, 2014, **2**, 25.
- 195 I. Kokal, K. V. Ramanujachary, P. H. L. Notten and H. T. Hintzen, *Mater. Res. Bull.*, 2012, **47**, 1932.
- 196 Y. Li, J.-T. Han, C.-A. Wang, H. Xie and J. B. Goodenough, *J. Mater. Chem.*, 2012, **22**, 15357.
- 197 R. Murugan, V. Thangadurai and W. Weppner, *Angew. Chem. Int. Ed.*, 2007, **46**, 7778.
- 198 I. Kokal, M. Somer, P. H. L. Notten and H. T. Hintzen, *Solid State Ionics*, 2011, **185**, 42.
- 199 A. C. Luntz, J. Voss and K. Reuter, *J. Phys. Chem. Lett.*, 2015, **6**, 4599.
- 200 K. Kerman, A. Luntz, V. Viswanathan, Y.-M. Chiang and Z. Chen, *J. Electrochem. Soc.*, 2017, **164**, A1731.
- 201 Y. Li, B. Xu, H. Xu, H. Duan, X. Lu, S. Xin, W. Zhou, L. Xue, G. Fu, A. Manthiram and J. B. Goodenough, *Angew. Chem. Int. Ed.*,

- 2017, **56**, 753.
- 202 X. Han, Y. Gong, K. Fu, X. He, G. T. Hitz, J. Dai, A. Pearce, B. Liu, H. Wang, G. Rublo, Y. Mo, V. Thangadurai, E. D. Wachsman and L. Hu, *Nat. Mater.*, 2017, **16**, 572.
- 203 R. Kanno, T. Hata, Y. Kawamoto and M. Irie, *Solid State Ionics*, 2000, **130**, 97.
- 204 R. Kanno and M. Murayama, *J. Electrochem. Soc.*, 2001, **148**, A742.
- 205 C. H. Lee, K. H. Joo, J. H. Kim, S. G. Woo, H. J. Sohn, T. Kang, Y. Park and J. Y. Oh, *Solid State Ionics*, 2002, **149**, 59.
- 206 T. Ohtomo, A. Hayashi, M. Tatsumisago and K. Kawamoto, *J. Solid State Electr.*, 2013, **17**, 2551.
- 207 T. Inada, *Solid State Ionics*, 2003, **158**, 275.
- 208 M. Tatsumisago, S. Hama, A. Hayashi, H. Morimoto and T. Minami, *Solid State Ionics*, 2002, **154-155**, 636.
- 209 A. Hayashi, *Solid State Ionics*, 2004, **175**, 637.
- 210 K. Joo, *Solid State Ionics*, 2003, **160**, 51.
- 211 N. S. Saetova, A. A. Raskovalov, B. D. Antonov, T. V. Yaroslavtseva, O. G. Reznitskikh and N. I. Kadyrova, *J. Non-Cryst. Solids*, 2016, **443**, 75.
- 212 A. V. Deshpande and V. K. Deshpande, *Solid State Ionics*, 2002, **154-155**, 433.
- 213 M. Tatsumisago, H. Yamashita, A. Hayashi, H. Morimoto and T. Minami, *J. Non-Cryst. Solids*, 2000, **274**, 30.
- 214 Y. Seino, T. Ota, K. Takada, A. Hayashi and M. Tatsumisago, *Energy Environ. Sci.*, 2014, **7**, 627.
- 215 Z. Liu, Y. Tang, X. Lu, G. Ren and F. Huang, *Ceram. Int.*, 2014, **40**, 15497.
- 216 Y. Seino, K. Takada, B. Kim, L. Zhang, N. Ohta, H. Wada, M. Osada and T. Sasaki, *Solid State Ionics*, 2006, **177**, 2601.
- 217 K. Ohara, A. Mitsui, M. Mori, Y. Onodera, S. Shiotani, Y. Koyama, Y. Orihara, M. Murakami, K. Shimoda, K. Mori, T. Fukunaga, H. Arai, Y. Uchimoto and Z. Ogumi, *Sci. Rep.*, 2016, **6**, 21302.
- 218 K. Takada, T. Inada, A. Kajiyama, H. Sasaki, S. Kondo, M. Watanabe, M. Murayama and R. Kanno, *Solid State Ionics*, 2003, **158**, 269.
- 219 E. Ranganamy, Z. Liu, M. Gobet, K. Pilar, G. Sahu, W. Zhou, H. Wu, S. Greenbaum and C. Liang, *J. Am. Chem. Soc.*, 2015, **137**, 1384.
- 220 J. Wei, H. Kim, D.-C. Lee, R. Hu, F. Wu, H. Zhao, F. M. Alamgir and G. Yushin, *J. Power Sources*, 2015, **294**, 494.
- 221 A. Hayashi, R. Komiya, M. Tatsumisago and T. Minami, *Solid State Ionics*, 2002, **152-153**, 285.
- 222 N. Kamaya, K. Homma, Y. Yamakawa, M. Hirayama, R. Kanno, M. Yonemura, T. Kamiyama, Y. Kato, S. Hama, K. Kawamoto and A. Mitsui, *Nat. Mater.*, 2011, **10**, 682.
- 223 S. Wenzel, S. Randau, T. Leichtweiss, D. A. Weber, J. Sann, W. G. Zeier and J. Janek, *Chem. Mater.*, 2016, **28**, 2400.
- 224 W. Zhang, D. A. Weber, H. Weigand, T. Arlt, I. Manke, D. Schroeder, R. Koerver, T. Leichtweiss, P. Hartmann, W. G. Zeier and J. Janek, *ACS Appl. Mater. Interfaces*, 2017, **9**, 17835.
- 225 P. Bron, S. Johansson, K. Zick, J. Schmedt auf der Gunne, S. Dehnen and B. Roling, *J. Am. Chem. Soc.*, 2013, **135**, 15694.
- 226 A. C. Kozen, A. J. Pearce, C.-F. Lin, M. Noked and G. W. Rubloff, *Chem. Mater.*, 2015, **27**, 5324.
- 227 A. J. Pearce, T. E. Schmitt, E. J. Fuller, F. El-Gabaly, C.-F. Lin, K. Gerasopoulos, A. C. Kozen, A. A. Talin, G. Rubloff and K. E. Gregorczyk, *Chem. Mater.*, 2017, **29**, 3740.
- 228 J. Glenneberg, F. Andre, I. Bardenhagen, F. Langer, J. Schwenzel and R. Kun, *J. Power Sources*, 2016, **324**, 722.
- 229 J. C. Li, C. Ma, M. F. Chi, C. D. Liang and N. J. Dudney, *Adv. Energy Mater.*, 2015, **5**, 1401408.
- 230 M. Tatsumisago, M. Nagao and A. Hayashi, *Journal of Asian Ceramic Societies*, 2013, **1**, 17.
- 231 M. Kotobuki and M. Koishi, *Ceram. Int.*, 2013, **39**, 4645.
- 232 V. Patil, A. Patil, S. J. Yoon and J. W. Choi, *J. Nanosci. Nanotechnol.*, 2013, **13**, 3665.
- 233 J. D. Nikolić, S. V. Smiljanjić, S. D. Matijašević, V. D. Živanović, M. B. Tošič, S. R. Grujić and J. N. Stojanović, *Process. Appl. Ceram.*, 2013, **7**, 147.
- 234 C. Liao, K. S. Han, L. Baggetto, D. A. Hillesheim, R. Custelcean, E. S. Lee, B. K. Guo, Z. H. Bi, D. E. Jiang, G. M. Veith, E. W. Hagaman, G. M. Brown, C. Bridges, M. P. Paranthaman, A. Manthiram, S. Dai and X. G. Sun, *Adv. Energy Mater.*, 2014, **4**, 1301368.
- 235 R.-c. Xu, X.-h. Xia, X.-l. Wang, Y. Xia and J.-p. Tu, *J. Mater. Chem. A*, 2017, **5**, 2829.
- 236 M. Eom, S. Choi, S. Son, L. Choi, C. Park and D. Shin, *J. Power Sources*, 2016, **331**, 26.
- 237 B. Huang, X. Yao, Z. Huang, Y. Guan, Y. Jin and X. Xu, *J. Power Sources*, 2015, **284**, 206.
- 238 R. B. Nuernberg and A. C. M. Rodrigues, *Solid State Ionics*, 2017, **301**, 1.
- 239 Z. Stoeva, I. Martin-Litas, E. Staunton, Y. G. Andreev and P. G. Bruce, *J. Am. Chem. Soc.*, 2003, **125**, 4619.
- 240 W. A. Henderson, N. R. Brooks and V. G. Young, *J. Am. Chem. Soc.*, 2003, **125**, 12098.
- 241 L. Y. Yang, D. X. Wei, M. Xu, Y. F. Yao and Q. Chen, *Angew. Chem. Int. Ed.*, 2014, **53**, 3631.
- 242 J. Zhang, L. Yue, P. Hu, Z. Liu, B. Qin, B. Zhang, Q. Wang, G. Ding, C. Zhang, X. Zhou, J. Yao, G. Cui and L. Chen, *Sci. Rep.*, 2014, **4**, 6272.
- 243 L. Porcarelli, C. Gerbaldi, F. Bella and J. R. Nair, *Sci. Rep.*, 2016, **6**, 19892.
- 244 Q. Pan, D. M. Smith, H. Qi, S. Wang and C. Y. Li, *Adv. Mater.*, 2015, **27**, 5995.
- 245 X. X. Zeng, Y. X. Yin, N. W. Li, W. C. Du, Y. G. Guo and L. J. Wan, *J. Am. Chem. Soc.*, 2016, **138**, 15825.
- 246 S. Klongkan and J. Pumchusak, *Electrochim. Acta*, 2015, **161**, 171.
- 247 F. Croce, L. Persi, B. Scrosati, F. Serraino-Fiory, E. Plichta and M. A. Hendrickson, *Electrochim. Acta*, 2001, **46**, 2457.
- 248 M. Dissanayake, P. Jayathilaka, R. S. P. Bokalawala, I. Albinsson and B. E. Mellander, *J. Power Sources*, 2003, **119**, 409.
- 249 E. M. Masoud, A. A. El-Bellihi, W. A. Bayoumy and M. A. Mousa, *J. Alloys Compd.*, 2013, **575**, 223.
- 250 W. Wang, E. Yi, A. J. Fici, R. M. Laine and J. Kieffer, *J. Phys. Chem. C*, 2017, **121**, 2563.
- 251 A. R. Polu and H.-W. Rhee, *J. Ind. Eng. Chem.*, 2016, **37**, 347.
- 252 D. Lin, W. Liu, Y. Liu, H. R. Lee, P. C. Hsu, K. Liu and Y. Cui, *Nano Lett.*, 2016, **16**, 459.
- 253 T. Jurkin and I. Pucić, *Polym. Eng. Sci.*, 2013, **53**, 2318.
- 254 C. W. Lin, C. L. Hung, M. Venkateswarlu and B. J. Hwang, *J. Power Sources*, 2005, **146**, 397.
- 255 S. Choudhury, R. Mangal, A. Agrawal and L. A. Archer, *Nat. Commun.*, 2015, **6**, 10101.
- 256 T. Itoh, Y. Ichikawa, T. Uno, M. Kubo and O. Yamamoto, *Solid State Ionics*, 2003, **156**, 393.
- 257 K. Kesavan, S. Rajendran and C. M. Mathew, *Polym. Compos.*, 2015, **36**, 302.
- 258 H. Y. Sun, Y. Takeda, N. Imanishi, O. Yamamoto and H. J. Sohn, *J. Electrochem. Soc.*, 2000, **147**, 2462.
- 259 Z. Y. Wen, T. Itoh, T. Uno, M. Kubo and O. Yamamoto, *Solid State Ionics*, 2003, **160**, 141.
- 260 C. Yuan, J. Li, P. Han, Y. Lai, Z. Zhang and J. Liu, *J. Power Sources*, 2013, **240**, 653.
- 261 K. Zhu, Y. Liu and J. Liu, *RSC Adv.*, 2014, **4**, 42278.
- 262 R. S. Kumar, M. Raja, M. Anbu Kulandainathan and A. Manuel Stephan, *RSC Adv.*, 2014, **4**, 26171.
- 263 F. Croce, L. Settini and B. Scrosati, *Electrochem. Commun.*, 2006, **8**, 364.
- 264 P. P. Chu, M. J. Reddy and H. M. Kao, *Solid State Ionics*, 2003, **156**, 141.
- 265 J. Xi, X. Qiu, X. Ma, M. Cui, J. Yang, X. Tang, W. Zhu and L. Chen, *Solid State Ionics*, 2005, **176**, 1249.
- 266 C. Shen, J. Wang, Z. Tang, H. Wang, H. Lian, J. Zhang and C.-n.

## REVIEW

## Journal of Materials Chemistry A

- Cao, *Electrochim. Acta*, 2009, **54**, 3490.
- 267 Y.-X. Jiang, J.-M. Xu, Q.-C. Zhuang, L.-Y. Jin and S.-G. Sun, *J. Solid State Electrochem.*, 2008, **12**, 353.
- 268 J. Xi, X. Qiu, J. Wang, Y. Bai, W. Zhu and L. Chen, *J. Power Sources*, 2006, **158**, 627.
- 269 J. Xi, X. Qiu and L. Chen, *Solid State Ionics*, 2006, **177**, 709.
- 270 A. Manuel Stephan and K. S. Nahm, *Polymer*, 2006, **47**, 5952.
- 271 E. M. Masoud, A. A. El-Bellihi, W. A. Bayoumy and M. A. Mousa, *Mater. Res. Bull.*, 2013, **48**, 1148.
- 272 Y.-J. Wang, Y. Pan and D. Kim, *J. Power Sources*, 2006, **159**, 690.
- 273 C. Wang, Y. Yang, X. Liu, H. Zhong, H. Xu, Z. Xu, H. Shao and F. Ding, *ACS Appl. Mater. Interfaces*, 2017, **9**, 13694.
- 274 J. Zheng, M. Tang and Y. Y. Hu, *Angew. Chem. Int. Ed.*, 2016, **55**, 12538.
- 275 J.-H. Choi, C.-H. Lee, J.-H. Yu, C.-H. Doh and S.-M. Lee, *J. Power Sources*, 2015, **274**, 458.
- 276 K. Fu, Y. Gong, J. Dai, A. Gong, X. Han, Y. Yao, C. Wang, Y. Wang, Y. Chen, C. Yan, Y. Li, E. D. Wachsman and L. Hu, *Proc. Natl. Acad. Sci. U. S. A.* 2016, **113**, 7094.
- 277 W. Liu, S. W. Lee, D. Lin, F. Shi, S. Wang, A. D. Sendek and Y. Cui, *Nat. Energy*, 2017, **2**, 17035.
- 278 W. H. Hou, C. Y. Chen and C. C. Wang, *Polymer*, 2003, **44**, 2983.
- 279 J. Zhang, J. Zhao, L. Yue, Q. Wang, J. Chai, Z. Liu, X. Zhou, H. Li, Y. Guo, G. Cui and L. Chen, *Adv. Energy Mater.*, 2015, **5**, 1501082.
- 280 J. C. Chai, Z. H. Liu, J. Ma, J. Wang, X. C. Liu, H. S. Liu, J. J. Zhang, G. L. Cui and L. Q. Chen, *Adv. Sci.*, 2017, **4**, 1600377.
- 281 Y. J. Lim, H. W. Kim, S. S. Lee, H. J. Kim, J.-K. Kim, Y.-G. Jung and Y. Kim, *Chempluschem*, 2015, **80**, 1100.
- 282 J. Li, Y. Lin, H. H. Yao, C. F. Yuan and J. Liu, *Chemsuschem*, 2014, **7**, 1901.
- 283 A. I. Horowitz and M. J. Panzer, *Angew. Chem. Int. Ed.*, 2014, **53**, 9780.
- 284 D. Zhou, R. Liu, Y.-B. He, F. Li, M. Liu, B. Li, Q.-H. Yang, Q. Cai and F. Kang, *Adv. Energy Mater.*, 2016, **6**, 1502214.
- 285 R. Bouchet, S. Maria, R. Meziane, A. Aboulaich, L. Lienafa, J.-P. Bonnet, T. N. T. Phan, D. Bertin, D. Gignes, D. Devaux, R. Denoyel and M. Armand, *Nat. Mater.*, 2013, **12**, 452.
- 286 Q. Ma, H. Zhang, C. Zhou, L. Zheng, P. Cheng, J. Nie, W. Feng, Y. S. Hu, H. Li, X. Huang, L. Chen, M. Armand and Z. Zhou, *Angew. Chem. Int. Ed.*, 2016, **55**, 2521.
- 287 I. Villaluenga, K. H. Wujcik, W. Tong, D. Devaux, D. H. Wong, J. M. DeSimone and N. P. Balsara, *Proc. Natl. Acad. Sci. U. S. A.*, 2016, **113**, 52.
- 288 Z. H. Li, C. Cheng, X. Y. Zhan, Y. P. Wu and X. D. Zhou, *Electrochim. Acta*, 2009, **54**, 4403.
- 289 J. Zhang, B. Sun, X. Huang, S. Chen and G. Wang, *Sci. Rep.*, 2014, **4**, 6007.
- 290 S. W. Choi, S. M. Jo, W. S. Lee and Y. R. Kim, *Adv. Mater.*, 2003, **15**, 2027.
- 291 Y. Zhu, F. Wang, L. Liu, S. Xiao, Y. Yang and Y. Wu, *Sci. Rep.*, 2013, **3**, 3187.
- 292 Z. Y. Tu, Y. Kambe, Y. Y. Lu and L. A. Archer, *Adv. Energy Mater.*, 2014, **4**, 1300654.
- 293 C. Xu, Z. Ahmad, A. Aryanfar, V. Viswanathan and J. R. Greer, *Proc. Natl. Acad. Sci. U. S. A.*, 2017, **114**, 57.
- 294 K. J. Harry, D. T. Hallinan, D. Y. Parkinson, A. A. MacDowell and N. P. Balsara, *Nat. Mater.*, 2014, **13**, 69.
- 295 S.-D. Gong, Y. Huang, H.-J. Cao, Y.-H. Lin, Y. Li, S.-H. Tang, M.-S. Wang and X. Li, *J. Power Sources*, 2016, **307**, 624.
- 296 M. Li, W. Zhu, P. Zhang, Y. Chao, Q. He, B. Yang, H. Li, A. Borisevich and S. Dai, *Small*, 2016, **12**, 3535.
- 297 Y. Li, K. W. Wong and K. M. Ng, *Chem. Commun.*, 2016, **52**, 4369.
- 298 F. Wu, N. Chen, R. Chen, Q. Zhu, J. Qian and L. Li, *Chem. Mater.*, 2016, **28**, 848.
- 299 G. Tan, F. Wu, C. Zhan, J. Wang, D. Mu, J. Lu and K. Amine, *Nano Lett.*, 2016, **16**, 1960.
- 300 F. Wu, N. Chen, R. Chen, L. Wang and L. Li, *Nano Energy*, 2017, **31**, 9.
- 301 I. Osada, H. de Vries, B. Scrosati and S. Passerini, *Angew. Chem. Int. Ed.*, 2016, **55**, 500.
- 302 J. H. Shin, W. A. Henderson and S. Passerini, *Electrochem. Commun.*, 2003, **5**, 1016.
- 303 A. S. Fisher, M. B. Khalid, M. Widstrom and P. Kofinas, *J. Power Sources*, 2011, **196**, 9767.
- 304 M. A. B. H. Susan, T. Kaneko, A. Noda and M. Watanabe, *J. Am. Chem. Soc.*, 2005, **127**, 4976.
- 305 A.-L. Pont, R. Marcilla, I. De Meatza, H. Grande and D. Mecerreyes, *J. Power Sources*, 2009, **188**, 558.
- 306 G. B. Appetecchi, G. T. Kim, M. Montanino, M. Carewska, R. Marcilla, D. Mecerreyes and I. De Meatza, *J. Power Sources*, 2010, **195**, 3668.
- 307 M. Li, L. Yang, S. Fang and S. Dong, *J. Membrane Sci.*, 2011, **366**, 245.
- 308 M. Doebbelin, I. Azcune, M. Bedu, A. Ruiz de Luzuriaga, A. Genua, V. Jovanovski, G. Cabanero and I. Odriozola, *Chem. Mater.*, 2012, **24**, 1583.
- 309 M. Li, L. Yang, S. Fang, S. Dong, S.-i. Hirano and K. Tachibana, *J. Power Sources*, 2011, **196**, 8662.
- 310 P.-L. Kuo, C.-H. Tsao, C.-H. Hsu, S.-T. Chen and H.-M. Hsu, *J. Membrane Sci.*, 2016, **499**, 462.

**Graphical Abstract:**

Recent progress in designing electrolytes for high voltage lithium ion batteries and solid-state lithium batteries is summarized.

